TRIBHUVAN UNIVERSITY

INSTITUTE OF ENGINEERING

PULCHOWK CAMPUS

B-13-BAS-2018/23

EXPERIMENTAL STUDY OF BLENDED WING BODY UAS WITH VTOL CONFIGURATION

BY

Mahesh Bhattarai (PUL075AER020)

Nabin Bhandari (PUL075AER024)

Roshani Sah (PUL075AER034)

A PROJECT REPORT

SUBMITTED TO THE DEPARTMENT OF MECHANICAL AND AEROSPACE ENGINEERING

IN THE PARTIAL FULFILLMENT OF THE REQUIREMENTS FOR THE DEGREE OF BACHELOR IN AEROSPACE ENGINEERING

DEPARTMENT OF MECHANICAL AND AEROSPACE ENGINEERING

LALITPUR, NEPAL

MARCH, 2023

COPYRIGHT

TRIBHUWAN UNIVERSITY

INSTITUTE OF ENGINEERING

PULCHOWK CAMPUS

DEPARTMENT OF MECHANICAL AND AEROSPACE ENGINEERING

The undersigned certify that they have read, and recommended to the Institute of Engineering for acceptance, a project report entitled "Experimental Study of Blended Wing Body UAS with VTOL Configuration" submitted by Mahesh Bhattarai, Nabin Bhandari and Roshani Sah in partial fulfillment of the requirements for the degree of Bachelor of Aerospace Engineering.

Supervisor, Ashish Karki

Assistant Professor

Department of Mechanical and Aerospace Engineering

External Examiner, Sanjiv Paudel

Managing Director, Machine Hub Nepal

Tribhuvan University
Institute of Engineering
Department of Mechanical and Aerospace Engineering
Pulchowk Campus

Committee Chairperson, Assoc. Prof. Dr. Surya Prasad Adhikari

Head

Department of Mechanical and Aerospace Engineering

17th, March 2023

Date:

ABSTRACT

The present study looked into the aerodynamic properties of blended-wing-body (BWB) unmanned aerial vehicles (UAS) with vertical takeoff and landing capabilities (VTOL). The UAS's innovative design allows for VTOL and hovering capabilities similar to multi-copter drones, as well as cruise flying efficiency comparable to fixed-wing aircraft in an effective and dependable manner. The creation of lift by the complete airframe and the decrease of drag in the wing body attachment are benefits of the BWB concept. Based on the calculated wing parameters, a baseline design was developed in XFLR5 and few parameters like sweep, dihedral and twist were varied continuously to obtain the most efficient design. The maximum L/D ratio obtained was 17 and calculated stall velocity was 12 m/s. The final design was then developed in CATIA and plane maker, and flight test was performed in X-Plane 11. By constructing parts out of Styrofoam and aluminum rod, a model was created. Four motors were used for vertical take-off and an electronic ducted fan was used for forward thrust. Pixhawk 4 was used as flight controller. The flight test was performed in three different modes: pure fixed wing, pure quad and hybrid VTOL mode. Initially, the fixed wing and quad mode test were performed individually. Then quad mode was enabled in the fixed wing configuration and transition from VTOL to fixed wing was performed. This report can serve as a comprehensive resource for learning about aerodynamic phenomena, fundamental design concepts, and fabrication techniques.

Keywords: BWB, VTOL, XFLR5, CATIA, Ducted Fan, Reflex Airfoil, Transition

ACKNOWLEDGEMENT

We are immensely grateful to the Department of Mechanical and Aerospace Engineering at IOE, Pulchowk Campus for giving us the opportunity to participate in this project and gain hands-on experience in the relevant field. Our heartfelt thanks go out to our supervisor, Asst. Prof. Ashish Karki, who provided unwavering support and guidance throughout the entire process. His presence and insights have been invaluable and we cannot express enough gratitude for the motivation and encouragement he provided. Furthermore, we would like to extend our sincere appreciation to Asst. Prof. Dr. Sudip Bhattarai for his invaluable advice and support. His expertise and guidance have greatly contributed to the success of this project.

We would like to present our sincere gratitude to Asst. Prof. Kamal Darlami, Head of IIEC, for his continuous support and providing us workspace at IIEC. Additionally, we would like to acknowledge the support of our seniors, juniors and classmates who helped us in various aspects of this project. We would also like to thank Department of Mechanical and Aerospace Engineering, Pulchowk Campus which provided us with the resources and equipment necessary for this project. Their support was crucial in allowing us to carry out our project.

TABLE OF CONTENTS

LIST OF FIGURES

LIST OF TABLES

ABBREVIATIONS

AOA	Angle of Attack
AR	Aspect Ratio
BWB	Blended Wing Body
CAD	Computer Aided Design
CG	Center of Gravity
CNC	Computerized Numerical Control
GPS	Global Positioning System
GSD	Generative Shape Design
IR	Infrared
MAC	Mean Aerodynamic Center
MTOW	Maximum take-off weight
PCL	Polycaprolactone
ROC	Rate of Climb
TR	Taper Ratio
UAS	Unmanned Aerial System
VTOL	Vertical Take-off and Landing

SYMBOLS

AOA, α	:	Angle of Attack
b or b_W	:	Span
C or c	:	Chord
Cd or C_d	:	Coefficient of drag.
CFx	:	Component integrated X force coefficient
CFy	:	Component integrated Y force coefficient
CFz	:	Component integrated Z force coefficient
C_{HT}	:	Coefficient for Horizontal Tail
Cl or C_l	:	Coefficient of lift
C_L	:	Lateral Moment Coeficient
$C_{L\beta}$	:	Lateral Moment Coefficient Slope
Cm	:	Pitching/Longitudinal Moment Coefficient
C_{m0}	:	Longitudinal Moment Coefficient at Zero Angle of Attack
$C_{m\alpha}$	:	Longitudinal Moment Coefficient Slope
Cmx	:	Component integrated X moment coefficient
Cmy	:	Component integrated Y moment coefficient
Cmz	:	Component integrated Z moment coefficient
C_n	:	Directional Moment Coefficient
$C_{n\beta}$	:	Directional Moment Coefficient Slope
C_{VT}	:	Coefficient for Vertical Tail
C_R	:	Root Chord
C_t	:	Tip Chord
L or L_β	:	Rolling Moment
L/D	:	Lift to drag ratio.
$L_{VT,}$ L_{HT}	:	Distance between wing and Vertical and Horizontal tail MAC

M	:	Pitching Moment
N	:	Yawing Moment
Re	:	Reynolds Number
S	:	Area of wing
S_{VT}	:	Vertical Tail Area
T	:	Thrust
W	:	Weight
X_{cg}	:	Distance of Center of Gravity from leading-edge
X_{np}	:	Distance of neutral point from leading-edge
β	:	Sideslip angle
ξ	:	Damping Ratio
λ	:	Taper Ratio
μ	:	Viscosity of air
ρ	:	Density of air

CHAPTER ONE: INTRODUCTION

1.1. Background

Blended Wing Body is an unconventional aircraft concept which was first proposed on older flying wing designs for significant improvements in future air transportation. The BWB is a tailless configuration that combines the wing and fuselage into one unit. It was originally designed as a one-of-a-kind platform for high-speed commercial airlines at the end of the 20th century. The most vital benefit that it holds is its lesser wetted area to volume ratio and significantly lower drag as compared to conventional airframe which results in an increased Lift-to-Drag ratio. This helps in significant payload advantages and increases fuel economy. It also has a larger internal room as well as sufficient area for installation of the engine on the top of the airframe.

(*Source: nasa.gov/x48*)

Fig 1. 1: Boing X-48B BWB prototype

The center body of BWB carries 31-43% of total lift which is a significant number compared to conventional airframes which carry only about 12-13%. Despite its unique characteristics and potential, the BWB is less likely to enter service until 2030s.

Due to its revolutionary form, which is also responsible for several issues and comfort difficulties, passenger safety, evacuation and cabin pressurization are some of the most critical challenges, and the BWB concept, despite continued research, cannot be considered a fusible alternative in the commercial airliner layout, at least for the time being.

VTOL UAS are unmanned systems that combine the features of multirotor and fixed-wing configurations. They have the feature to take-off, fly and land vertically and allow access to difficult-to-reach areas, hover over points of interest, and, in some situations, give enhanced portability. Their main flaw is that their engines consume a lot of power, limiting flying time and cargo weight. VTOL UAS can be further sub-categorized into several groups such as tail-sitter, tail rotor, dual-system UAS, and so on.

(*Source: arcarosystems.com*)

Fig 1. 2: e-Starling, BWB UAS with VTOL Configuration.

Ducted fans, also known as shrouded propellers, show potential as components for propulsion systems with high static thrust. They typically create more static thrust than an isolated propeller of the same diameter and power loading. Furthermore, because the rotating fan is enclosed in the duct, the ducted fan system provides an additional

safety element, making it an appealing option for many advanced unmanned aerial system configurations. The design and flight control are more difficult than with a multirotor platform, but the advantages in terms of safety, payload, noise, precision hover, resilience, and control make it worthwhile. The ducted fan UAS can be used to a wide range of complicated conditions and carry out demanding tasks. It's small, with a compact and adaptable design. It can maneuver in any direction in addition to hovering and vertical takeoff and landing, allowing it to do some unique tasks.

1.2. Objectives

The main and specific objectives of this project are mentioned below:

1.2.1. Main Objective

- To design, study, fabricate and test a VTOL type blended wing body UAS.

1.2.2. Specific objectives

- To design and analyze stability and performance of BWB.
- To fabricate designed model.
- To perform manual and autonomous test flight in quad and fixed wing mode.
- To perform smooth transition from vertical take-off to cruise.

1.3. Application

VTOL (Vertical Take-Off and Landing) BWB (Blended Wing Body) UAS have several applications in various industries:

1) Military: They can be used for surveillance, reconnaissance, and attack missions.
2) Agriculture: BWB UAS with VTOL capabilities can be used for crop monitoring and mapping, providing a cost-effective way to gather data and make informed decisions.
3) Emergency Response: VTOL BWB UAS can be used in disaster management and search and rescue operations to provide real-time aerial imagery and video to aid in decision-making.

4) Infrastructure Inspection: These UAS can inspect bridges, pipelines, power lines, and other infrastructure assets with ease, reducing the risk to human inspectors and improving the efficiency of inspections.
5) Environmental Monitoring: VTOL BWB UAS can be equipped with sensors to monitor air quality, track wildlife, and monitor forests for signs of degradation.
6) Delivery: BWB UAS with VTOL capabilities can be used for delivery of small packages and supplies in urban areas, reducing delivery time and increasing efficiency.
7) Filmmaking: VTOL BWB UAS can be used in the film industry to capture aerial footage, providing filmmakers with a cost-effective alternative to manned aircraft.

1.4. Features

Some of the feature of VTOL BWB are mentioned below:

1) Vertical take-off and landing: They can take off and land vertically without the need for a runway.
2) Blended wing body design: They have a unique aerodynamic shape with a wide, flat body that blends seamlessly into the wings, providing increased lift and reduced drag.
3) Increased efficiency: Due to their aerodynamic design, they typically have a longer flight time and greater payload capacity compared to traditional drone designs.
4) Multi-mission capabilities: They can be used for a variety of missions, such as aerial photography, surveillance, and delivery.
5) Autonomous flight: They are often equipped with advanced navigation systems and autopilot software that enable them to fly autonomously.

1.5. Feasibility Analysis

1.5.1. Economic Feasibility

The initial cost estimation of our project was NRs. 91,000 which is relatively very high. But as we had availibility of the electronic components such as: transmitter, PX 4 controller, GPS module, telemetry, servo, ESC, brushless motors, and ducted fan for

throttle, our cost dropped significantly. The only expenses we had to manage were the cost of structural components which we was affordable. Hence, our project was economically feasible.

1.5.2. Technical Feasibility

Since our project was design and fabrication of BWB UAS, the technological requirements were for the design, analysis and flight test software and hardware and manufacturing tools for fabrication. As XFLR 5, CATIA V5, X-PLANE 11 are sufficient for design and analysis works. As well as we had Flight simulator that ease the flight testing for the designed UAS.

Moving towards fabrication process, we had CNC LASER Cutting Machine that was used to cut ribs in plywood, CNC Hot Wire Cutting Machine used for cutting Styrofoam to give the required airfoil shape form to the central structural part. Although due to the limitations of CNC Hot wire Cutting Machine, it was not possible to cut the Styrofoam automatically but it was used to manually cut the airfoil shape and form spar holes in the designed wing segments. Besides CNC Cutting Machines, we had 3D printer which was used for printing servo connectors using PCL.

1.5.3. Operational Feasibility

The purpose of our BWB VTOL UAS is for surveillance in the wild lives reserves in Himalayan region where it is not possible to have sufficient runway for takeoff and landing. But as it is well known that there is no regulation for regulation and operation of UAS in Nepal, it cannot be commercialized till a proper regulation is established. Whereas if there is a proper established regulation for regulation and operation of UAS, it could be one of the best and most feasible means for doing night surveillance in such regions using IR camera. Since, BWB are capable of carrying more payload and greater range compared to conventional UAS, the problem for power supply will be less frequent.

1.6. System Requirement

1.6.1. Software requirement

1.6.1.1. XFLR5

XFLR5 serves as a software program that facilitates the design and analysis of aircraft components such as wings, airfoils, and planes. On the other hand, XFOIL is an interactive tool primarily used for designing and analyzing individual subsonic airfoils. By inputting the coordinates that define a 2D airfoil's shape, Reynolds, and Mach values, XFOIL can provide information on the pressure distribution of the airfoil, as well as its lift and drag characteristics. Along with accepting input in the form of airfoil coordinates, returning an airfoil shape and doing analysis on it based on those criteria, XFLR5 also offers inverse foil design, which determines the shape of various airfoils depending on the desired airfoil properties.

For the examination of wing shapes that are outside the scope of the LLT, a VLM approach is used as an alternative. A VLM works on the premise of summarizing the vortices spread throughout the wing's planform to represent the perturbation produced by the wing. Each vortex's strength is calculated to satisfy the necessary boundary conditions (BC), i.e., non-penetration conditions on the panels' surface.

When it comes to plane analysis, XFLR5 offers both static and dynamic stability analysis of planes, along with an Eigen value matrix for dynamic stability analysis.

1.6.1.2. Airfoil Maker

A new airfoil can be created using the airfoil maker, and an old airfoil can also be opened in view mode and modified. The amount that the airfoil wants to lift up, pull back, and pitch up can be used to produce a new airfoil in the airfoil creator. For the purpose of creating an airfoil, different lift, drag, and moment data are provided, including: Cl intercept, Cl slope, Cl curvature near stall, Clmax, Cdmin, Cl at minimum Cd, Cd curvature, laminar drag bucket location, laminar drag bucket curvature, Cm at low and high AOA change points, stall minimum and maximum AOA, and the values of Cl, Cd, and Cm at specific AOAs.

1.6.1.3. Plane Maker

Almost any airplane that can be imagined can be constructed with this software. The design made on plane maker is used in X-Plane 11 simulator which is capable of predicting the flight behavior of an aircraft. All the parameter of wing, control surfaces, empennage, and landing gear can be assigned in the design. Beside this type of engine and its specification, customized airfoils can be assigned to the design.

1.6.1.4. X-Plane 11

X-Plane 11 is a software for flight simulator. It is versatile instrument that caters to the needs of pilots seeking to enhance their skills through realistic simulation, engineers keen on predicting the performance of new aircraft, and aviation enthusiasts eager to unravel the mysteries of flight dynamics. It predicts the performance and handling of almost any aircraft.

The designed aircraft can be flown in a variety of modes with X-Plane 11, including Phugoid, Short-Period, Dutch roll, and spiral, to obtain the dynamic stability characteristics of an aircraft. Additionally, the aircraft's saw-tooth ascent and descent, roll sensitivity, and pitch sensitivity can be tested.

1.6.1.5. CATIA V5

CATIA is used for CAD, CAM, and CAE design. CATIA ensures quicker analysis, design, and manufacturing process with numerous approaches to product design and development. It features large number of workbenches for design and analysis of parts and product from simple 3D part design to complex shape designs, surface design and assembly design. In this Project, mostly the Mechanical Part Design, Generative Shape Design and Assembly Design workbench have been used to design each component of the Blended Wing Body Aircraft as well as the complete Planform and the assembly of all components.

1.6.1.6. RD Works

RD Works is a software application used for laser cutting and engraving. It is used to create, edit, and carry out tasks involving laser cutting and engraving. Editing vector graphics, preview and simulation, parameter modification, cutting and engraving optimization. The laser machine may also be controlled remotely, allowing users to

control it from a separate place. It was utilized in this project to set up the ribs drawing geometry from the CATIA V5.dxf file and prepare it for CNC LASER cutting.

1.6.1.7. QgroundControl

QGroundControl is an open source software that offers a user interface for managing mission planning, system setup, and monitoring of unmanned system. It includes sensor calibration, safety feature setup, and several flight mode configurations. By altering the characteristics of the program, such as the flight speed, altitude, and camera settings, users can modify the behavior of their vehicle. QGroundControl delivers live telemetry data from the UAS, including GPS position, altitude, battery level, and other crucial data.

1.6.1.8. Mission planner

Mission planner is used to design and manage autonomous missions for drones and UAS similar to QgroundControl. It also enables the user to map out a UAS's flight path, set waypoints, and customize different settings like altitude, speed, and camera settings. By choosing particular waypoints on a map interface, users of Mission Planner can plan their flight paths. The UAS can conduct activities such as hovering or changing altitude, direction, speed, or flying modes by being given the ability to set height and speed at each waypoint. It consists of a lot of parameters to customize the UAS configuration as per the requirement.

1.6.2. Hardware Requirement

1.6.2.1. CNC LASER Cutting Machine

A CNC laser cutter utilizes a concentrated laser beam to perform a range of cutting, engraving, and marking tasks with exceptional accuracy. The process is entirely non-contact and thermally-based, with a laser head featuring a nozzle and focusing lens directing the laser beam onto the work piece. The laser's heat melts and shapes the material, resulting in a precise cut that conforms perfectly to the desired 2D shape.

1.6.2.2. Hot Wire CNC

Hot wire CNC foam cutters enable virtually any product with the most complex shapes to be produced quickly, precisely, and reasonably priced A hot wire, or a particular kind of resistance wire that becomes extremely hot when current flows through it, is

the key component of this gadget. When the hot wire passes through the foam, it melts or vaporizes it, allowing us to precisely and quickly create whatever shape we choose.

1.6.2.3. Fixed Based Flight Simulator

A flight simulator is a device that artificially re-creates the experience of flying an aircraft. It is employed in the fields of education, research, and entertainment. There are many different kinds of flight simulators, including desktop simulators, professional-grade simulators, full motion simulators, fixed base simulators, simulators for basic training, and virtual reality flight simulators. The hardware consists of an exact reproduction of a cockpit that is furnished with controls and tools that are comparable to those used in real airplanes and that give the user a realistic simulation experience.

1.6.2.4. Control Stick

A joystick is a handheld device that is used to control movement in a computer game or simulation. A joystick functions by converting physical stick motion into computer-interpretable electrical impulses. Joysticks can be used to precisely control the movement of objects in racing games, flight simulators, and other situations. With the joystick, we had access to more control input elements than we needed, such as trim tabs, roll, yaw, and throttle control.

1.6.2.5. Pixhawk 4

Pixhawk is a flight controller that can transform any fixed-wing aircraft, rotary-wing aircraft, multirotor aircraft, boats, and even cars into a fully autonomous system; capable of performing a wide range of tasks, even pre-programmed GPS missions with waypoints. The most recent flight controller version, Pixhawk 4, features the most cutting-edge processing technology and a NuttX real-time operating system, giving it remarkable controllability, versatility, and performance.

1.6.2.6. Other Equipment and Tools

Beside the above mentioned hardwares, there were several equipment that we used throughout the manufacturing process of our model. Some of them are: Drill machine to drill holes aluminum structure, Hex saw to cut spar segments from the aluminum tube, aluminum C section to get the segment of required length, glue gun to attach the

structural components with each other, soldering iron for making wire connections, sand paper to blend the Styrofoam wing segment and other general tools for manufacturing.

CHAPTER TWO: LITERATURE REVIEW

2.1. History of Blended Wing Body (BWB)

Blended wing body (BWB) aircrafts are more centered aerodynamically and structurally efficient aircraft. The evolution of BWB aircraft started when NASA Langley Research Centre challenged aerospace companies to design an aircraft with 800 seats, a range of 700 miles, and a Mach 0.85 service speed, BWB aircraft were developed [1]**.** When the design team at McDonnel Douglas Boeing began selecting the configuration taking passenger cabin problem as their major challenge for the design, they started with three canonical configurations i.e., Spherical, Cylindrical, and disc. Since Sphere has the minimum surface area but wasn't streamlined so it was rejected initially. Then from the remaining two with equal surface area, they discovered disc configuration to have 33% reduced total weighted area compared to the cylinder when wings and control surfaces were added. With this, the BWB configuration arises to be the most efficient in terms of payload, empty operating weight, thrust requirement, and fuel consumption. But it doesn't end there, with the advantages of payload and lift there came challenges in flight mechanics and control system of BWB which are still under investigation. But the benefits of BWB of improved system performance and highly fuel-efficient over conventional aircraft are so high that it has always been in research for commercialization.

Present studies on configuration of aircraft incorporates BWB as a potential candidate for large body sub-sonic transport aircraft. The present aerial compatibility restrictions limited the BWB's wing span at 80 meters. One of the major advantages of BWB is significant reduction in Skin friction drag if the laminar flow technique is successfully implemented. The study found BWB to be not so suitable for smaller size transport system due to its large wetted surface area increasing drag penalty and a large trim drag due to substantial negative pitching moment of the aircraft. [2][3]

A conceptual design is a tool that enables users to quickly modify an airplane's geometry and analyze the impact on key performance characteristics such as flight, stability, weight, and passenger accommodation. It is ideal for optimizing aircraft design and streamlining the design process. Three major different configurations for the BWB is presented: the conventional one with aft sweep and aft engine, one with aft swept and forward mounted engine under wings and the one with forward swept

with wing mounted engine and the pros and cons of each are discussed. The conventional one is found to have maximum lift to drag ratio with least fuel consumption, while the one with engine mounted under wings provides highest Wing loading at MTOW since it has maximum lift coefficient due to undisturbed flow over the upper surface of wing. Similarly, the forward swept wing has the advantage of least operational empty takeoff weight providing greater payload capacity and range with least CG travel throughout the mission. [4][5]

Based on an aerodynamically optimized design with fixed planform and pitching moment, performance analysis of BWB with varying sweep angle has been studied. The grid analysis was performed for both forward sweep and aft sweep. It was found that the L/D ratio increases with increase in sweep angle for sweep back configuration and provide negative pitching moment with increase in incidence angle signifying stability of the aircraft. While in case of forward sweep BWB, L/D was found to be least without any significant change with sweep angle and gave nose up tendency with increase in incidence angle making the aircraft more unstable. Along with the problem of instability the additional problem of shock wave formation at body wing junction. Hence even having the benefit of reduced wing tip stall, the penalty of drag divergence and longitudinal instability of forward sweep wings make those BWB configuration not feasible for application. [6]

The application of UAS in detecting forest fire and its direction of spread is presented depending upon the path traced. The algorithm has been developed to evaluate the delay time for transmitting data to checkpoint and base station using single UAS and multiple UAS assigning different paths. [7]

2.2. History of Fixed-Wing VTOL Aircrafts

Fixed Wing VTOL aircraft blends the advantage of hover flight with the high speed, longer range, and larger payload capacity of fixed-wing aircraft without compromising the efficiency of the aircraft. The major challenge of the past half-century has been to increase the top speed of VTOL without compromising lift to power in hover and efficiency during long-range flight [8].

The Major VTOL configurations are tilt-wing rotor VTOL, tilt-rotor VTOL, tilting ducted fan VTOL, and tilt jet VTOL, Aerodyne VTOL, and thrust vector-controlled VTOL [9]. Quantix tail-sitter UAS, NASA GL-10 tilt-wing UAS, Rotormast V-22 tilt-rotor UAS, Dronetech's AV-1 Albatross, and ALTI transition are some examples of Fixed-Wing VTOL aircraft currently in use. In some only the propulsive unit is tilted for transition while in others the whole wing is tiled.

Since the use of tilt rotors in UAS is still in the experimental phase. Canard Configuration with the full tilt of wing and canard was found to be the best so far in cruise performance, hover efficiency and payload [10].

The transition of the same aircraft from hover to forward flying to make it more robust. At the same time, it increases the complexity of handling the stability of aircraft. Since the use of traditional design method for fixed-wing design and momentum theory for rotor dynamics becomes incompatible with the incorporated design making them more unstable. To tackle such problem, the preliminary design method with additional lifting area and reduced dead weight was introduced [11].

The challenges of flight transitions and the factors that must be considered while designing aircraft which expresses thrust requirement and lifting area being the major consideration that affects the stability of the air-frame while in the transition phase [12].

In the initial design phase, two distinct flying wing models were analyzed using a range of techniques including established analytical methods, less precise Vortex-Lattice Method evaluations, and modified semi-empirical/statistical methods specifically suited for lightweight flying wing drones. The most suitable model was selected based on its aerodynamic performance and ability to perform vertical takeoff and landing (VTOL). The selected design is currently undergoing further development and refinement in the preliminary design phase [13].

2.3. Overview of Design Process

Conceptual design is the first step in the design process. During this phase, the designers consider a variety of aircraft configuration concepts, conduct trade studies

of the designs and requirements, and then choose one best design and, with significant customer input, choose a well-balanced set of requirements. The design requirements are employed in conceptual design to direct and assess the creation of the overall aircraft configuration arrangement.

When the significant adjustments are finished, preliminary design might be deemed to start. The major issues, such whether to utilize an aft tail or a canard, have been settled. Although minor changes could yet happen, it can be predicted that the configuration arrangement will mostly stay the same as it is in the existing drawings.

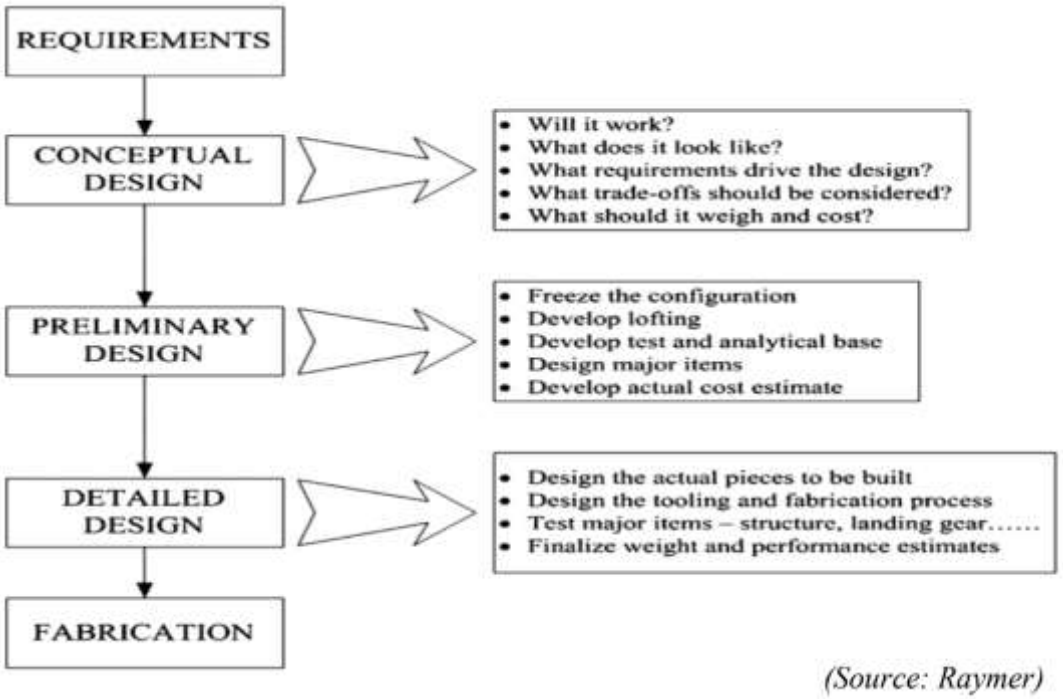

(Source: Raymer)

Then the phase of detail design starts, assuming that it is decided favorably to move further with full-scale development. The real parts are designed in "depth" at this time. After that, you fabricate the components, put them all together, and fly. Not a single "build-to" drawing is produced during the whole conceptual and preliminary design processes. All of the individual structural sections are developed in detail.

2.4. Airfoil Selection for Tailless Aircraft

The parameters for choosing an airfoil varies depending on the type of tailless aircraft since stability needs are important. The optimum performance is produced by airfoils with low moment coefficients for the majority of tailless aircraft [14].

The shape of an airfoil is composed of two parts: thickness distribution along the camber line and camber distribution along the camber line. The shapes and wing twist distributions needed for different types of tailless aircraft can be determined based on this. To achieve a positive moment coefficient and the necessary lift, reflexed camber line airfoil is used [15].

The shape of the camber line and the moment coefficient Cm are connected. Modifying the rear half of the camber line can produce the desired Cm, but it also results in a decrease in lift at a certain angle of attack and a lower lift coefficient overall. This occurs because the lift vs. drag polar is moved downward when a reflex is added to the camber line to increase the moment coefficient [16].

Reflexed camber lines are a commonly used design feature in the development of aircraft wings, as they provide several advantages in terms of aerodynamic performance. However, the related velocity distributions are sensitive to low Reynolds numbers, which can lead to problems with stall behavior. Low Reynolds numbers occur at low air speeds, such as those experienced by light aircraft during takeoff and landing. In these situations, the airflow over the wing may separate prematurely, causing a loss of lift and an increase in drag [17].

To mitigate these effects, designers must carefully consider the shape and position of the camber line when designing aircraft wings. A moderate reflex with a maximum camber located near the leading edge and a relatively blunt nose has been found to be an effective compromise for light, tailless aircraft. This design provides high lift coefficients, which are essential for safe takeoff and landing, while also reducing the risk of premature stall. Additionally, the position of the maximum camber near the leading edge helps to maintain stability and control at low speeds [18].

CHAPTER THREE: RELATED THEORY

3.1. Stability

Equilibrium and stability are important concepts in aircraft design and operation. Equilibrium refers to a state where the forces and moments acting on an aircraft are balanced, resulting in a steady and unchanging flight condition. If an aircraft is in a state of equilibrium, then the resultant force and moment acting on it must both be equal to zero.

Stability refers to the ability of an aircraft to return to its original equilibrium state after being disturbed. A stable aircraft will tend to return to its original flight condition after being perturbed, whereas an unstable aircraft will continue to deviate from its original condition. Static stability and dynamic stability are two different types of stability.

3.1.1. Static Stability

Static stability refers to the ability of an aircraft to remain in a stable and level flight even when faced with external disturbances such as turbulence or wind gusts.

An aircraft with positive static stability will return to its original position after being disturbed, while an aircraft with negative static stability will continue to deviate from its original position. Positive static stability is considered desirable for flight safety, as it increases the margin of error for the pilot to correct any disturbances. The stability of an aircraft is affected by its center of gravity, wing sweep, dihedral angle etc.

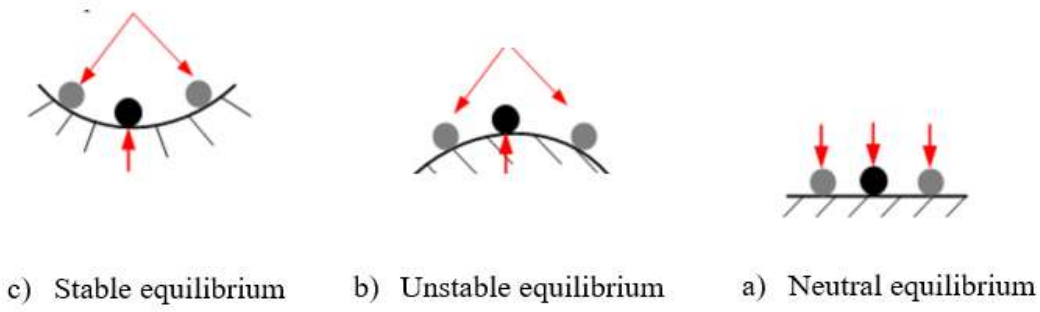

(*Source: Pamadi*)

Fig 3. 1: Equilibrium position

There are three type of Static Stability: Longitudinal Static Stability, Static Directional Stability and Static Lateral Stability

3.1.1.1. Longitudinal Static Stability

The longitudinal static stability of an aircraft refers stability in the pitch axis. When aircraft is subjected to nose down pitching moment it is considered to be longitudinally statically stable if the nose up pitching moment generated to counter the effect. To put it in simpler terms, for an aircraft to be considered stable in the pitch axis, the slope of the curve representing the relationship between the Coefficient of Moment and the angle of Attack must be negative.

To achieve pitch trim, the net pitching moment about the center of gravity must be zero. It is crucial for an aircraft to be capable of maintaining a trimmed state at all values of angle of attack within the permissible range, in order to be considered flyable.

The criterion for longitudinal or pitch stability can be expressed mathematically as,

$$\frac{dM}{d\alpha} < 0 \qquad \frac{dC_m}{d\alpha} < 0$$

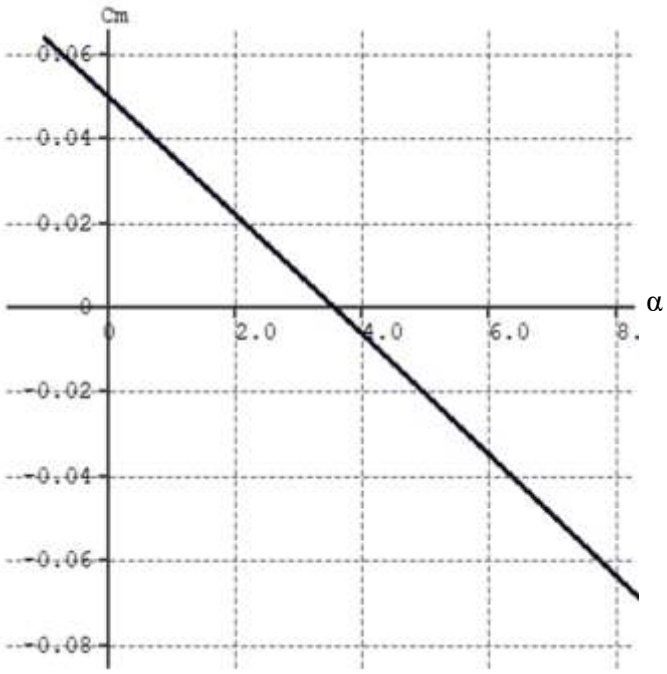

Fig 3. 2*:* Coefficient of moment (Cm) vs alpha (α) curve

To establish a stable pitch trim the necessary and sufficient conditions are,

If, $C_{mo} > 0$ And, $\frac{dC_m}{d\alpha} < 0$

$C_{m\alpha} < 0$ Or, $C_{mo} < 0$

3.1.1.2. Directional Static Stability

When an aircraft experiences a disturbance in its horizontal plane during steady level flight, such as a gust of wind or rudder deflection, it may encounter a sideslip. The aircraft's ability to effectively eliminate this disturbance in sideslip and realign itself along the direction of the resultant wind is known as its static directional stability. In this scenario, the aircraft's orientation in space may change in response to the disturbance, but its heading remains the same with respect to the Earth. The aircraft automatically adjusts itself to achieve zero sideslip and returns to a balanced state. The criterion can be expressed mathematically as:

$N_\beta > 0$ $C_{n\beta} > 0$

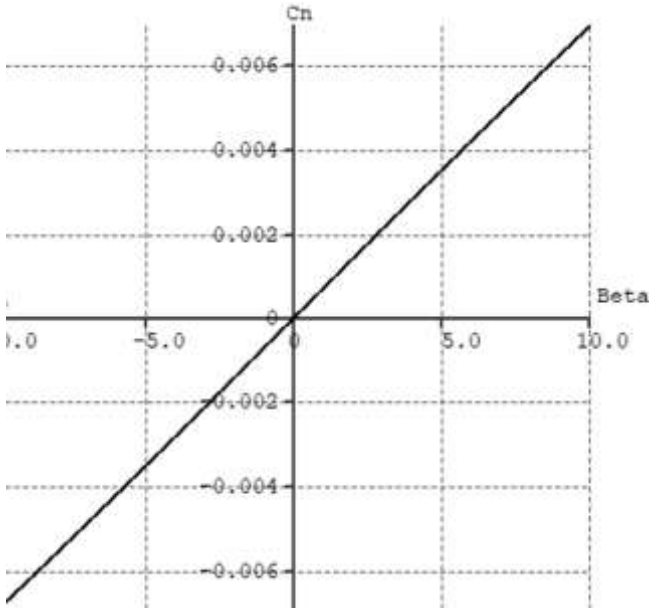

Fig 3. 3: Yawing moment (N) vs sideslip angle (β)

3.1.1.3. Lateral Static Stability

Lateral stability refers to the ability of an airplane to counteract a disturbance in its bank angle. If the airplane is banked, a sideslip is generated in the direction of the bank and it is considered lateral stable if this sideslip results in a restoring rolling moment

eliminating sideslip. However, if the rolling moment does not restore it is said to be laterally unstable. When the induced rolling moment is zero and the airplane remains constantly banked and continues to sideslip, it is considered neutrally stable.

The criterion can be expressed mathematically as:

$$L_\beta < 0 \qquad C_{l\beta} < 0$$

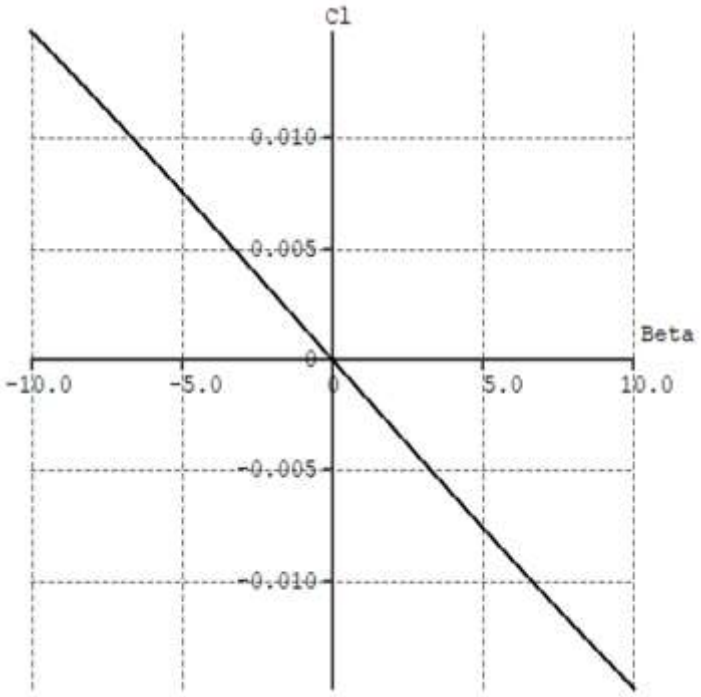

Fig 3. 4: Coefficient of rolling moment (Cl) vs sideslip angle (β)

3.1.1.4. Static Stability Analysis

Static stability analysis is a method used to evaluate the stability of an aircraft. The process involves analyzing the aircraft's inherent stability characteristics and determining whether the aircraft will remain in a stable condition or move away from its original state after being disturbed.

The results of the static stability analysis are used to determine the aircraft's stability characteristics, including its longitudinal and lateral stability, and to make any necessary modifications to improve the aircraft's stability. The process is typically repeated until the aircraft has a satisfactory level of stability.

3.1.2. Dynamic Response of aircraft

Dynamic stability is a measure of a system's ability to recover its initial state after being subjected to external disturbances. It is usually quantified by the time it takes for the disturbance to reduce by half or double, depending on whether the motion is stable or unstable, respectively. In oscillatory motions, the frequency and period of the motion are critical factors in assessing dynamic stability.

Dynamic stability is essential for ensuring the safe and stable flight of aircraft. The dynamic stability of an aircraft can be affected by a variety of factors, including its design, weight and balance, and operating conditions. A highly dynamic stable aircraft will be able to recover quickly and effectively from disturbances, such as turbulence or gusts, and return to its original flight path.

3.1.2.1. Phugoid Mode or Long-Period Mode

The phugoid mode is a dynamic response of an aircraft characterized by a long-period oscillation in both altitude and airspeed. It occurs when an aircraft experiences a small disturbance, such as a gust of wind or a change in weight distribution, and is an important factor in determining the stability and performance of aircraft.

In the phugoid mode, the aircraft experiences a slow oscillation in altitude, with a corresponding change in airspeed. The aircraft will first climb, then descend, and continue to oscillate back and forth until the disturbance is dampened. The frequency of the phugoid mode is usually very low, typically around 0.1 Hz, making it a slow-moving mode compared to other aircraft responses.

The phugoid mode is primarily influenced by the lift-to-drag ratio of the aircraft, and it is important for designers to carefully consider this characteristic when designing aircraft. A higher lift-to-drag ratio can result in a more stable phugoid mode, while a lower lift-to-drag ratio can make the aircraft more prone to oscillating in this model.

3.1.2.2. Short Period Mode

The short period mode refers to the rapid, small-amplitude, oscillatory motion of an aircraft about its longitudinal axis in the pitch direction. This mode is characterized by

its relatively short period of oscillation, typically a few seconds, and its relatively low frequency, usually less than one cycle per second.

The short period mode is the result of a change in the angle of attack (AOA) of an aircraft, causing the lift and weight forces to oscillate. The motion is typically dampened by the airframe's mass and elastic properties, as well as by the aerodynamic damping of the wings. The short period mode is an important factor in the stability and control of aircraft, and it is critical to understanding the behavior of an aircraft in flight.

The dynamic response of the short period mode is usually analyzed using linear mathematical models, which allow for the determination of the aircraft's natural frequency, damping ratio, and stability derivatives. These parameters are used to design and optimize the aircraft's control systems, including its stabilizers and elevators, to ensure safe and stable flight.

3.1.2.3. Spiral Mode

The dynamic response of an aircraft's spiral mode refers to the behavior of the aircraft when it experiences a spiraling motion. This motion can occur when the aircraft is subjected to a disturbance, such as a strong gust of wind or an imbalance in the control inputs. The spiral mode is characterized by a continuous rolling motion that increases in amplitude over time, leading to a tight, spiraling descent.

In an aircraft with poor dynamic stability, the spiral mode can quickly become unstable and can lead to a dangerous situation. In these cases, the aircraft will continue to roll and yaw, causing an increasingly steep descent, unless the pilot takes corrective action.

However, in aircraft with good dynamic stability, the spiral mode is typically well-damped, meaning that the rolling and yawing motion will quickly decay and the aircraft will return to its original flight path. The ability to quickly recover from the spiral mode is critical for the safe and stable operation of aircraft.

To enhance the dynamic stability of an aircraft, engineers use various design techniques, including the use of winglets, vortex generators, and aerodynamic modifications. Additionally, the use of fly-by-wire systems and stability augmentation

systems can also help to improve the dynamic response of an aircraft in the spiral mode.

3.1.2.4. Dutch Roll

Dutch roll is a type of dynamic response that can occur in an aircraft. It is a yawing and rolling motion that can arise as a result of conflicting demands between the lateral and directional stability of the aircraft.

In an aircraft, the lateral stability system provides stability about the roll axis and the directional stability system provides stability about the yaw axis. When these two systems have different natural frequencies or damping ratios, a Dutch roll motion can occur. The motion consists of a slow rolling motion combined with a quick yawing motion, giving the impression of a weaving or fishtailing motion.

Dutch roll is often caused by a mismatch between the lateral and directional stability systems of the aircraft, such as having a wing with a low dihedral angle and a rudder with high authority. It can also be exacerbated by certain atmospheric conditions, such as turbulence or wind shear.

It is important to note that Dutch roll can lead to a loss of control of the aircraft if not properly addressed. To mitigate the effects of Dutch roll, aircraft manufacturers can design the lateral and directional stability systems to have similar natural frequencies and damping ratios. Pilots can also reduce the risk of Dutch roll by using proper control inputs and by avoiding excessive yawing and rolling motions.

3.1.2.5. Dynamic Stability Analysis

Dynamic analysis in XFLR5 is performed to evaluate the stability and dynamic performance of an aircraft. It involves using mathematical models of the aircraft to calculate the aircraft's response to disturbances and to assess its stability.

The following steps were carried out while performing a dynamic analysis in XFLR5:

1) Linear stability analysis: To perform a linear stability analysis of the aircraft. This involves using the aircraft's mathematical model to calculate the stability

derivatives, such as the lateral state matrix, and to determine the aircraft's response to disturbances.

2) Eigenvalue analysis: The eigenvalue analysis is performed to determine the aircraft's natural frequencies and modes of motion. The eigenvalues represent the natural frequencies of the aircraft's motion, while the eigenvectors represent the aircraft's natural modes of motion.
3) Damping ratio analysis: The damping ratio analysis is performed to determine the stability margins of the aircraft. The Phillips formulae is used to calculate the damping ratio and the frequency of the aircraft's motion in response to disturbances.

After the Completion of this, Flight Simulation is performed using ‘X-Plane 11’. This involves using the aircraft's mathematical model to simulate the aircraft's motion and to assess its stability. The results of the flight simulation are used to validate the stability analysis and to design the aircraft's control systems.

CHAPTER FOUR: METHODOLOGY

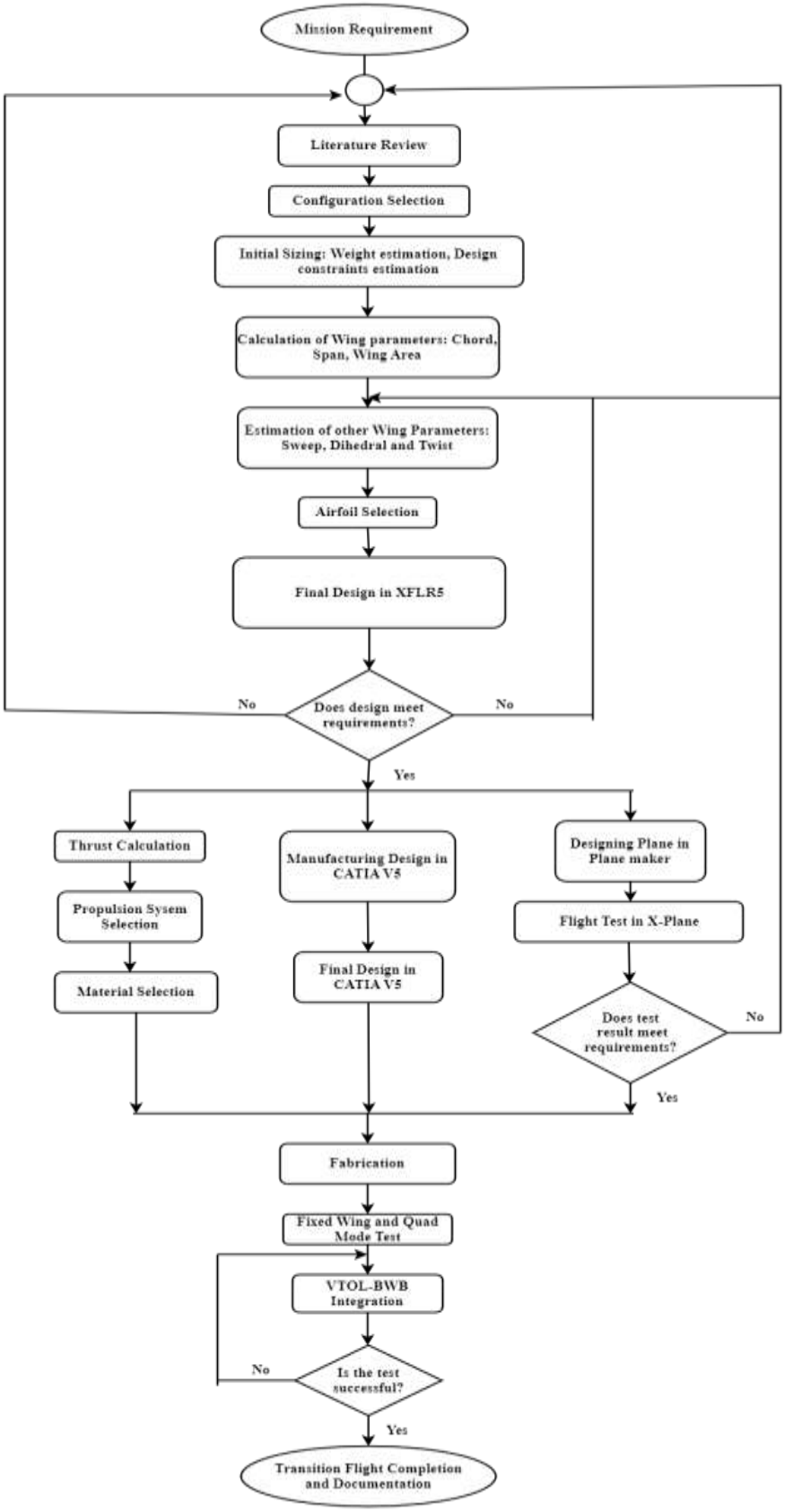

Fig 4. 1: Methodology flowchart

This chapter covers our approach to solving the statement problem of the project and describes the methods that we will be using during our project. The steps are briefly explained below.

4.1. Conceptual Design

Traditionally, the conceptual design stage is where an airplane is first created. The primary goal of the conceptual phase is to ascertain whether an aircraft that satisfies some stated or presumptive design requirements can be constructed. Therefore, given fundamental mission objectives, top-level exploration of the design space is carried out during the conceptual design phase using quick and easy methodologies. This makes it possible to develop and assess a number of notions. The most practical concept is then chosen for more examination. At the conceptual stage, few specifics are needed.

4.1.1. Configuration Selection

Just like any other aircraft, a BWB can also be designed in many different configurations. The configuration of a BWB UAS is determined by its size, weight, manufacturing complexity, structural limit, payload capacity and other features. Some of the configurations that a BWB can be modelled are aft-swept wing, fwd-swept wing, single fin, double fin, BWB with winglet, BWB with separate horizontal tail and many more.

Since the inboard stall of forward-swept wing leads in pitch up and a BWB doesn't have tail to compensate it, the selection of aft-swept wing is a default choice for us. The aft-swept wing also has lesser aero elastic fluttering tendency. A double fin configuration exhibits greater directional stability and better directional control and also helps to shield the engine noise, so we decided to proceed with double fin type. Also, a winglet needs greater structural strength at the wing tip which will significantly increase the weight, so it is never a good option for a small scale BWB.

Considering all these, the most optimum configuration for our requirements seemed to be an aft-swept, body mounted double fin BWB. We also decided to incorporate the Vertical Take-Off and Landing (VTOL) feature in our BWB reducing the challenges

of take-off and landing which also provides us flexibility to take-off and land anywhere which is a major requirement of our mission as well.

4.1.2. Weight Estimation

Mass prediction is vital in every aircraft design process. It vastly affects the performance characteristics as well as entire structure of an aircraft. The initial estimation of total mass of our BWB was performed based on the individual masses of each component and structural mass.

Table 4. 1 : Mass calculation

Accessories	**Mass**	**Quantity**	**Total Mass**
Wing and Structure	900 gm	1	900gm
Battery (4S, 5200 mAh)	450 gm	1	450 gm
Battery (4S, 2200 mAh)	250 gm	1	250 gm
Motor and Propellers	150 gm	4	600 gm
Ducted Fan	180 gm	1	180 gm
ESC 50A	70 gm	4	280 gm
ESC 60A	70 gm	1	70 gm
Servos	20 gm	2	40 gm
Controller	100 gm	1	100 gm
Miscellaneous	130 gm		130 gm
TOTAL			3000 gm

4.1.3. Propulsion System Selection

The propulsion system should be selected such that it provides maximum efficiency while consuming minimal energy. It must also be able to generate enough thrust to lift off and maintain flight while still being lightweight and compact enough for the UAS's size and payload requirements. Furthermore, it must be reliable and cost-effective so that it can be used for a variety of applications.

For our requirement, we selected propeller for vertical take-off and land as they are light weighted. For thrust, we opted Electronic Ducted Fan (EDF) for their higher power, less noise, robustness and higher efficiency than multi-copters in higher altitude.

4.2. Preliminary Design

Selected concepts are developed and validated by thorough analysis and computer simulations throughout the preliminary design process. Creating an optimum configuration with enough specifics and potentials to move on to the detailed design phase is the goal of this phase.

The design process involves few parameters to be assumed and few to be chosen from all the literature surveys that is being made.

4.2.1. Design Constraints

There are several design constraints that must be taken into consideration when designing a UAS. These constraints may include different parameters like size and weight of the aircraft, its cruise speed, the type of propulsion system used, wing loading, etc. These design constraints must be thoroughly understood to create a UAS that is optimized for specific task.

Few parameters that we assumed based on the selected configuration and mission requirements are:

- Weight = 3 kg
- Wing Loading = 8 kg/m^2
- Aspect Ratio = 6
- Taper Ratio = 0.15
- Cruise Speed = 25 m/s
- Cruise Altitude = 4000 m

These variables serve as a starting point for the calculation of other required parameters.

4.2.2. Wing Parameters

Wing design is one of the most crucial tasks to complete during the aircraft design process. A designer must optimize a lot of wing geometrical factors in order to achieve an efficient wing geometry that complies with design requirements.

4.2.2.1. Wing Area

Since our entire airplane is made up of wings, the wing area is a significant variable for us. It must be big enough to generate enough lift during every phase of flight, but not so big that it exceeds the size and weight limit.

The wing area can be calculated from wing loading and weight by following formula:

$$\text{Wing Area} = \frac{W}{W/S} = \frac{3}{8} = 0.37\ m^2$$

4.2.2.2. Wing Span

The distance between the tips of each wing on an airplane is known as its wingspan. Regardless of wing form or sweep, an aircraft's wingspan is always calculated in a straight line from wingtip to wingtip. Wing span is directly related to the aspect ratio and total wing area. The aspect ratio can be expressed in terms of wing span as:

$$\text{Aspect Ratio} = \frac{b^2}{S}$$

$$b = \sqrt{AR * S} = 1.5\ \text{m}$$

4.2.2.3. Root Chord

The distance between the leading and trailing edges of a wing in the airflow direction is used to calculate the chord of the wing. Since many wings are not square or rectangular, they contain various chords in various span wise locations. The chord length typically increases from the point where the wing attaches to the aircraft's fuselage (referred to as the root chord) and reduces as it travels toward the wing's tip (the tip chord). The root chord can be calculated as:

$$\text{Root Chord } (C_R) = \frac{2 * Wing\ Area}{b(1+\lambda)}$$

$$= 0.57\ \text{m}$$

4.2.2.4. Tip Chord

It is the total chord length at the tip of the wing. It can be calculated as:

$$\text{Tip Chord } (C_t) = \lambda * Root\ Chord$$

$$= 0.15 * 0.57$$

$$= 0.09 \text{ m}$$

4.2.2.5. Other Parameters

Sweep: Wings of BWB aircraft are frequently swept and twisted to achieve longitudinal static stability. By sweeping the wing back, the center of lift moves rearward thus producing stabilizing moment and it also increases the control effectiveness of control surfaces by increasing the moment arm from CG. However, it comes at a cost of maximum lift coefficient.

BWB has leading edge sweep of 30 degree. The sweep is highest at the root section to minimize drag and have positive directional stability. The sweep is reduced at the outboard section in order to increase the lift coefficient since sweep reduces CL.

Twist: Twist is varied from +3 degree to -3 degree from root to tip section. It is +3 degree from root section to 0.22 m of span. Then the twist value is 0 degree at 0.33 m and -3 degree from 0.42 to 0.75 m span. This is done primarily to achieve elliptical lift distribution.

Dihedral: Dihedral angle has crucial stabilizing effects on aircrafts. It greatly impacts the lateral-directional stability of the aircraft. BWB has a total of 3 degree dihedral at every section.

4.3. Vertical Tail Parameters

Vertical stabilizers are incorporated into BWB due of their stability with regard to sideslip and rudder inputs. We choose vertically mounted twin stabilizer design. The volume coefficient design approach is used to size the vertical tail. The tail volume coefficient is taken as 0.05 from historical data. The location of vertical tail is defined with respect to the location of trailing edge from wing's MAC. The distance of vertical

tail's MAC from wing's MAC is 0.15, so required vertical tail area can be calculated as:

$$C_{VT} = \frac{L_{VT} S_{VT}}{b_{WT} S_w}$$

$$\therefore S_{VT} = 0.02\ m^2$$

Considering Aspect Ratio as 2.8, the span comes out to be 0.12 m. considering taper ratio as 0.7, the root and tip chord is calculated as 0.1 m and 0.07 m.

Table 4. 2: Tail parameter

Tail Parameters	**Value**
Tail Area	0.02 m^2
Span	0.24 m
Aspect Ratio	2.8
Taper Ratio	0.7
Root Chord	0.1 m
Tip Chord	0.07 m

4.4. Airfoil Selection

The choice of an appropriate airfoil is likely the most crucial step in the design of any tailless aircraft since, in the absence of a tail, the airfoil itself is hugely responsible for the overall stability of the craft.

The Reynolds number value at different chord location can be calculated as:

$$\text{Re} = \frac{\rho V L}{\mu}$$

Since our BWB is designed to operate in high Himalaya region (about 4000 m), so approximated density value at that altitude is 0.82 kg/m^3 and viscosity at about 5° C is 1.75*10^{-5} Pa.s.

Hence, for root:

Re_{root} = 667,714

For Tip:

Re_{tip} = 105,428

4.4.1. Criteria of Selection for Root

The center body of a BWB UAS generates the majority of the lift. It was necessary to select a high lift airfoil at the root chord. Also, the airfoil must have positive moment coefficient for large range of Reynolds number since BWB lacks proper elevator for pitch balance. Another important criteria for the selection of root airfoil is the maximum thickness since the airfoil must be thick enough to be able to have enough space for electrical components.

Large set of airfoils were studied first and five airfoils were shortlisted for detailed analysis. Those airfoils along with their characteristics are:

Table 4. 3: Airfoil characteristics for root

Airfoil	$C_{l\max}$	$C_{m\max}$	**Thickness**	$C_{d\min}$	**Stall AOA**
MH78	1.4	+0.02	14.45%	0.01	16
MH81	1.6	-0.015	13%	0.01	15
NACA 23012	1.4	-0.02	12%	0.015	15
E334	1.45	-0.06	11.9%	0.01	14
MH91	1.35	+0.015	14.97%	0.02	16

Based on our preferences, every parameter was carefully investigated. The following list includes both their traits and preferences:

Table 4. 4: Characteristics and preferences for root

Characteristics	**Preferences**
$C_{l max}$	High Values are preferred
C_m	Least negative value is satisfactory Small Positive value is preferred
Thickness	High enough to accommodate electrical components (14-16 % is the optimum value)
L/D_{max}	High Values are preferred
$C_{d min}$	Minimum Values are preferred
Stall Angle of Attack	High Values are preferred

Above table suggests than MH78 would be the best option for us due to its positive moment coefficient, good amount of maximum thickness, higher stall angle and less drag coefficient.

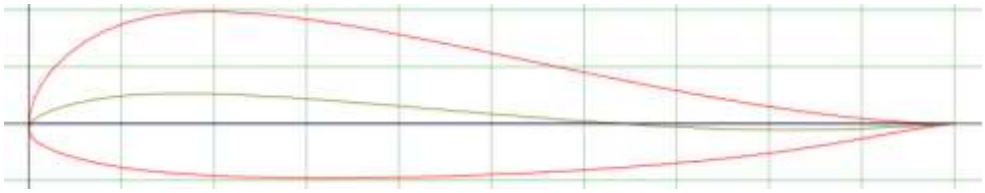

Fig 4. 2: Profile of MH78 airfoil

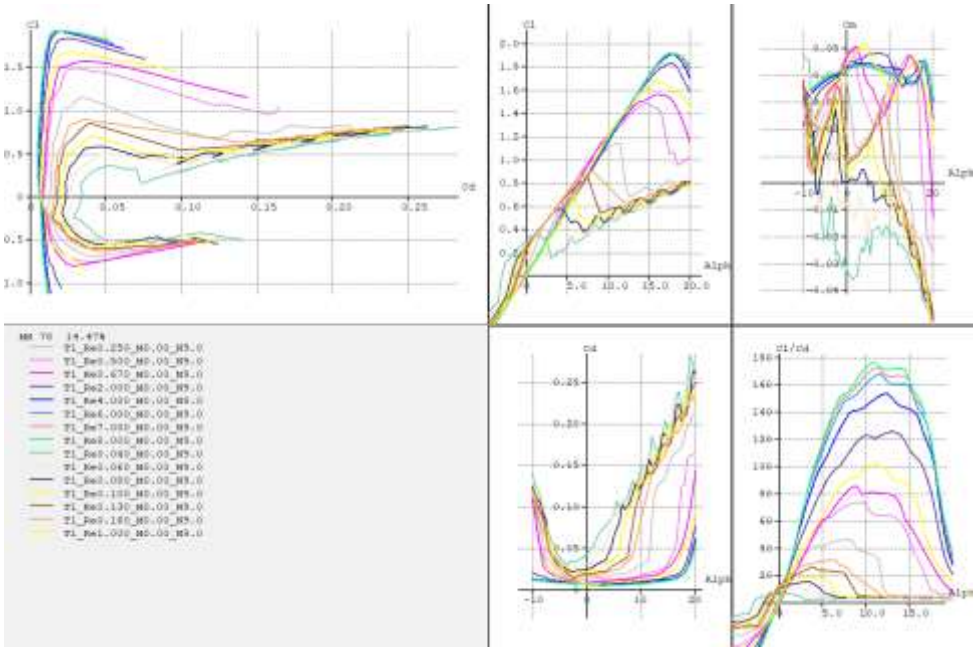

Fig 4. 3: Airfoil batch analysis of MH 78 for different Reynolds number

4.4.2. Criteria of Selection for Tip

For tip airfoil selection, the main criteria is to have least negative moment coefficient along with high lift coefficient.

Three airfoils were shortlisted for detailed analysis. Those airfoils along with their characteristics are tabulated below:

Table 4. 5: Airfoil characteristics for root

Airfoil	**C_{lmax}**	**C_{mmax}**	**Thickness**	**C_{dmin}**	**Stall AOA**
MH45	1.2	-0.02	10%	0.01	14
S5010 10%	1.4	-0.01	10%	0.005	14
E330	1.3	+0.02	11.04%	0.015	11

Below is the list of individual characteristics and our selection preferences for the shortlisted airfoils:

Table 4. 6: Characteristics and preferences for tip

Characteristics	**Preferences**
C_m	Least negative value is preferred
L/D_{max}	High Values are preferred
Stall Angle of Attack	High Values are preferred
Thickness	Neither thicker than root chord, nor lesser than 10%
C_{lmax}	High Values are preferred
C_{dmin}	Minimum Values are preferred

Despite having slight negative moment, s5010 10% airfoil is the most optimum choice for us based on our preferences.

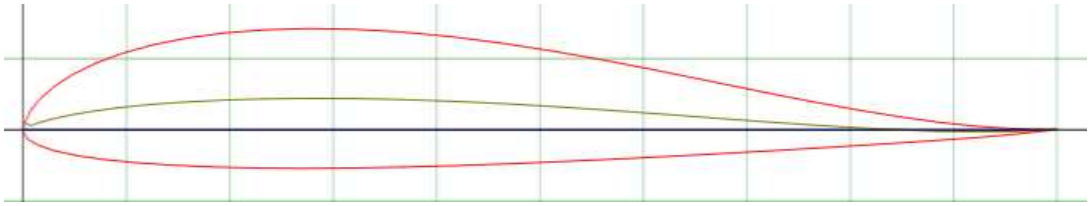

Fig 4. 4: Profile of S5010 airfoil

The XFLR analysis of S5010 airfoil is presented below:

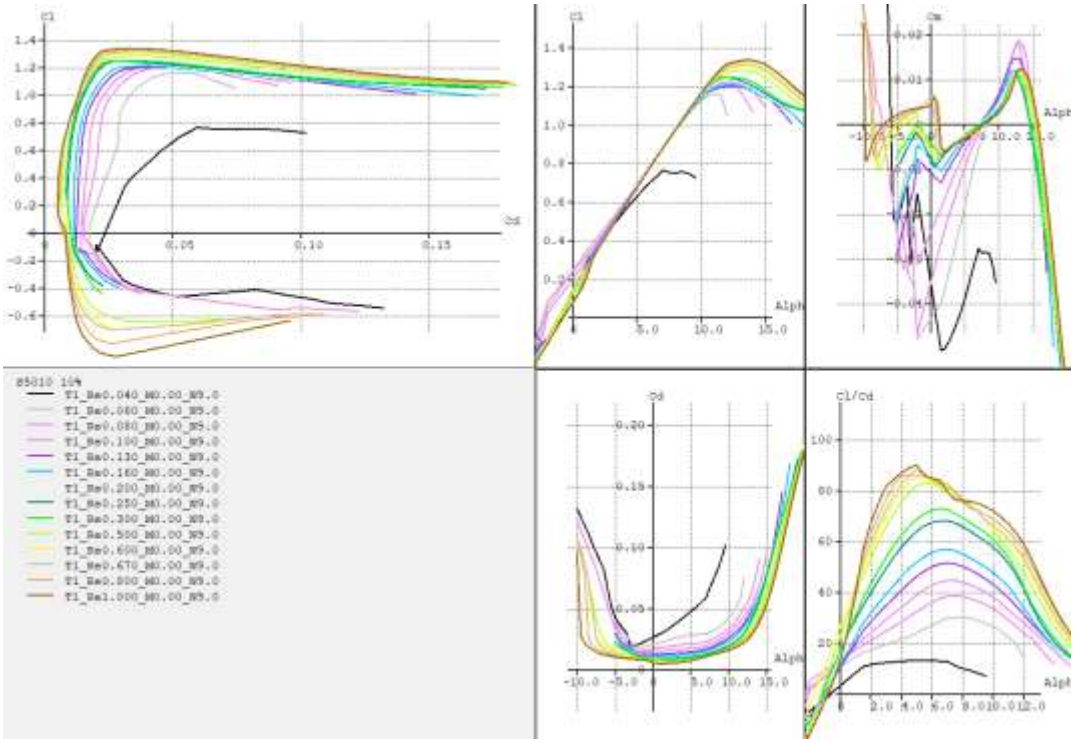

Fig 4. 5: Airfoil batch analysis of S5010 for different Reynolds number

MH78 is used from root to 0.22m of span and S5010 is used from 0.42m to tip of the wing. In order to have further improved performance and smoother planform, MH80 airfoil is also used at span wise location of 0.33m. Its maximum thickness of 12% also acts as a filler and avoids the transition of maximum thickness from high 14.47% to low 10%.

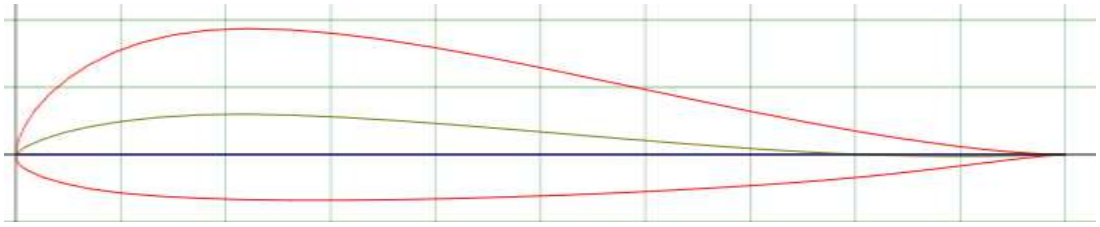

Fig 4. 6: Profile of MH80 airfoil

The XFLR analysis of MH80 airfoil is presented below:

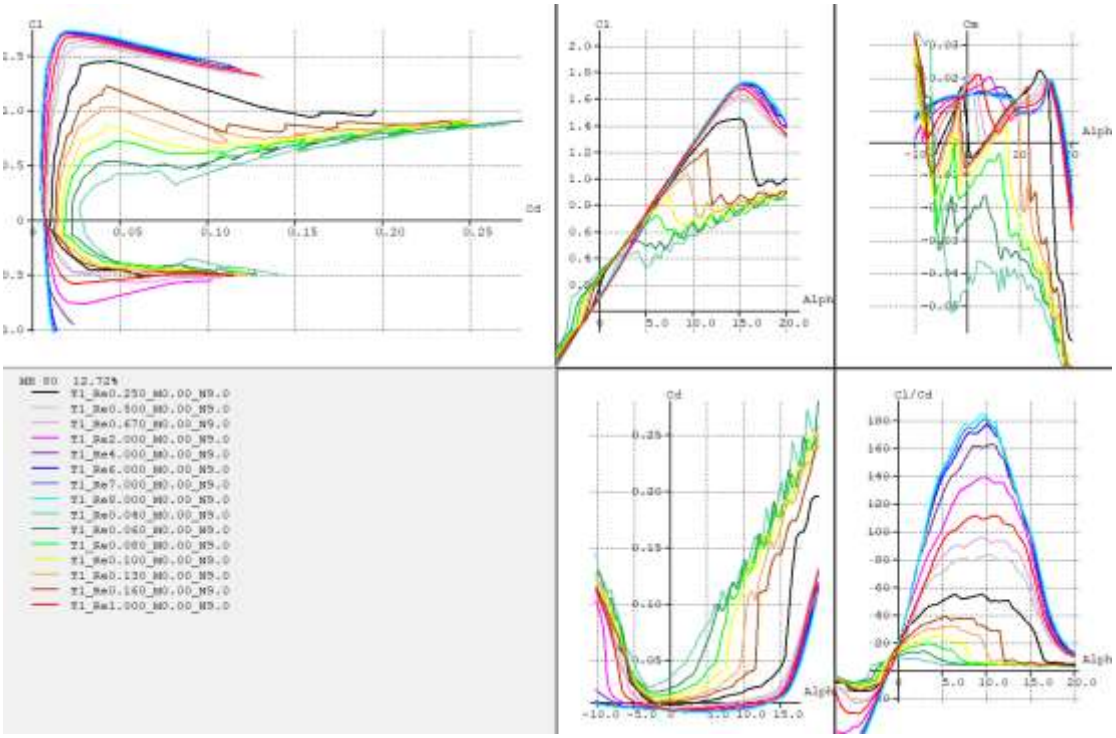

Fig 4. 7: Airfoil batch analysis of MH80 for different Reynolds number

4.4.3. Criteria of Selection for Fin

Normally, a symmetrical airfoil is preferred for vertical tail. The thickness should be between 9% and 15% to achieve a good balance between maximum side force and structural effectiveness. We selected NACA 0012 for this purpose.

Fig 4. 8: Profile of NACA 0012 airfoil

The XFLR5 analysis of NACA 0012 airfoil is presented below:

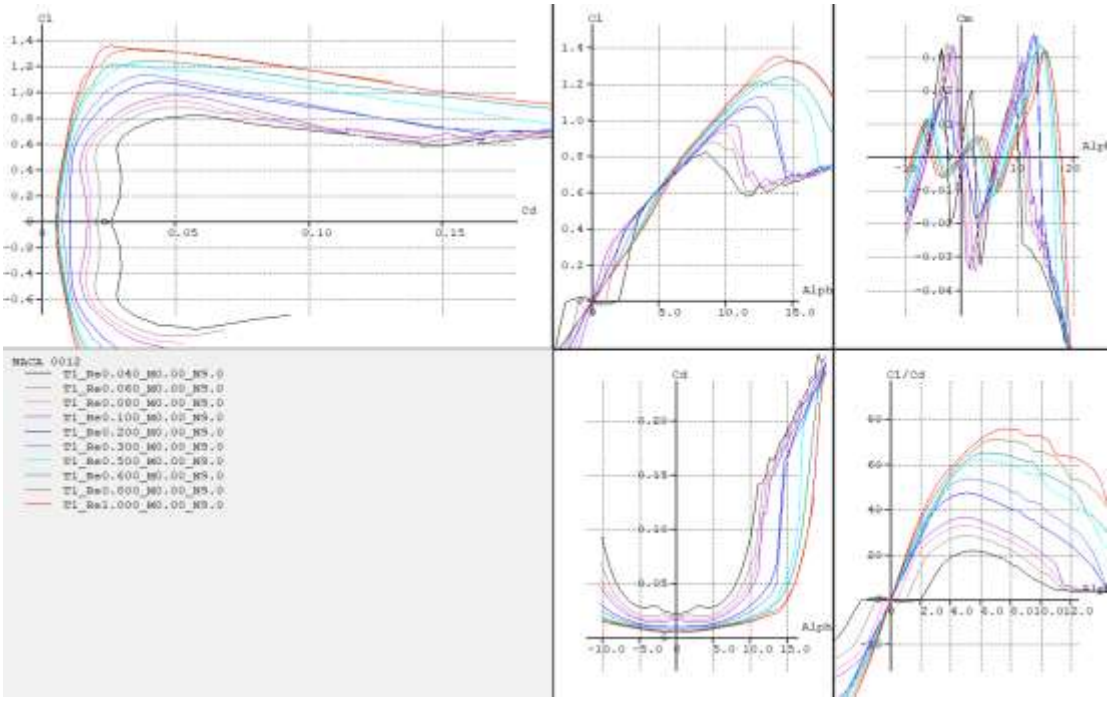

Fig 4. 9: Airfoil batch analysis of MH80 for different Reynolds number

4.5. Control Surface Sizing

Other than its primary wing, a tailless aircraft has no other horizontal surfaces. The primary wing incorporates the aerodynamic control and stabilization functions for both pitch and roll. The three primary control surfaces namely flaps, ailerons and rudders are chosen based on the historical data.

Table 4. 7: Control surface parameters

Control Surface	**Chord Ratio**	**Span**	**Airfoil**
Elevons	0.3	0.3 m	S5010
Rudders	0.3	0.1 m	NACA 0012

4.6. Final Design

The final design of our BWB was created in XFLR5, Plane maker, and CATIA for our necessary doings based on all the parameters mentioned above.

Table 4. 8: *Major parameters of BWB planform*

Parameters	**Value**
Wing Loading	8 kg/m^2
Maximum Takeoff Weight	3 kg
Wing Area	0.372 m^2
Wing Span	1.5 m
Aspect ratio	6
Taper Ratio	0.15
Root Chord	0.57 m
Tip Chord	0.09 m
Leading Edge Sweep	30°
Dihedral Angle	3°

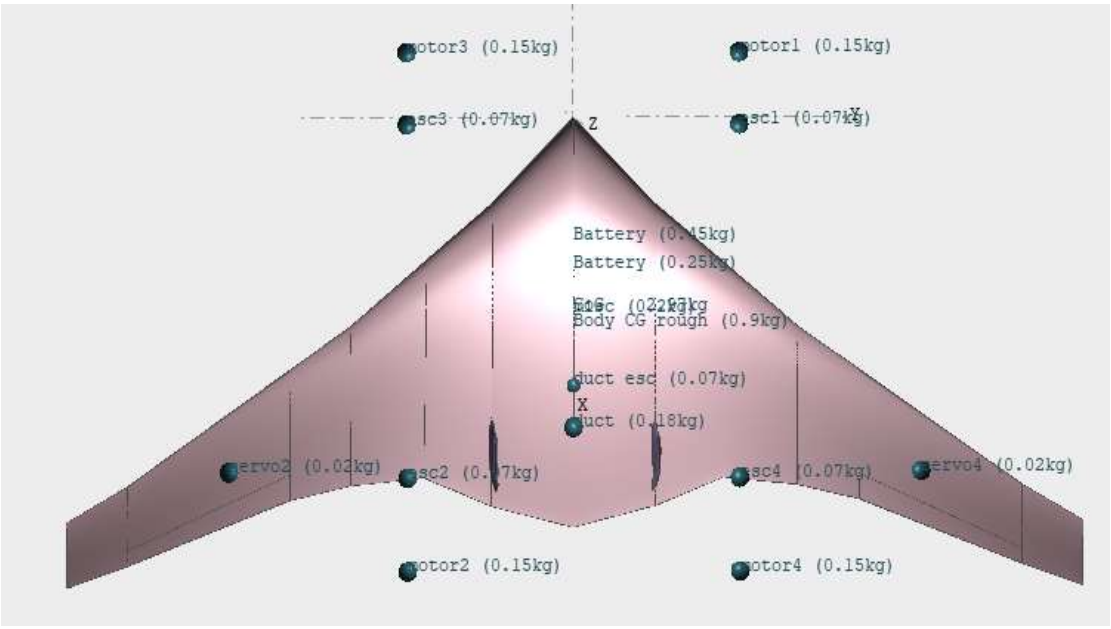

Fig 4. 10: *Mass distribution*

4.7. Propulsion System Specifications

One of the main factors that have the most impact on VTOL UAS design are the power requirements. Battery selection and, thus, take-off weight are substantially impacted

by power estimations. In addition, the VTOL UAS's flying time and range are enhanced by the reduced power requirement.

4.7.1. Propulsion System for Take-off and Landing Phase

For take-off and landing, we preferred propellers for propulsion. We will be using four brushless motors for take-off and landing phase. For vertical take-off and landing, the required thrust must be greater than the weight of aircraft. Since we do not have any type of take-off constraints to be fulfilled and also do not have any type of acrobatic maneuver to be performed, the vertical thrust just greater than weight will work fine for our requirement. So, the thrust-to-weight ratio of somewhere around 1.5 will be ideal for us.

$$\frac{T}{W} = 1.5$$

$$\therefore T = 4.5 \text{ kg}$$

This means, a thrust of 1125 gm per motor is the requirement for us in order to have smooth vertical take-off and landing.

We were provided Motor of 1000 KV rating. The motor specification manual suggests that using propeller of diameter 10*4.5 inch can provide about 2200 gm thrust. So, we decided to use 1000 kV motor with 10*4.5 inch propeller.

4.7.2. Propulsion for Cruise

For cruise, we decided to use Electronic Ducted Fan (EDF). The thrust required for cruise can be estimated from the lift-to-drag ratio at cruise angle of attack and can be calculated as:

$$\frac{T}{W} = \frac{1}{L/D_{cruise}} = \frac{1}{16} = 0.0625$$

$$T = 0.2 \text{ kg}$$

For safety margin, we considered the required thrust as 0.5 kg.

Here, is a plot of thrust vs velocity:

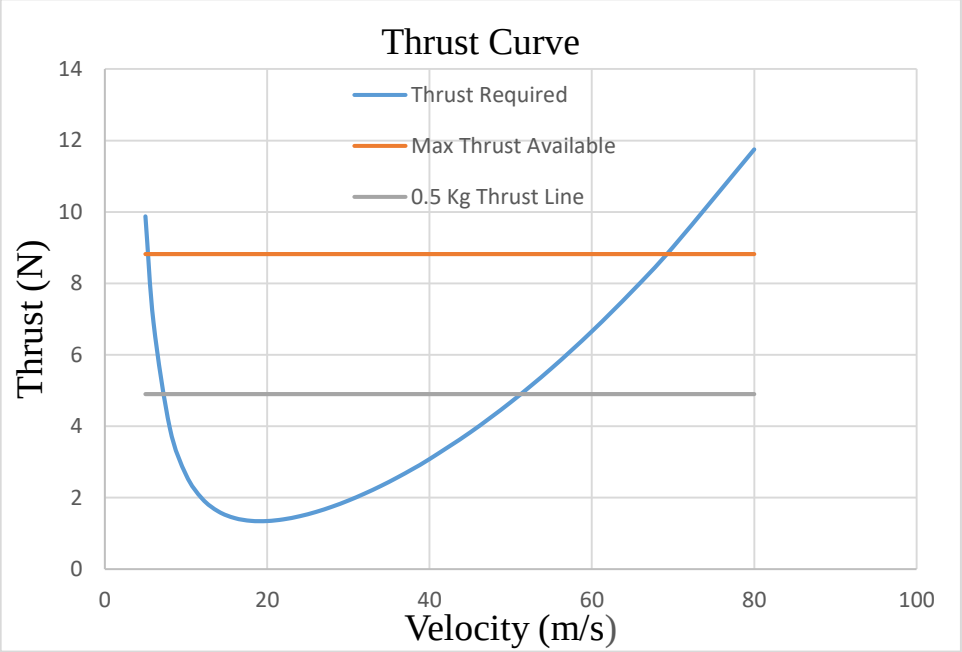

Fig 4. 11: Thrust vs velocity graph

There exist two equilibrium airspeeds for a given thrust setting:

- Low speed, high CL, high α
- High speed, low CL, low α

In our case, the two equilibrium airspeed for cruise thrust setting are 8 m/s and 50 m/s. Since our stall speed is 12 m/s, the lower equilibrium speed is lower than the stall speed. So, the lowest possible airspeed for our BWB is 12 m/s.

4.8. Detail Design

The configuration, layout, and size of the UAS have already been decided upon at this stage of the design process through the Conceptual Designing and Preliminary Designing processes. The process of creating actual parts that will be manufactured and put together to form the actual aircraft body is known as detail design. Every component that will be integrated into the aircraft body during this design phase must have exact calculated dimensions that take into account manufacturing viability and the availability of the material of choice. The detail design process is where the

intricate structural and system pieces have to be designed, down to the smallest of connections and assembly requirements.

The structural component of the airplane is the first thing to be designed. Since we selected a blended wing body aircraft, obtaining the necessary wing form is our main concern. The materials chosen for manufacture are 3mm plywood for the ribs, foam for the central body and wing structure, and aluminum rods for the spars and other structural integration components because we are developing and constructing this model for experimental project work.

The method of detail designing involved initially designing the ribs, followed by the placement of the spars and the central body structure, system components, and assembly parts. CATIA V5 was used for the design work for the detain design of blended wing body aircraft.

4.8.1 Final Design Specifications

The final sizing and structure of BWB was determined from the aerodynamic analysis in XFLR5. The following specifications were obtained in order to go on to the manufacturing design on the basis of the necessary data from XFLR5.

4.8.1.1 Main Body Wing Specifications:

Table 4. 9: Main body wing specification

Lateral Location mm	Airfoil	Chord Length mm	Twist degree	Leading Edge Sweep (Longitudinal Offset) mm	Dihedral (3^0) (Vertical Offset) mm
0	MH78	570	3	0	0
120	MH78	420	3	120	6.34
220	MH78	300	3	200	11.728
330	MH80	220	0	290	17.434
420	S5010	180	-3	350	22.19
660	S5010	110	-3	510	34.87
750	S5010	90	-3	560	39.306

4.8.1.2 Fin Specifications

Table 4. 10: Main fin specification

Vertical Location mm	Airfoil	Chord Length mm	Leading Edge Sweep (Offset) mm
0	NACA0012	100	0
120	NACA0012	70	18

On the basis of these specifications the initial planform of the BWB was designed in CATIA V5.

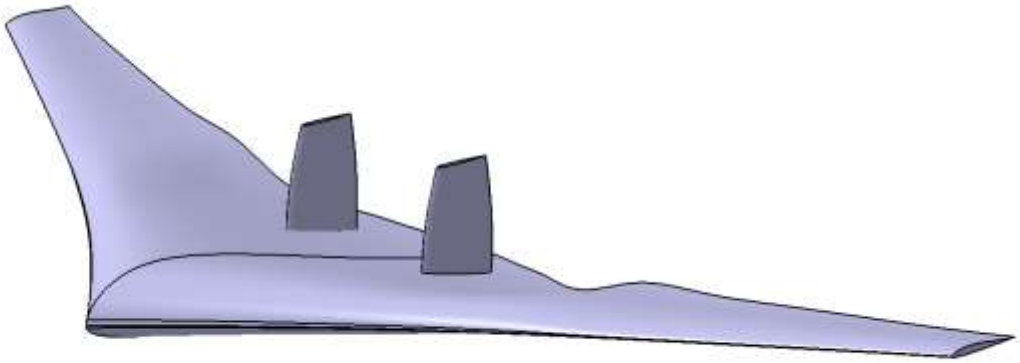

Fig 4. 12: Planform of BWB in CATIA

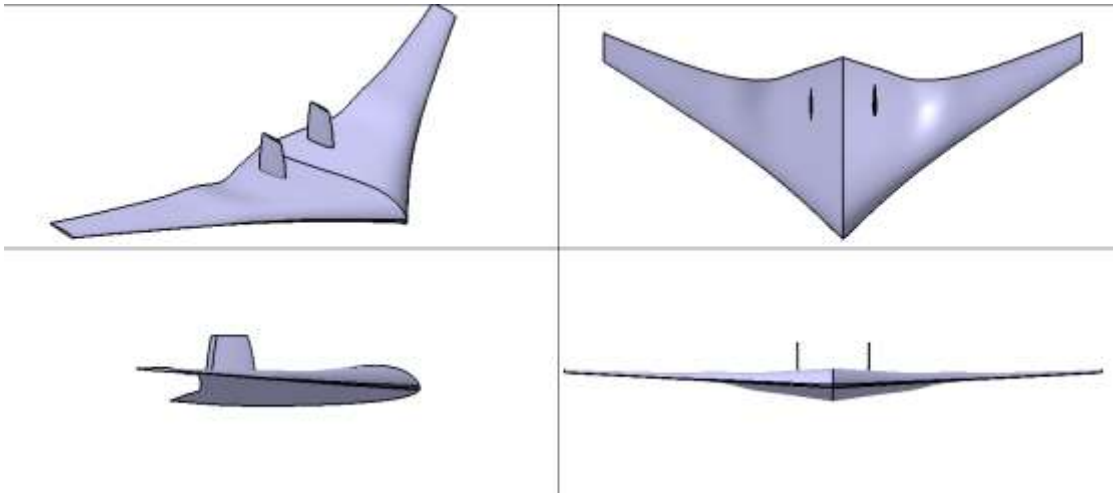

Fig 4. 13: 3D-View of BWB in CATIA

Studying the shape of the structure and materials that could be used for manufacturing the structural components to be included was decided. Then the structural component that can be integrated to form the aircraft structure were proceeded for manufacturing design.

4.8.2. Components Design

The structural components to be designed were categorized in ribs, spars, structural support, central body structure, Propulsion system components and electronic components.

4.8.2.1. Ribs

It is necessary to first collect the crucial airfoil coordinates in order to create the genuine solid 3D body of the rib in CATIA. The chord length and pitch angle inputs were used in the airfoil plotter to generate the coordinates of MH78, MH80, and S5010 in order to obtain the data points for the essential airfoils.

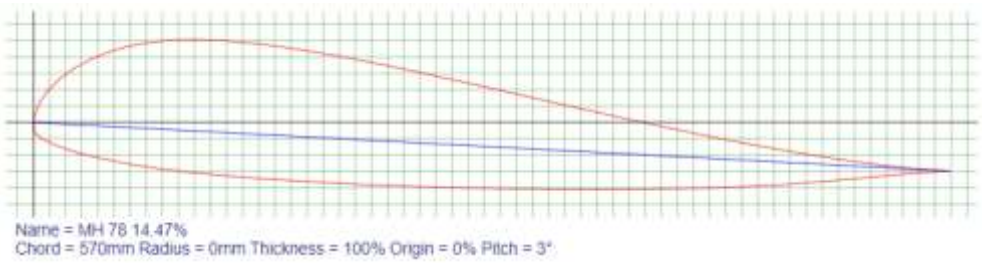

Fig 4. 14: MH 78 14.47% airfoil

After obtaining the airfoil coordinates, GSD Micro was used to retrieve the data points for the airfoils in the CATIA part design, which, when projected, revealed the airfoil curve. The sweep and dihedral were preserved for each section using the Generative Shape Design workbench. Finally, the desired placements and required dimensions of the ribs were acquired.

Each airfoil's offset dimensions in the lateral and vertical axes were determined from the sweep and dihedral. Then cuts for structural components at the bottom were created, along with spar holes at 25% of the chord for the entire span and spar holes at 50% of the chord for the main body.

Fig 4. 15: Rib alignment in CATIA

Numerous cuts were made in the ribs to lessen the weight because it is always necessary to lower the weight of structural components as much as possible when constructing an aircraft for light weight criteria.

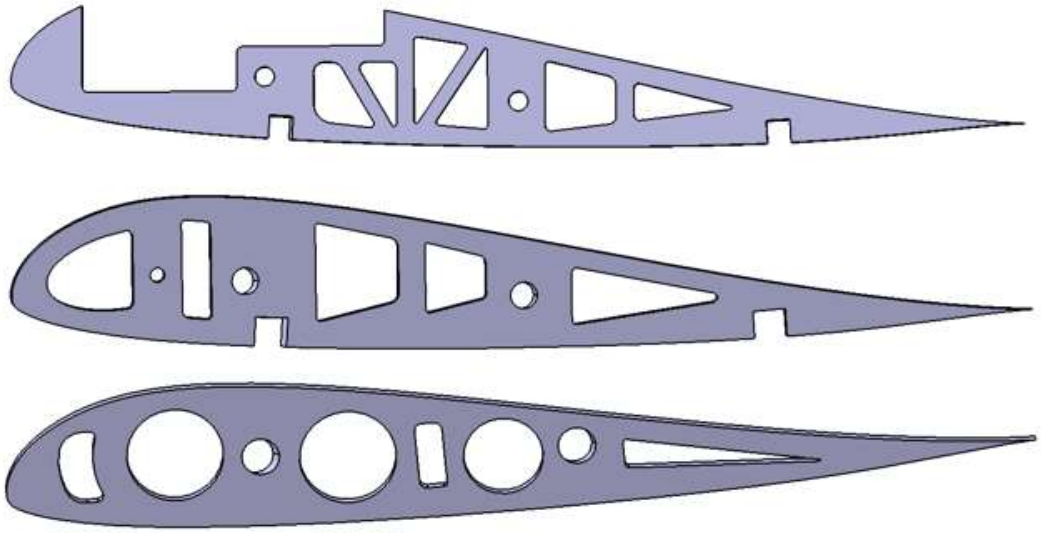

Fig 4. 16: Rib design in CATIA

The revised rib design was now prepared for CNC laser cutting. The CAD drawing .dxf file was imported into RD Works before being sent to the CNC machine.

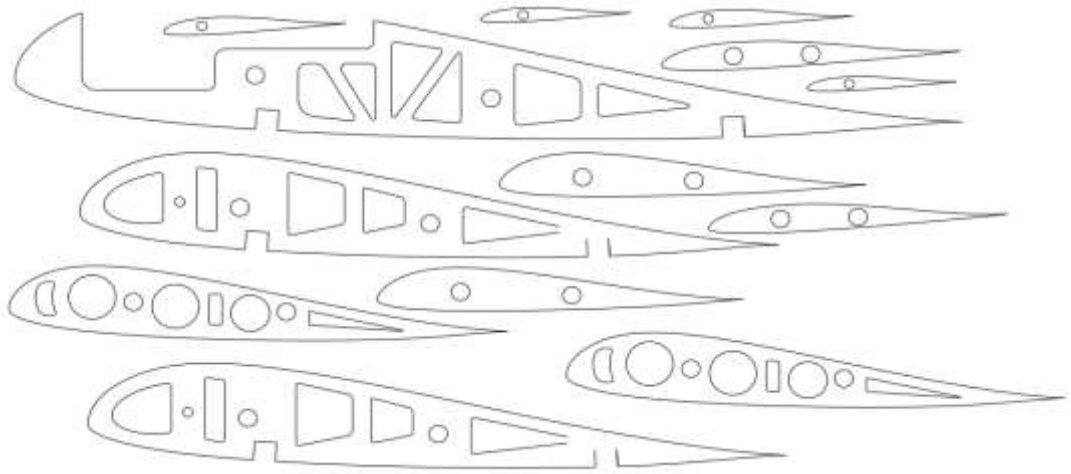

Fig 4. 17: 2D- Drawing for CNC LASER cutter

4.8.2.2. Spars and Structural support

The spar of aluminum rod with outer diameter 9mm thickness 1mm was in main body at the locations of 25% chord and 50% chord up to just before the section of wing where ailerons starts. And considering the thickness of tip airfoil thickness 6mm spar were used afterwards at 25% chord of each wing segment. For supporting the body structure itself and propulsion system integration a pentagon structure was designed on the bottom center of body that was extended forward and afterward to integrate four motor propeller system for the purpose of vertical takeoff and landing.

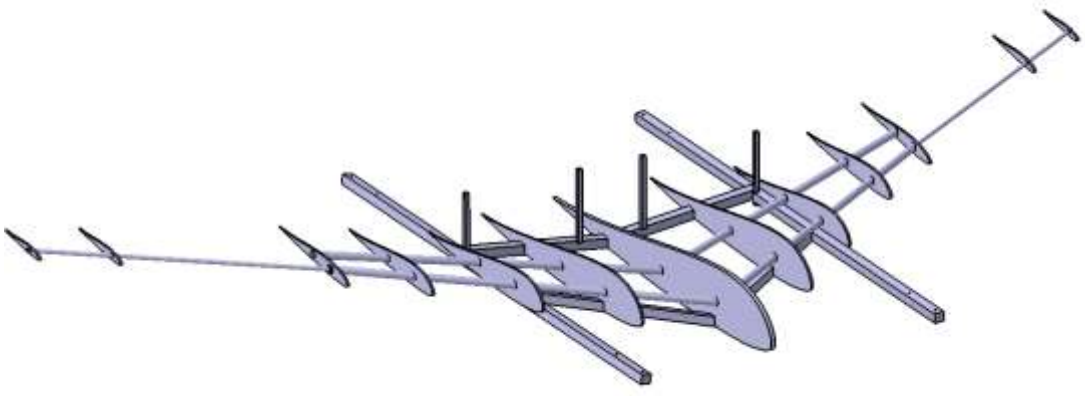

Fig 4. 18 : Internal structure of BWB in CATIA

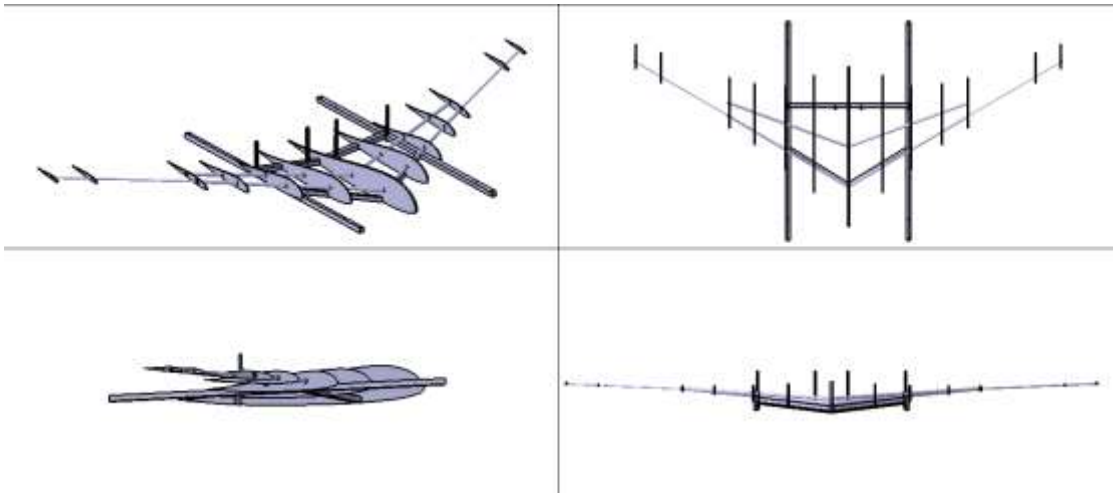

Fig 4. 19: 3D- View of internal structure

The structural support is made with 13mm Aluminum C Channels joined together using Aluminum plate in the form of lap joint using rivet as shown in figure below.

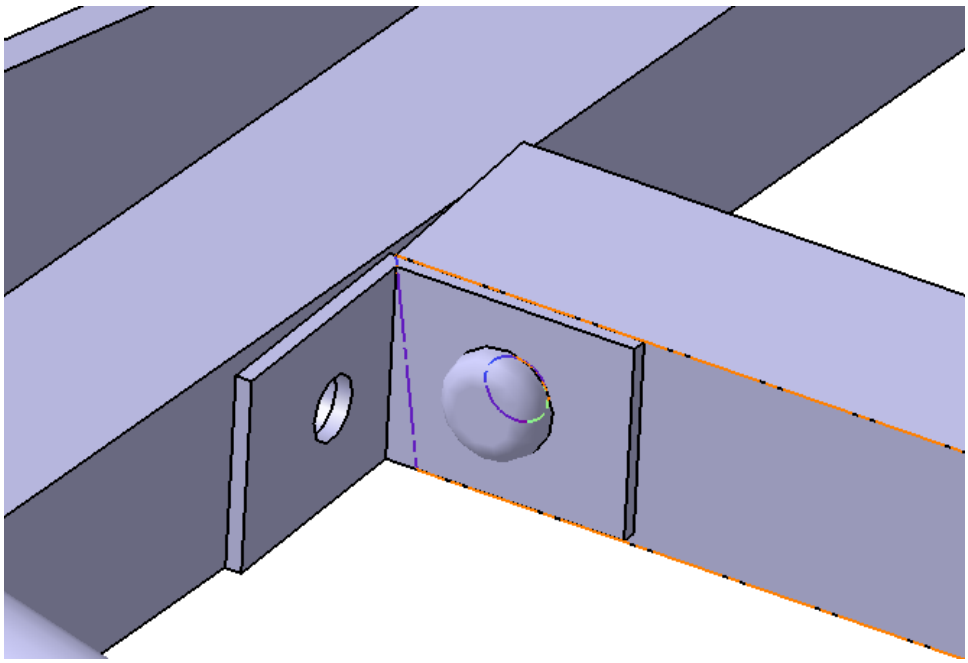

Fig 4. 20: Joint at rectangular spar

4.8.2.3. Centre Body Structure:

Since the body structure has varying twist angle from root to tip as well as change in sweep angle between central body and wing portion, the body should be made in parts. Beside that three different airfoils were blended to form the structure so the ribs were

placed exactly at the locations were twist and airfoil changed. Hence to include ribs in the structure, the central foam body part is to be made piece wise. Along with that to add ailerons and flaps/elevators the cutouts in foam block is made. From the calculations, the aileron of size 20% of chord length extending from 420mm to 660mm lateral distance. Similarly, the flaps of 15% of chord length were added from center to 120mm lateral distance on both sides. With this, the part wise design of central body portion was completed.

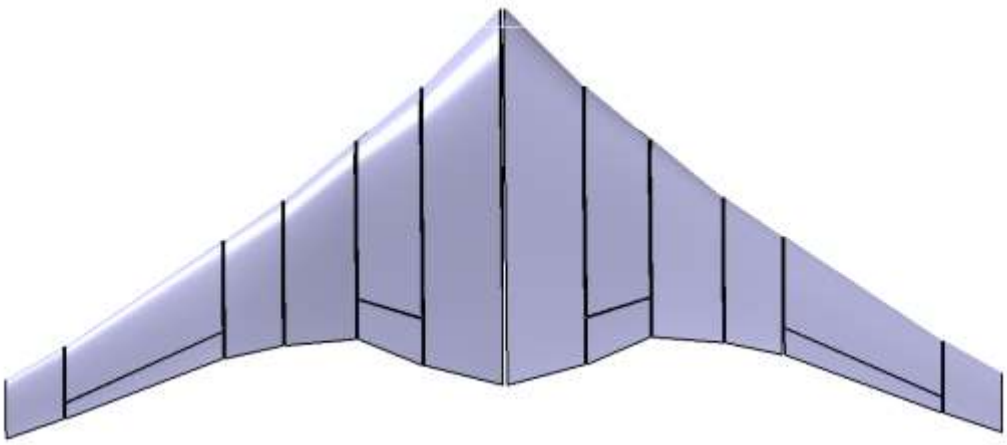

Fig 4. 21: Top view after addition of control surface

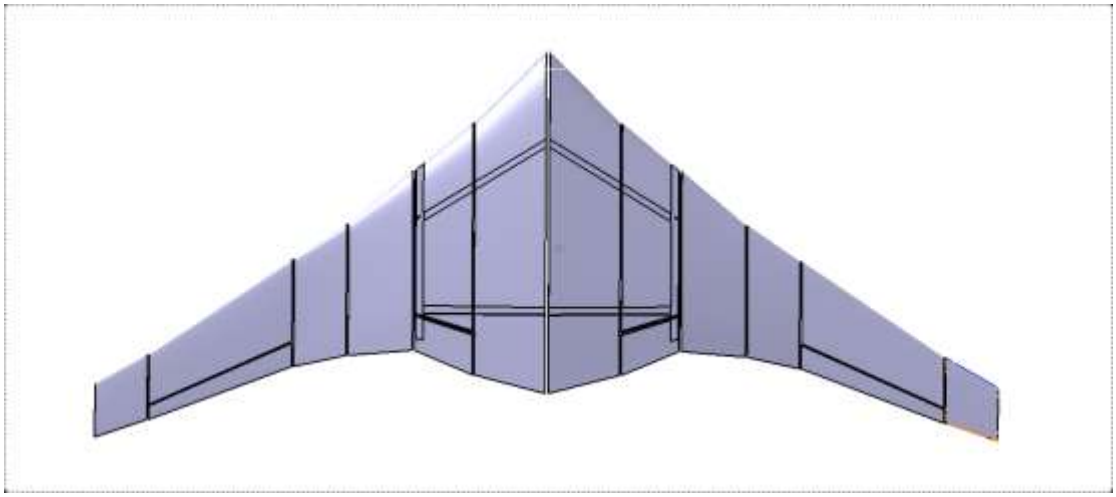

Fig 4. 22: Bottom view after addition of control surface

4.8.2.4. Propulsion System:

The selection of propulsion system was based on the thrust requirement and weight criteria for both VTOL and cruise. Since for VTOL more thrust is required to lift the aircraft straight upward and the thrust should be balanced both laterally and longitudinally, four propellers of 7inch diameter and 5inch pitch was chosen for the purpose.

As it will be of no use to just increase such huge amount of weight by integrating four ducted fan even though they generate huge amount of thrust compared to propellers. Whereas for the purpose of cruise flight ducted fan is used as a single ducted fan is sufficient to take the weight and drag during the flight and is best suited for positioning above the body of the aircraft a bit beyond the cg of aircraft in longitudinal direction.

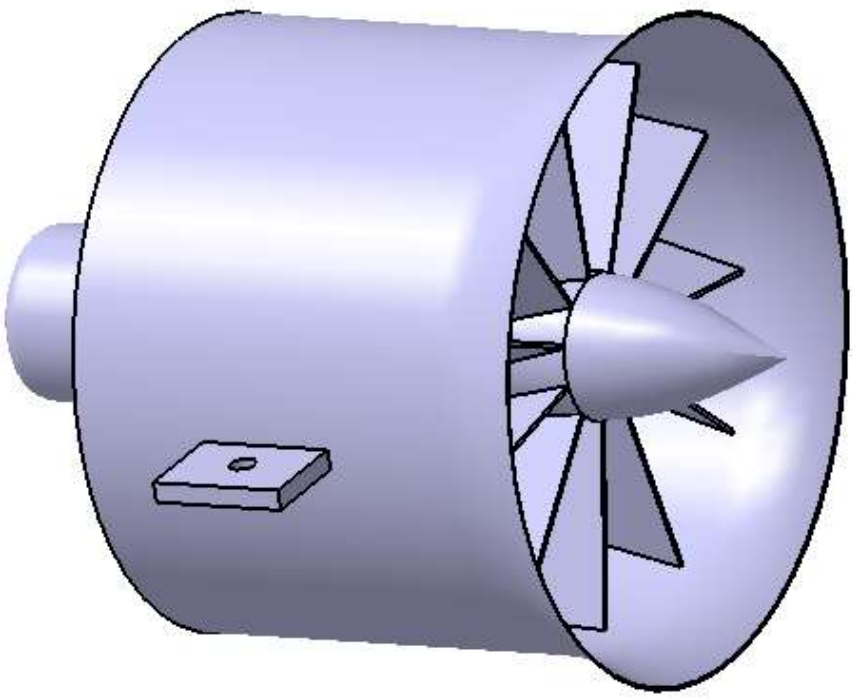

Fig 4. 23: Duct fan

Fig 4. 24: Propeller Blade

4.9. Assembly Design

After all the components were designed with the calculated dimensions, each component is assembled together in CATIA Assembly Design Workbench using the concentric, offset and surface contact features. To provide the necessary width for the engine's four-sided support, the motor and propeller were installed over the enlarged frame using a motor mount. The complete assembled design along with assembled design with material added for each component are shown below.

Fig 4. 25: Final assembly design of BWB in CATIA

4.10. Material and Structure

Structures and Materials, a crucial step in the design process, addresses the strength of the airplane and the materials that will be utilized to construct it. Particularly in our situation, it is crucial for our BWB to be as light as feasible. A lighter aircraft can travel farther since its engines don't have to work as hard. So, for the wing section, low-dense

Styrofoam is used and for the structure, aluminum rods of circular and three faced cross section are used.

4.11. Fabrication:

4.11.1. Center Body Structure

We started our fabrication process by building the center body structure. We constructed a pentagon shaped structure for our center body. It forms the foundation for the entirety of our production process. We connected them with rivets and 13mm*13mm three-faced aluminum rod.

Fig 4. 26: Center body structure

4.11.2. Ribs

Ribs are the lateral structural components of wing that shapes the wing and provides it required aerodynamic curvature. We inserted ribs at various span wise locations to aid in the joining of the foam cores to the main spar and to have a hole that is a push-fit to the main wing spar. Since we have number of individual wing sections to be joined

together, ribs provide large attachment area to assist bonding the wing sections together. We used a 4 mm thick ply and the CNC laser cutter to cut required ribs for our BWB.

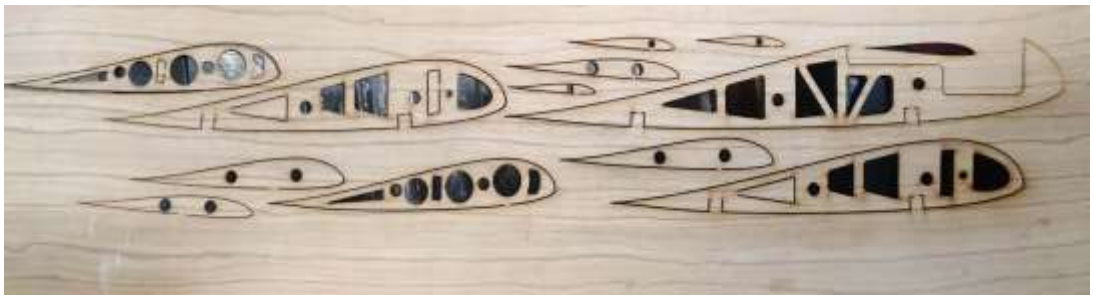

Fig 4. 27: CNC LASER cutting of ribs

4.11.2. Spars

The spar, which typically runs span wise in a fixed-wing aircraft, is the primary structural part of the wing. It supports the weight of the wings and flying loads and helps to transfer the aerodynamic loads to the center body. We generated a tubular opening in each wing sections and inserted the spars at desired locations. The spars we used were circular aluminum rods of different diameters. We used a 9mm diameter rod up to 0.42 m span wise location and a 6 mm diameter rod at the remaining location due to lesser thickness of wing section. For further strength and moment resistance, we used another spar up to 0.33 m span.

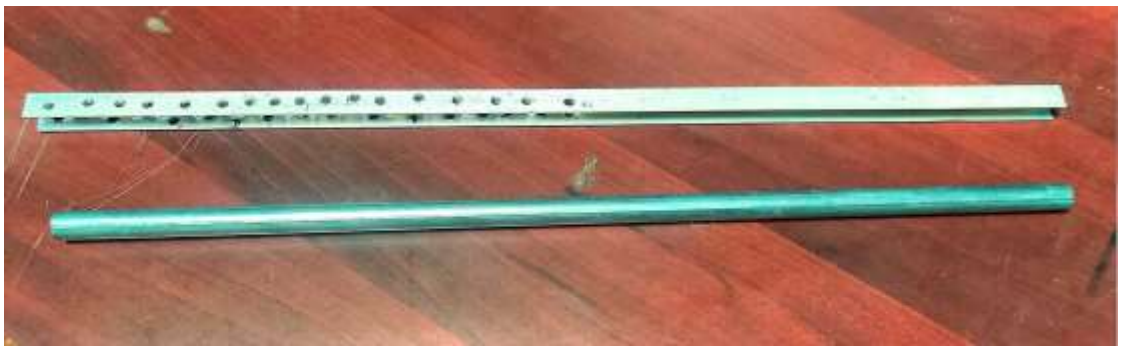

Fig 4. 28: Circular and C-section spars

4.11.3. Wing Sections

We had to divide our entire wing section into a number of parts and build each one separately because of diverse chord length, sweep, dihedral, variable geometric twist, as well as various airfoils at various locations along the span wise axis. Due to the

inability of the available CNC to accurately cut higher sweep wing portions, we manually cut all sections except the tip section.

4.11.4. Assembly

To begin the assembly process, we first attached the pentagon to the center wing sections by cutting a channel from lower side of wing at desired locations and used hot glue gun to join them together tightly. Then two spars were inserted at their respective locations and glued. The remaining process was then quite simple. We continued inserting the ribs and remaining wing sections one after another till the final assembly is completed. Once the wing assembly is complete, the control surfaces were cut and taped together with the wing.

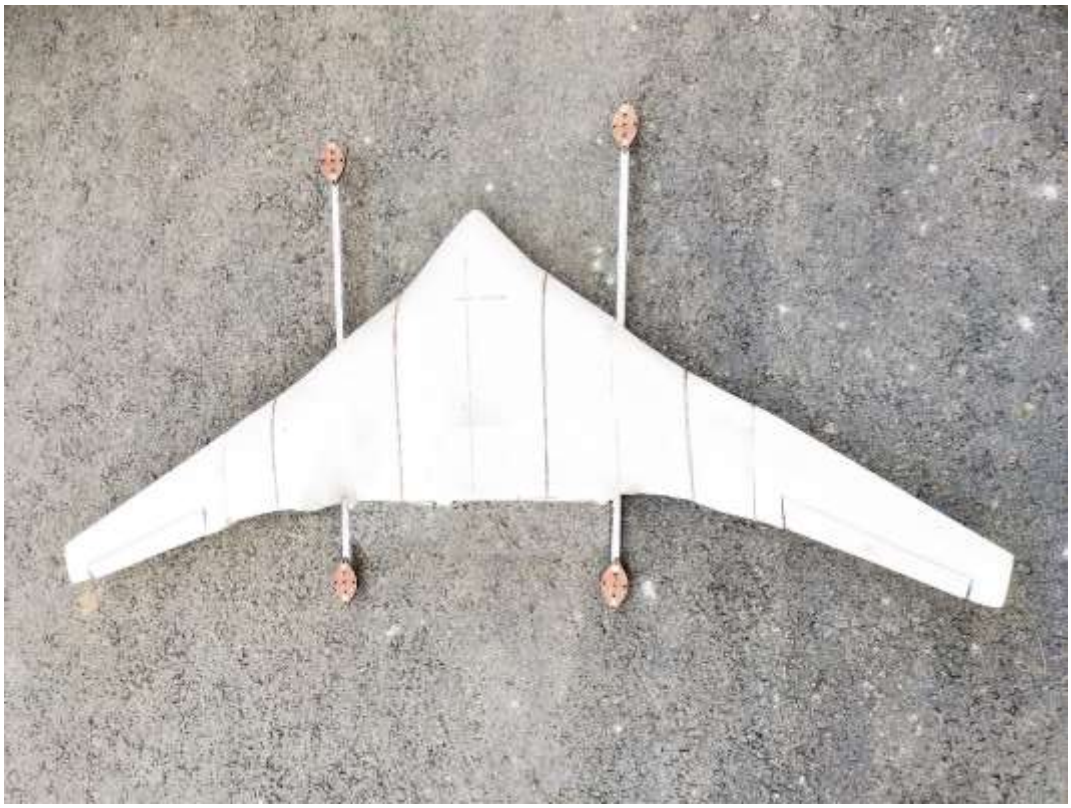

Fig 4. 29: Final assembly design

At this point, we started testing the individual electrical components like ducted fan and servos and began integrating each one of them into the airframe in their respective locations. This completes the overall assembly of our BWB.

4.12. Final Fabricated Model

After finishing the fabrication process and successfully deploying the control mechanism, we will perform test flights. If the test flight becomes successful, that will be the end of this project. If not, the entire process will be reviewed to identify what went wrong until a satisfactory test flight is obtained.

Fig 4. 30: Final fabricated design model

4.13. Electronic Components

In this study, no particular electronic design was implemented. The majority of electronic components, including the battery/charger, radio frequency modules, control module and motor are commercially available items. All the electronic components used in our system along with their respective ratings are presented below.

4.13.1. Motors and Propellers

The right selection of motor and propeller depends on the application of system. Since we want to fly high and the weight of our system is also relatively more, slightly large

propellers and motors capable of carrying such propellers are better choice for us. So, we selected 1000 KV motors with 10*4.5 propellers.

Thrust stand was used to measure the thrust of selected motor and propeller combination. The combination provided 2196 gm of maximum thrust with 4S battery which was sufficient for the vehicle.

Fig 4. 31: Measurement of thrust using thrust stand

4.13.2. Battery

The selected battery must be able to continuously provide sufficient current for sufficient period of time. The availability also needs to be considered. We initially selected 3S battery as per the battery manual but the motors were facing problem while operating. The battery was solved once 4S battery was used. So, we opted 4S battery of 5200 mAh.

4.13.3. ESC

The current rating is the most vital parameter to be considered while selecting an ESC. The maximum current which motor can draw as per the manual was 40A. so, 50A ESC for four quad motors and 60A ESC for ducted fan were selected.

4.13.4. Flight Controller

A flight controller is simply a circuit board with sensors that can recognize user commands and with this information, all the motors and actuators move accordingly. We used Pixhawk PX4 flight controller for our system because of its reliability and versatility.

4.13.5. Others

We used PM07 as our power management board and telemetry to communicate our ground control station with Pixhawk. A GPS module was used with Pixhawk for accurate positioning information and a receiver and transmitter was used for manual control as well as to trigger different flight modes.

4.13.6. Electronics Layout

The VTOL-electrical UAS's wiring diagram is shown in the diagram below. The Pixhawk Flight Control Unit is the system's brain. The PM board provides power to all four quad motors. The two servo's and signal wire of pusher motor were connected to the FMU PWM port and the signal wire of four quad motors were connected to the I/O PWM port in Px4. All the components were connected as shown in the figure.

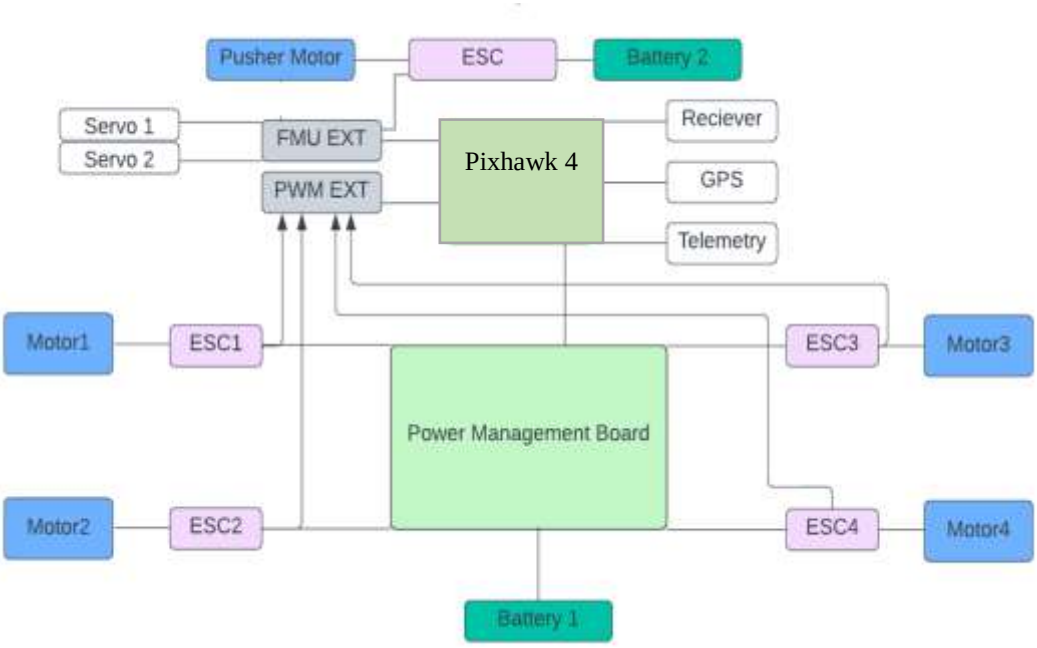

Fig 4. 31: Electronic Circuit Diagram

Fig 4. 32: Final model after installation of electronic components

4.14. System Setup for Testing

For testing, we divided our testing process into three divisions: pure fixed wing mode, pure quad mode and VTOL hybrid mode. The vehicle setup for each testing are presented below:

4.14.1. System Setup for Fixed Wing Mode Testing

QgroundControl is used as ground control station for pure fixed wing mode testing. The latest version of Pixhawk firmware from Qgroundcontrol in Pixhawk was installed. The selected system configuration was Generic Flying Wing. Once calibrating all the sensors and setting up all the required parameters, mission that included five waypoints was setup. The flying altitude and flying velocity were 10 m and 15 m/s respectively. The vehicle was launched by hand and it worked quite satisfactorily in the fixed wing mode.

4.14.2. System Setup for Quad Mode

For quad mode, the selected system configuration was Generic Quadcopter. Same firmware which was used before for fixed wing mode testing was used. Set of missions were performed by varying velocity to ensure that the quad mode is working fine and to check the altitude variance due to the excessive drag of vehicle's surface area. The altitude of 10m was set constant at every waypoints and speed was varied mission-wise from 5m/s to 20 m/s.

4.14.3. System Setup for Hybrid VTOL Mode

Initially, Qgroundcontrol and the same firmware as used before, for hybrid mode testing was used. Vertical Technologies Deltaquad as our system configuration was selected. All the MAIN and AUX ports were connected as mentioned in the Pixhawk documentation. A transmitter switch was used to trigger the transition from quad mode to fixed wing mode. After setting up all the required parameters, ground testing to check the response of system was initiated. Everything else worked perfectly except the ducted fan. It wasn't receiving signal from Pixhawk and was not spinning even after triggering the transition switch. We checked the connection multiple times and even modified the connection slightly as per our own assumption but nothing really worked. We also assigned a very low transition speed of 1 m/s and manually provided it that velocity assuming that it may not supply signal to the pusher motor unless the transition speed is obtained. This also couldn't solve the problem and we shifted towards Mission Planner as our ground control station.

We installed Arduplane firmware from Mission Planner in Pixhawk and selected Pixhawk as our platform. Since there aren't any VTOL options in Mission Planner so we first selected Arduplane as our firmware and then we started adding VTOL elements on top of it. We first enabled the quad feature in our system by setting the Q_ENABLE parameter to 1. It introduces changes in the firmware that allows all the VTOL features to be integrated into it. All the Q parameters starts appearing after enabling the Q_ENABLE parameter.

4.14.3.1. Plane Parameter Setup

- ARSPD_FBW_MIN is the minimum airspeed parameter. We set the value of minimum cruise speed i.e. 14 m/s for the plane.

- ARSPD_FBW_MAX is the maximum airspeed parameter. We set this to the value of maximum cruise speed i.e. 25 m/s for the plane.
- TRIM_ARSPD_CM is the cruise airspeed parameter. We set this to the value of intended cruise speed i.e. 20 m/s for the plane.

Parameters	**Value**
ARSPD_FBW_MIN	14 m/s
ARSPD_FBW_MAX	25 m/s
TRIM_ARSPD_CM	20 m/s

4.14.3.2. VTOL Setup

Frame Setup

We set up the frame for quadplane by first setting the frame class as Quad and then setting the frame type to H frame as per our final design. For this, the Q_FRAME_CLASS value was set as 1 and Q_FRAME_TYPE was set as 3.

Motor Ordering

The motor output channel can be set in SERVOX_FUNCTION for motors 1, 2, 3 & 4. The output channels for four motors were set as SERVO 9, 10, 11 and 12 respectively. The FMU PWM OUT port was used to provide signal to the quad motors.

Servo Ordering

We set the output channels for control surface servo and pusher motor as SERVO 1, 2 and 3 respectively. The I/O PWM OUT port was used to provide signal to the control surface servos and pusher motor.

Quad Setup

Since we don't have any kind of vertical takeoff and landing constraints, we tried to keep those values as less possible to ensure a smooth vertical flight. Keeping that in mind, we set both the takeoff and landing speed as 1 m/s.

Throttle Setup

The throttle parameters along with their corresponding assigned values are presented below:

Cruise = 100 %

Min = 0 %

Max = 100%

Slew Rate = 40%

The cruise throttle was set at its maximum value. The slew rate was set as 40% which suggests that the throttle will ramp up at a rate of 40% per second.

Transition Parameters Setup

The key transition parameters that were set are given below:

- ARSPD_FBW MIN: The quad motors will continue to supply lift and stability until this speed is reached even after transitioning to fixed wing mode.
- Q_TRANSITION MS: Once the ARSPD_FBW_MIN airspeed is reached, the quad motors will slowly drop in power over this period of time.
- Q_ASSIST_SPEED: Quad motors will provide assistance if the airspeed of the quadplane is below this value.
- Q_ASSIST_ANGLE: If there is attitude error, quad motors will provide assistance if the error is greater than this value.
- Q_ASSIST_ALT: Quad motors will support if the aircraft drops below this altitude.
- Q_ASSIST_DELAY: It represents the time delay between the assistance threshold triggered and assistance activation.

The corresponding values of these parameters are presented below:

Parameters	**Value**
ARSPD_FBW_MIN	14 m/s
Q_TRANSITION_MS	5000 ms
Q_ASSIST_SPEED	14 m/s

Q_ASSIST_ANGLE	30°
Q_ASSIST_ALT	5m
Q_ASSIST_DELAY	0.5 sec

Once the parameter setup was completed, we started the test flight and performed few fully autonomous missions.

CHAPTER FIVE: RESULT AND DISCUSSION

An aircraft's stability, controllability, and flying characteristics are examined as part of the performance and stability analysis, which also determines if the aircraft is capable of carrying out the intended mission. The static margin and trim parameters of the aircraft are evaluated using the stability analysis used in this study. On the other side, point and mission performance are included in the performance analysis. The point per-performance evaluates the aircraft's capacity to carry out necessary maneuvers while carrying out its task.

5.1. Aerodynamic Performance

It is vital to explore an aircraft’s aerodynamic performance across its entire flight envelope. To develop a better design, different sets of parameters should be thoroughly investigated throughout the design process. We performed the performance analysis of our BWB using XFLR5. The analysis setup was defined as below:

Table 5. 1: Analysis definition in XFLR5

Polar Type	Fixed Speed
Velocity	25 m/s
Analysis Method	Ring Vortex (VLM2)
Viscous Effect	Enabled

The Coefficient of lift relates the lifting force generated by the aircraft when flown at certain velocity. The above CL vs Alpha graph shows that the maximum lift coefficient of our BWB is 1.1 and the minimum Cd is about 0.01. The Cm vs Alpha graph indicates that the trim angle is 3.5 degree.

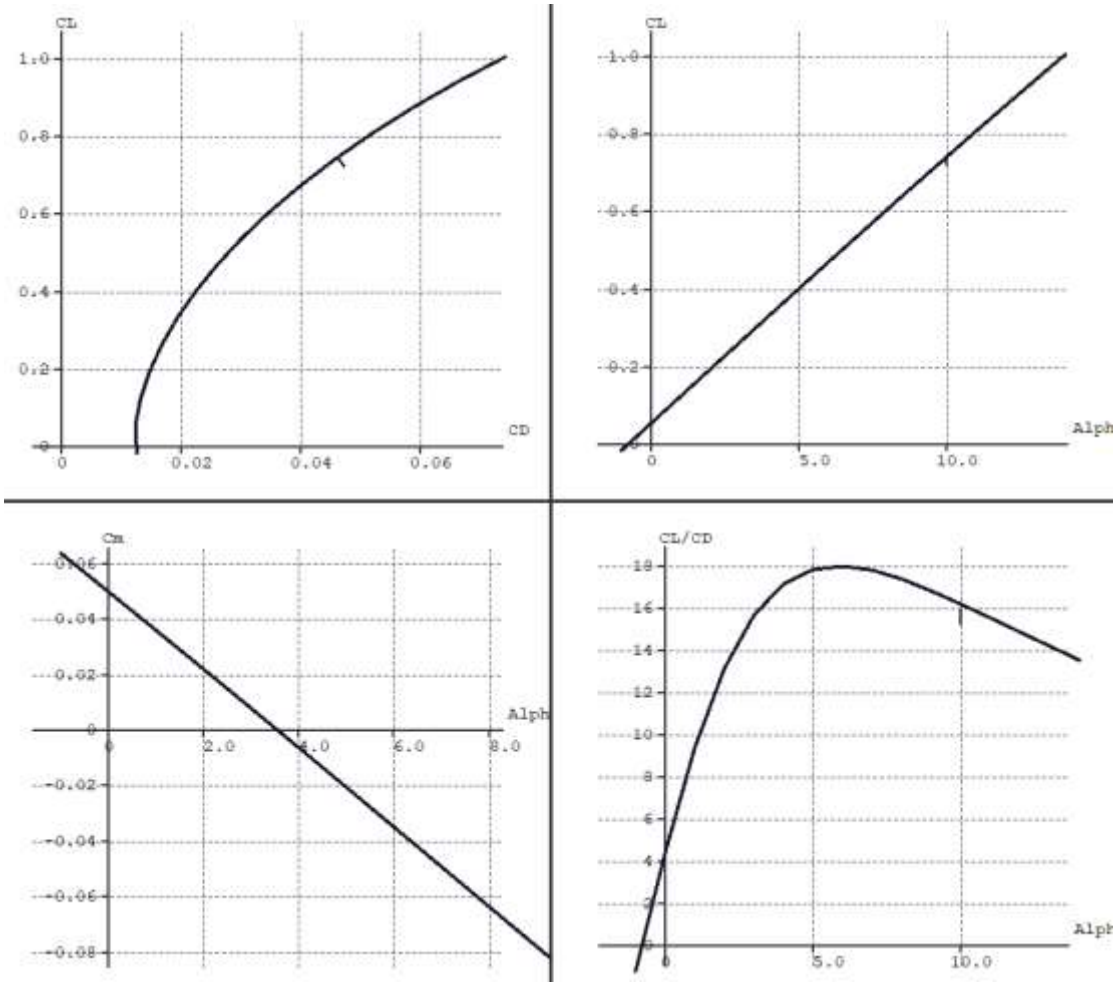

Figure 5. 1 : XFLR5 Performance Analysis

The (L/D) ratio of an aircraft is the measure used to describe the aerodynamic effectiveness of the aircraft. It is one of the key variables needed to estimate the flight performance of an aircraft. A greater L/D value indicates superior flying performance, which is frequently aimed for by aircraft designers for increased flight time, endurance, and power consumption efficiency. The maximum L/D ratio of our BWB is 17 at about 3.5 degree AOA which is trim angle. This indicates that our BWB is having L/D value closer to the maximum value when being flown at AOA equal to trim angle.

5.2. Static Stability

A plane's initial propensity to settle back into place after being disturbed indicates its static stability. As a result, the effort of the pilot is reduced and the aircraft can maintain consistent flight conditions and recover from disruptions. The Cm vs Alpha graph is a key indicator of aircraft's longitudinal static stability. As discussed in earlier sections,

for an aircraft to be statically stable, the Cm value at zero AOA must be positive and the slope of Cm vs Alpha curve should be negative.

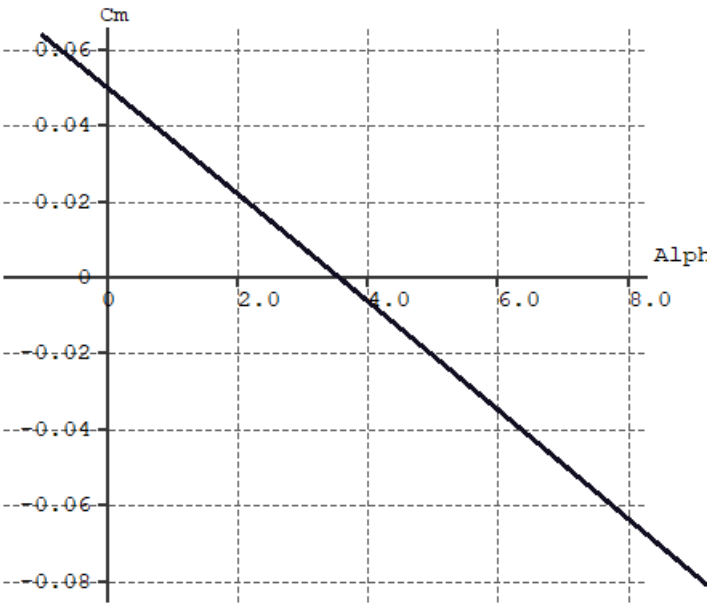

Figure 5. 2: Cm vs alpha curve

The above Cm vs Alpha curve verifies that our aircraft satisfies the above two conditions since the Cm value at zero AOA is around 0.05 and the plot also has negative slope. So, this indicates that our aircraft is statically longitudinal stable.

After the mass components such as ducted fan, motor, electronic speed controller (ESC), battery, etc. were placed at their estimated places, the computed location of the C. G. was discovered to lay at 0.27m, and the neutral point of the aircraft was discovered to be at 0.338m.

Since the mean aerodynamic chord is 0.323m, the static margin can be calculated as:

$$\text{Static Margin} = \frac{0.338-0.27}{0.323} * 100\%$$

$$= 21\%$$

The positive value of static margin also ensures the longitudinal static stability of our aircraft.

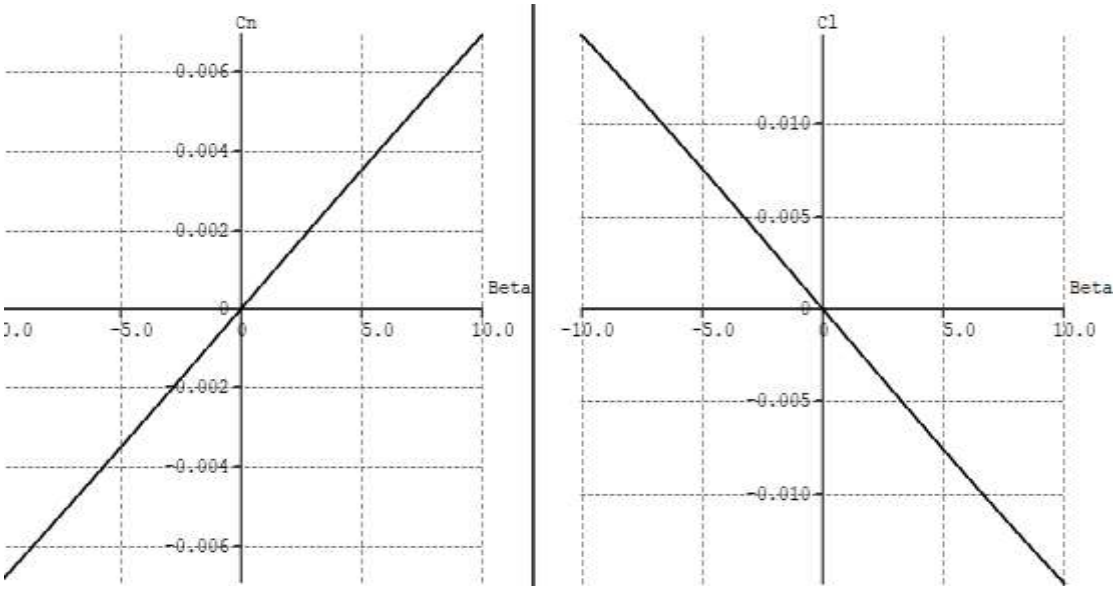

Fig 5. 1: Cn vs beta and Cl vs beta curve

Similarly, for directional static stability, the slope of graph between directional moment coefficient (C_n) and sideslip angle (Beta) should be positive and for lateral static stability, the slope of graph between lateral moment coefficient (C_l) and sideslip angle (Beta) should be negative. Above graphs validate both these conditions which ensures that the aircraft is both laterally and directionally stable.

5.3. Dynamic Stability

5.3.1. Control Derivatives

Control derivatives are a critical component of dynamic analysis in aircraft design and flight dynamics. They describe the relationship between the aircraft's control inputs, such as elevator deflection or aileron deflection, and the aircraft's response to these inputs.

In aircraft dynamics, control derivatives are used to determine the aircraft's response to changes in control inputs, such as changes in elevator deflection or aileron deflection. These derivatives are used to determine the aircraft's stability and control characteristics, such as stability margins, control effectiveness, and maneuverability.

Control derivatives are typically calculated using mathematical models of the aircraft, such as a transfer function or a state-space representation. The models are used to

predict the aircraft's response to changes in control inputs, and the results are used to determine the aircraft's control derivatives.

Following are the longitudinal and lateral derivatives value obtained from XFLR5 stability analysis.

Table 5. 2 : Longitudinal and lateral control derivatives

Control Derivatives			
Longitudinal Derivatives		**Lateral Derivatives**	
Xu= -0.1481	Cxu=-0.0362	Yv= -0.52361	CYb= -0.1282
Xw= 0.6734	Cxa= 0.1650	Yp= -0.11692	CYp= -0.0382
Zu= -2.6781	Czu= 0.0099	Yr= 0.13261	CYr= 0.04337
Zw= -16.1550	Cla= 3.9582	Lv= -0.41526	Clb= -0.06790
Zq= -3.0704	CLq= 4.6644	Lp= -1.5800	Clp= -0.3449
Mu= -0.0009	Cmu= -0.0007	Lr= 0.25818	Clr= 0.056356
Mw= -0.9802	Cma= -0.7446	Nv= 0.09361	Cnb= 0.01530
Mq= -0.4063	Cmq= -1.9135	Np= -0.1538	Cnp= -0.0335
		Nr= -0.00856	Cnr= -0.00187

For longitudinal dynamic stability:

MwZw – ZuMu > 0

(-0.9802 * -16.1550) – (-2.6781* -0.0009) > 0

15.83269 > 0

This represents longitudinal dynamic stability.

5.3.2. Longitudinal State Matrix

The Longitudinal State Matrix in XFLR5 consists of state variables that describe the aircraft's motion in the longitudinal (pitch) axis. The matrix is comprised of the following values:

- Velocity: The velocity of the aircraft in the longitudinal axis.

- Attitude: The attitude of the aircraft in the longitudinal axis, which is the angle between the aircraft's longitudinal axis and the horizon.
- Altitude: The altitude of the aircraft in the longitudinal axis.
- Angular Velocity: The angular velocity of the aircraft in the longitudinal axis, which is the rate of change of the attitude.
- Acceleration: The acceleration of the aircraft in the longitudinal axis.

These values are used to calculate the aircraft's stability derivatives, which describe the aircraft's response to disturbances in the longitudinal axis. The stability derivatives are used to determine the aircraft's damping ratios, oscillation frequencies, and natural modes of motion. Longitudinal state matrix obtained from XFLR5 stability analysis:

$$\begin{bmatrix} -0.059615 & 0.271015 & 0 & -9.81 \\ -1.07767 & -6.50115 & 16.7008 & 0 \\ -0.0115189 & -13.2494 & -5.49144 & 0 \\ 0 & 0 & 1 & 0 \end{bmatrix}$$

5.3.3. Lateral State Matrix

Lateral state matrix is a mathematical representation of the aircraft's lateral (roll) motion. It is used in the dynamic stability analysis of an aircraft to determine the aircraft's response to lateral disturbances. The lateral state matrix is a square matrix that contains information about the aircraft's lateral motion. It includes the aircraft's lateral state variables, such as roll angle, roll rate, and yaw rate, and the relationships between these variables. The lateral state matrix is used to determine the aircraft's dynamic response to lateral disturbances, such as gusts or turbulence, and to evaluate the aircraft's lateral stability.

In XFLR5, the lateral state matrix is used to perform a linear stability analysis of the aircraft's lateral motion. This involves using the aircraft's mathematical model to calculate the lateral stability derivatives and determine the aircraft's response to lateral

disturbances. The results of the lateral stability analysis are used to determine the aircraft's lateral stability characteristics and to design the aircraft's lateral control systems. Lateral state matrix obtained from XFLR5 stability analysis:

$$\begin{bmatrix} -0.210707 & -0.04705 & -17.883 & 9.81 \\ -8.61009 & -32.3327 & 5.31148 & 0 \\ 1.11762 & 0.0601708 & -0.286928 & 0 \\ 0 & 1 & 0 & \end{bmatrix}$$

5.3.4. Eigen Value and Eigen Vector for Different Mode:

Eigen values and Eigen vectors are mathematical concepts that are used in the dynamic stability analysis of an aircraft. They provide important information about the stability and motion of the aircraft.

Eigen values are scalar values that are used to characterize the behavior of a system. In the context of aircraft stability analysis, Eigen values represent the natural frequencies of the aircraft's motion. These frequencies determine the rate at which the aircraft will oscillate in response to disturbances. Positive Eigen values indicate a stable system, while negative Eigen values indicate an unstable system.

Eigen vectors, on the other hand, are vectors that are used to characterize the direction of the motion. In the context of aircraft stability analysis, Eigen vectors represent the aircraft's natural modes of motion. These modes of motion determine the direction in which the aircraft will oscillate in response to disturbances. The information provided by Eigen values and Eigen vectors is used to determine the aircraft's dynamic stability characteristics.

For Longitudinal Mode:

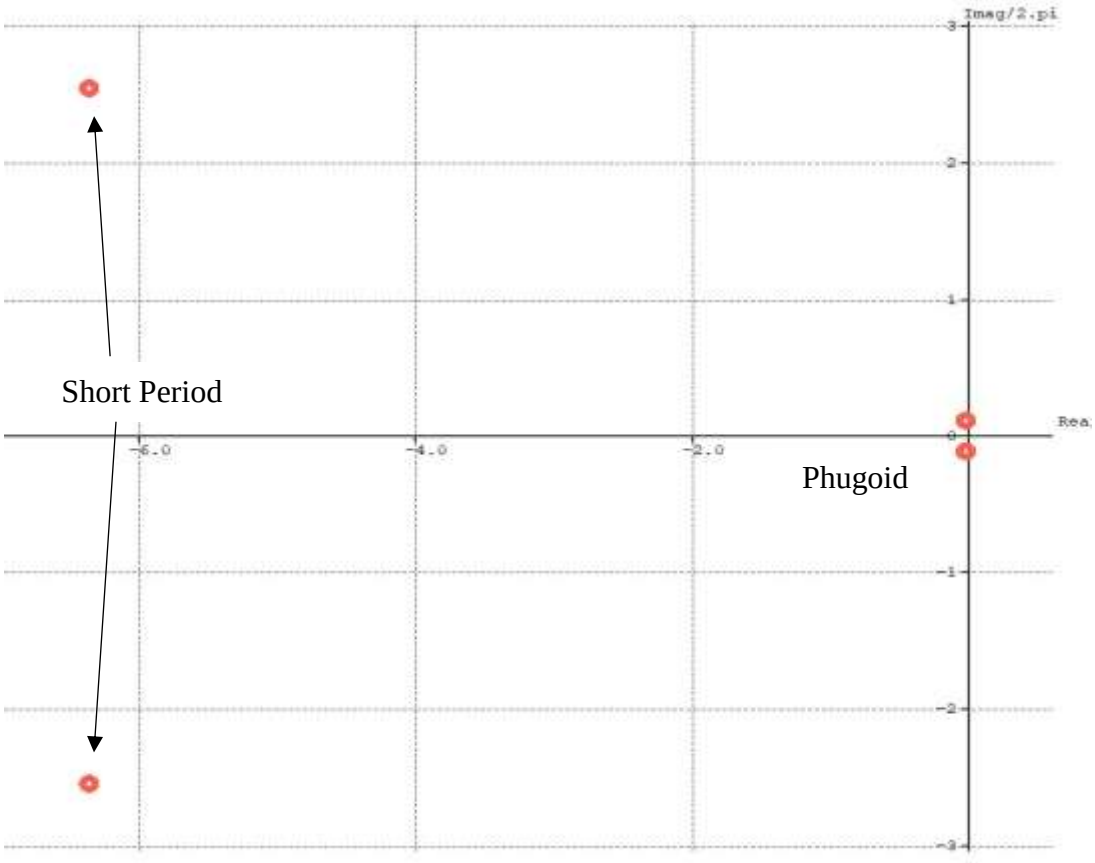

Fig 5. 2: Root locus graph for longitudinal mode

Table 5. 3: Eigen value and Eigen vector value for longitudinal mode

Mode	**Short Period**	**Short Period**	**Long Period**	**Long Period**
Eigen Value	-6.006+-14.86i	-6.006+ 14.86i	-0.021+-0.737i	-0.021+ 0.737i
Eigen Vector	1+ 0i 46.11+ 20.43i 19.61+-40.43i 1.88+ 2.079i	1+ 0i 46.11+-20.43i 19.61+ 40.43i 1.88+ -2.079i	1+ 0i -0.024+0.002i 0.0554+0.002i -0.005+0.075i	1+ 0i -0.024+-0.003i 0.056+-0.002i -0.0047+-0.08i

For Lateral Mode:

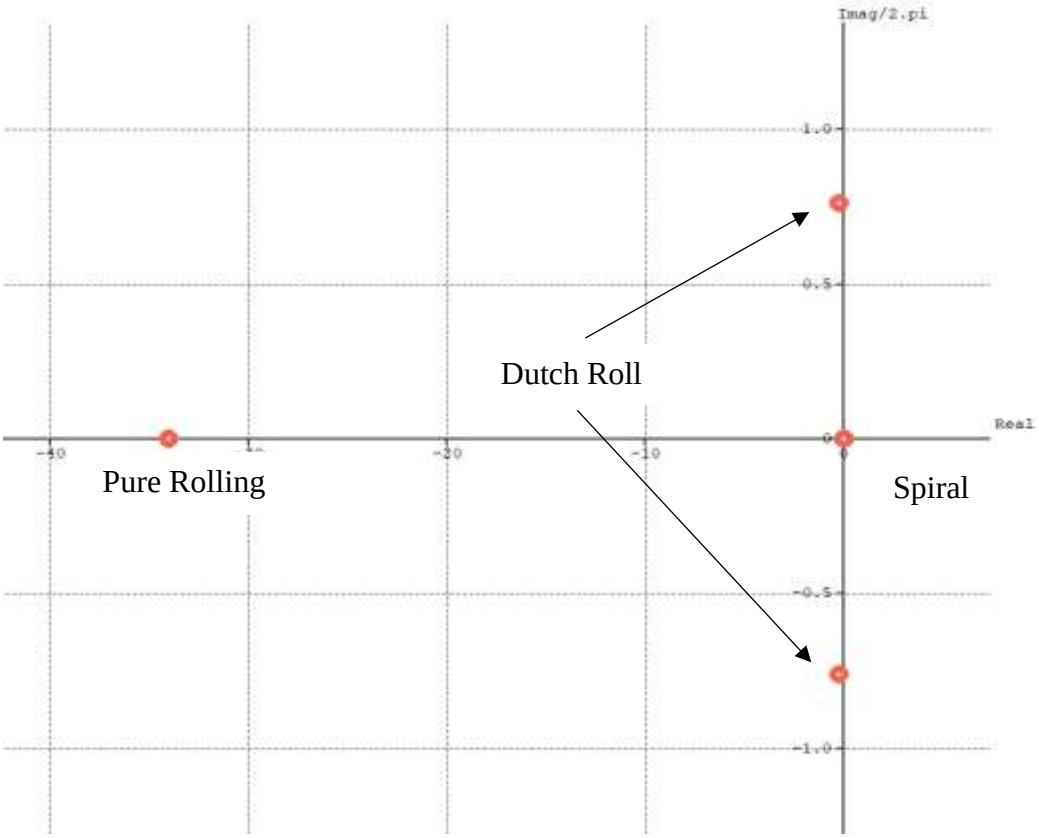

Fig 5. 3: Root locus graph for longitudinal mode

Table 5. 4: Eigen value and Eigen vector value for lateral mode

Mode	**Roll**	**Dutch Roll**	**Dutch Roll**	**Spiral**
Eigen Value	-32.43+ 0i	-0.225+-4.724i	-0.225+-4.724i	0.04688+ 0i
Eigen Vector	1+ 0i 103.9+ 0i -0.2293+ 0i -3.204+ 0i	1+ 0i -0.268+-.0007i 0.0031+-0.23i 0.003+-0.057i	1+ 0i -0.268+-.0007i 0.0031+-0.23i 0.003+-0.057i	1+ 0i 0.2919+ 0i 3.401+ 0i 6.227+ 0i

Using Phillips formulae, we get:

For Phugoid mode: Frequency: 0.115 Hz

Damping Ratio: 0.008

For Dutch Roll: Frequency: 0.752 Hz

Damping Ratio: 0.032

5.3.5. Flight Simulation in X-Plane 11

X-Plane 11 is a flight simulation software that can be used to analyze the dynamic response of an aircraft. This software can simulate the aircraft's response to various conditions, including changes in airspeed, altitude, and attitude, as well as turbulence and other external disturbances. And finally, different dynamic response mode were simulation under SLUF condition.

5.3.5.1. Phugoid Mode:

For phugoid mode control input was applied to pitch up about 20 degrees nose up and 10% of the aircraft speed was allowed to bleed off, and then the pitch control was released. It was observed that initial pitch up moment was observed after 8 sec approximately when pitch of 25 degree applied. Fluctuation in pitching moment was seen minimum after 45 sec and complete damping was seen after 80 sec.

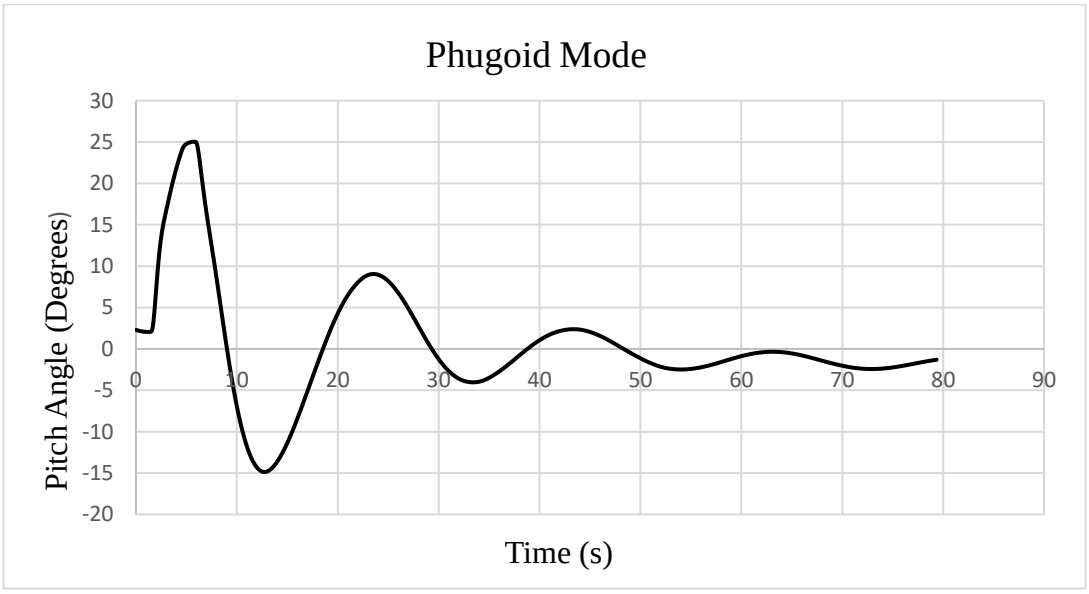

Fig 5. 4: Pitch vs time graph in phugoid mode

5.3.5.2. Short Period Mode:

For short period mode control input was applied quickly in order to obtain sharp pitch up then pitch down and then the pitch control was released. It was observed that initial pitch up moment was observed after 5 sec approximately. Fluctuation in pitching moment was seen minimum after 6 sec and complete damping was seen after 80 sec.

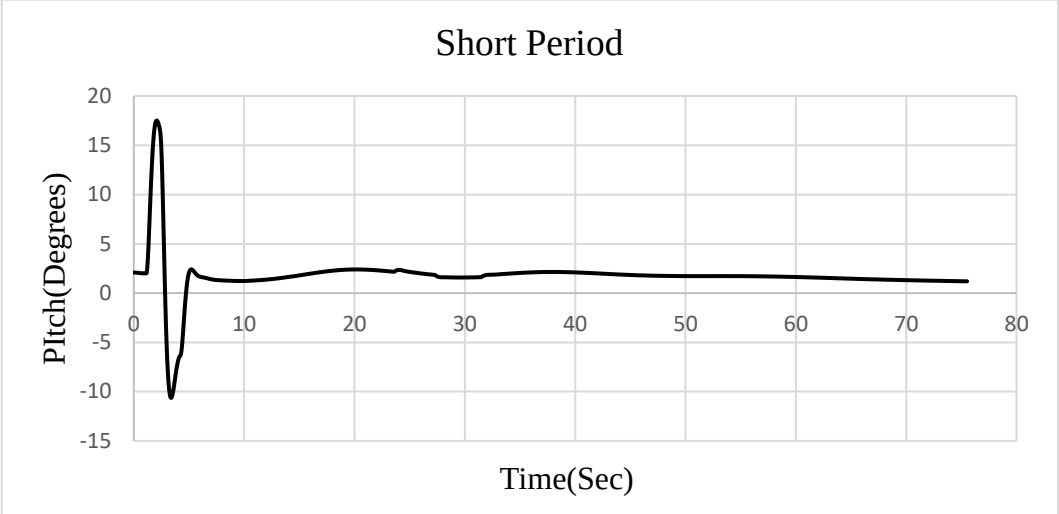

Fig 5. 5: Pitch vs time graph in short period mode

5.3.5.3. Dutch Roll

For Dutch roll mode, control input was applied quickly in rudder such that it deflect fully in one way then in other way and then rudder control was released. Initial rudder deflection of negative 15 degree and positive 18 degree was given at the time interval of 6 sec. It was observed that, aircraft retains its initial position within 2 sec.

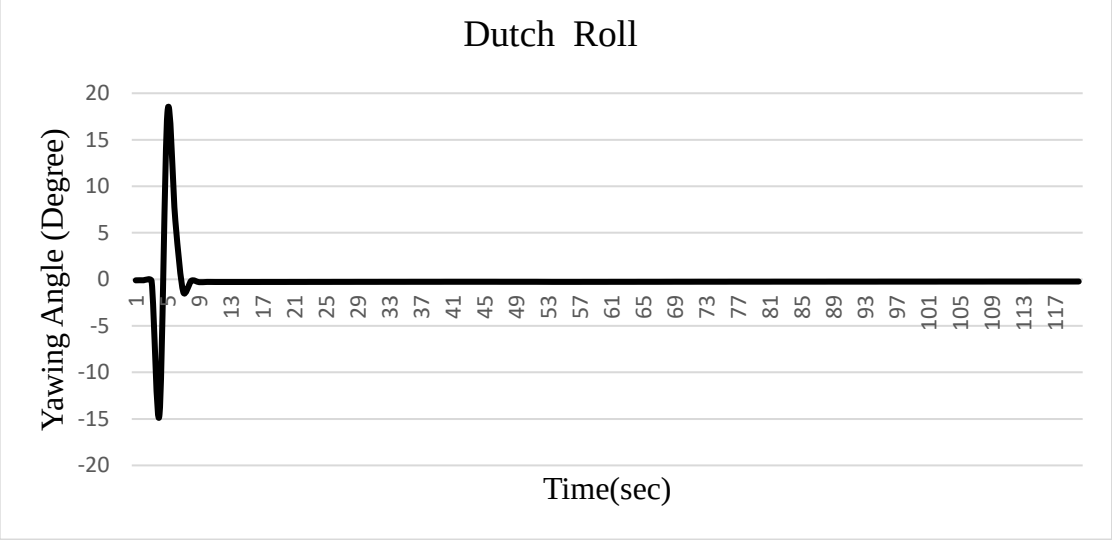

Fig 5. 6: Yawing angle vs time graph in Dutch roll mode

5.3.5.4. Spiral Mode

For spiral mode control input was applied in order bank the aircraft, and the control is released. In Spiral mode the time taken to double the bank angle is measured if it does not double itself, data of bank angle for 1minute time period is taken. Initially bank angle of negative 45 degree was applied which result in restoration of the initial condition which took almost 63 sec.

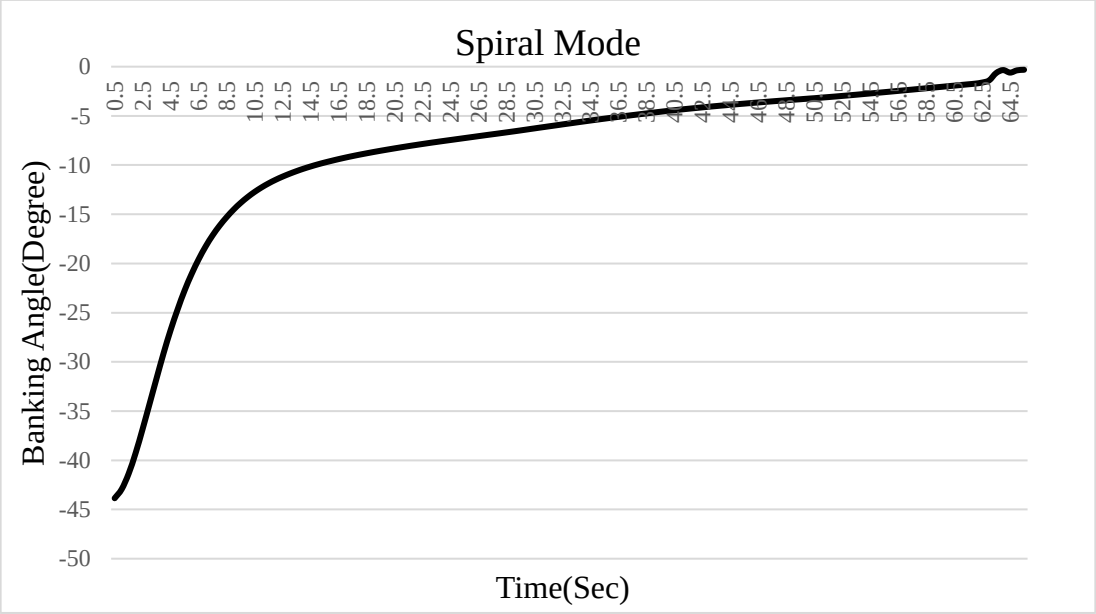

Fig 5. 7: Banking angle vs time graph in spiral mode

5.4. Flight Testing

The flight test is the finalized fabricated model with electronic setup embedded into it. Qgroundcontrol was used as ground control station and the latest Pixhawk firmware was installed. We, at first, performed pure quadcopter as well as pure fixed wing flight test. For pure quadcopter testing, we selected Generic Quad system configuration and for pure fixed wing, we selected Flying Wing configuration. All the sensors were calibrated and required flight modes were set. ESC's were calibrated following the given commands and few parameters were changed as per our requirements.

5.4.1. Fixed Wing Mode Testing

We initially performed pure fixed wing mode testing to ensure that the system is flyable. The flight test was manual and the result was satisfactory. We then proceed to pure quad testing.

5.4.2. Quadcopter Mode Testing

QGround Control software was used for the flight control and system setup. We performed several missions on pure quadcopter mode at different velocities. The maximum velocity we got during pure quad mode test was about 11.5 m/s. The sink rate was not so high even at that speed. The outcomes of an autonomous mission in pure quad mode are presented below:

Fig 5. 8: Mission path

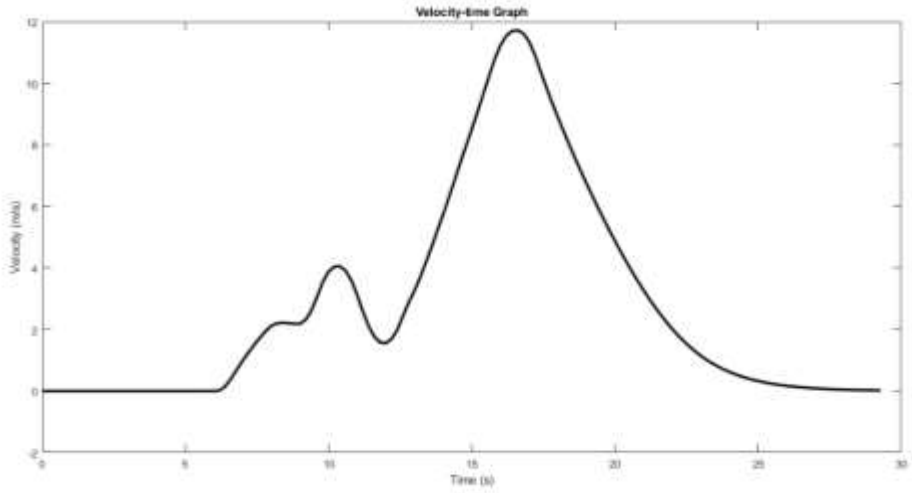

Fig 5. 9: Velocity change throughout the mission

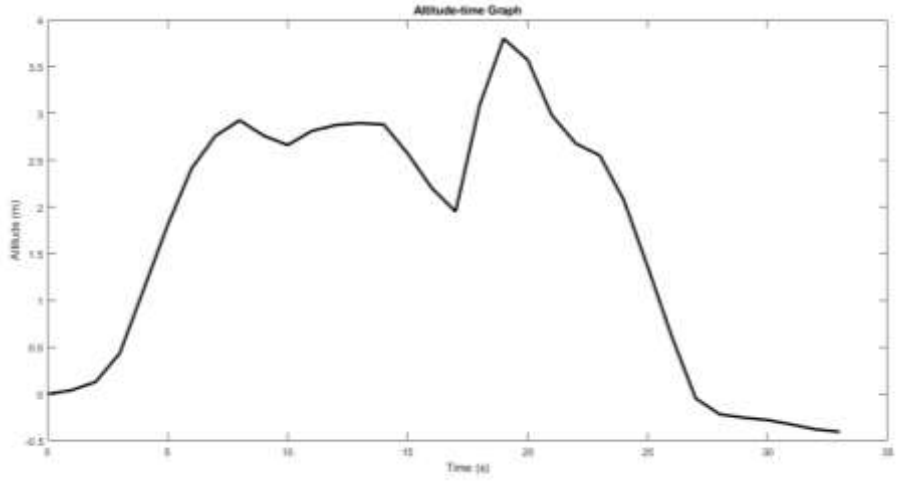

Fig 5. 10: Altitude change throughout the mission

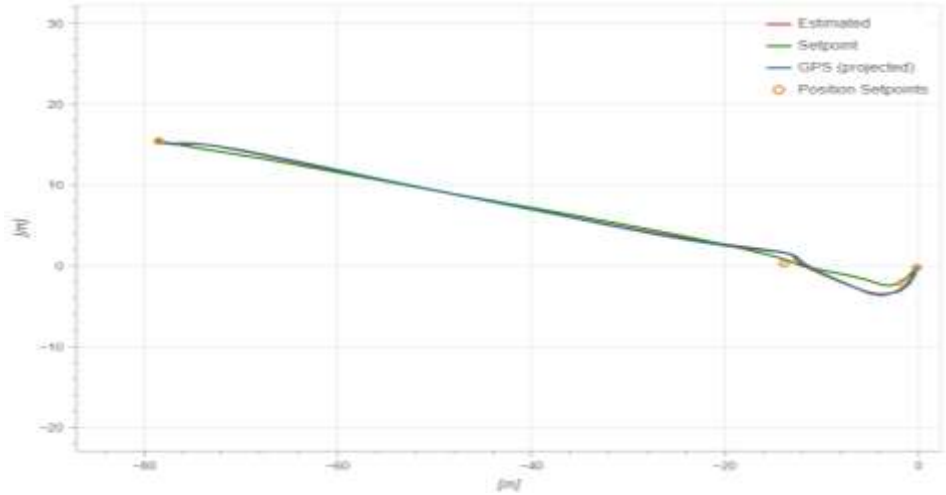

Fig 5. 11: Projected path and actual path

During the autonomous quad mission, it was noted that the UAS followed all the waypoint markers closely. At some point it was observed that altitude being dropped down due to negative lift during forward flight. However, it was successful to retain its initial altitude given at different waypoints. It was also observed that the quadcopter's larger surface area hindered its ability to achieve the necessary speed in quadcopter mode. As the quadcopter tilted forward to gain speed, it encountered surface drag, which restricted its maximum speed to 11.5 m/s. Nonetheless, it is possible to surpass this speed during the transition phase by pusher motor, while using the control surface to maintain level flight. This approach minimizes surface drag and enables the UAS to achieve higher speeds.

We also performed manual test in stabilized mode to observe its response. The vehicle was well responding according to the given input and was quite stable as well. However, there was a little time delay in response.

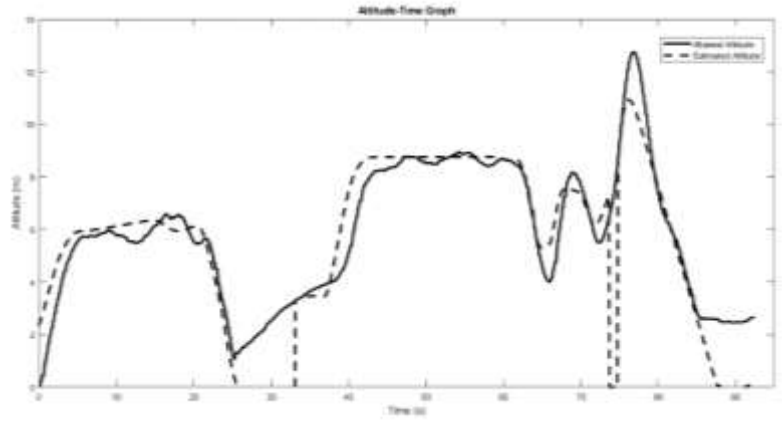

Fig 5. 12: Estimated and Actual Altitude

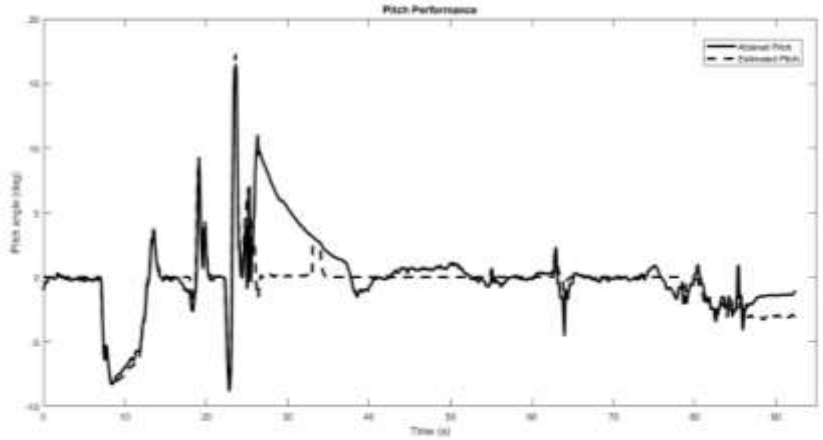

Fig 5. 13: Estimated and Actual Pitch Angle

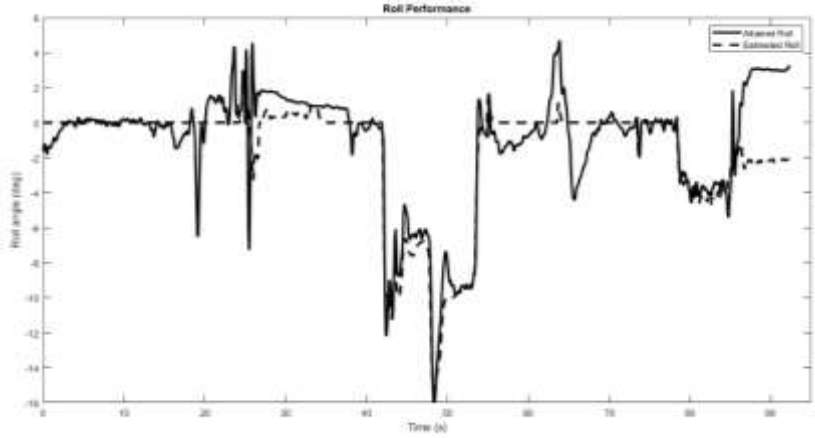

Fig 5. 14: Estimated and Actual Roll Angle

5.4.3. Transition Testing

After completing the Hybrid VTOL setup, we tested a simple quad mission to test the quad motors. We prepared an auto mission with commands as shown below:

Takeoff ⟶ Loiter (15 sec) ⟶ Land

The successful completion of this mission confirmed that the quad worked perfectly fine in quad mode.

Then, a complete autonomous hybrid VTOL mission was prepared in Mission Planner. The altitude was set as 15m at every waypoints. Auto mode was set as one of the flight mode that triggers the entire mission. DO_VTOL_TRANSITION command was used to trigger the transition at waypoint 2.

Following figure shows the mission plan of VTOL transition in mission planner.

Fig 5. 15: Mission plan of VTOL transition

Following the above mission plan, autonomus hybrid VTOL mission was completed starting from VTOL takeoff to VTOL transition and VTOL land sucessfully, providing following sets of graph:

5.4.3.1. Altitude Vs Distance Graph:

The flight path graph indicates that the vehicle followed the given mission closely. The plot shows takeoff altitude to be around 16m which is deviated by 1m from the given altitude of 15m. The altitude is dropped slightly at the initial stage because of the negative lift produced by the vehicle due to its nose down orientation at initial cruise. Once the transition starts, the vehicle has maintained its altitude. The landing trajectory of system shows slight inconsistency with the mission plan. This may be the consequence of gusty wind and GPS error at the time of testing.

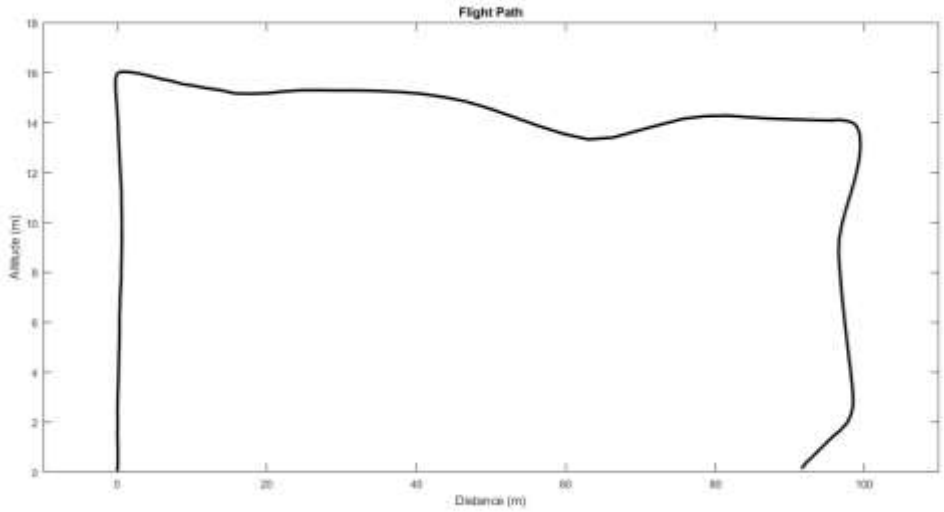

Fig 5. 16: Actual traced flight path

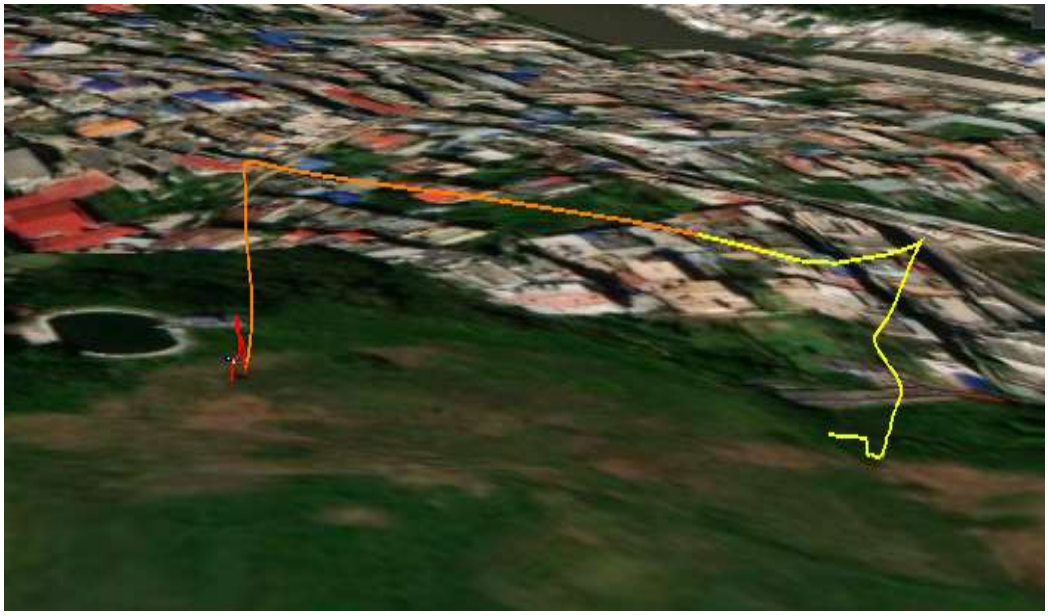

Fig 5. 17: 3D view of Flight Path

5.4.3.2. Altitude and Throttle vs Distance Graph:

The pusher has behaved just the way it has to. Transition has started right after covering slight forward distance. The waypoint radius of 5m defined while planning the mission led to transition trigger earlier than actually reaching the second waypoint. The forward throttle has been constant to its maximum value till the system starts back transition. When back transition triggers, the pusher throttle started slowing down and quad motors started ramping up.

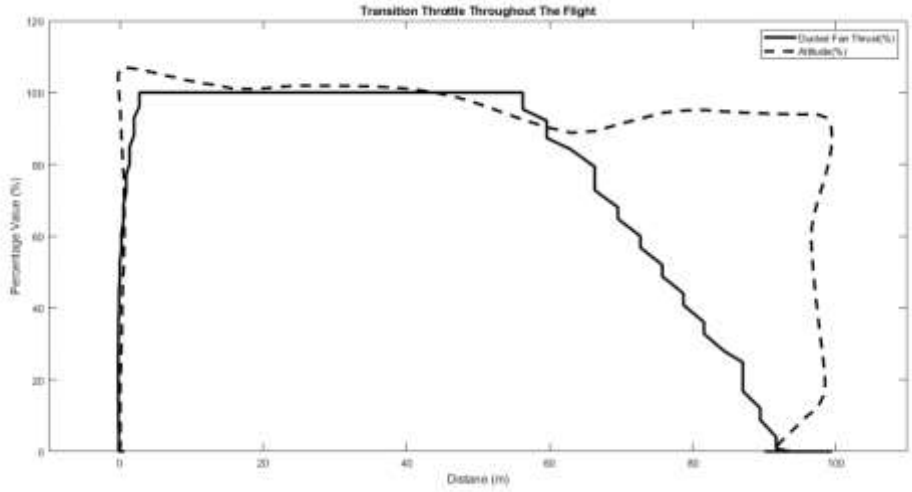

Fig 5. 18: Altitude and throttle Vs time graph

5.4.3.3. Roll, Pitch and Yaw Performance of the UAS:

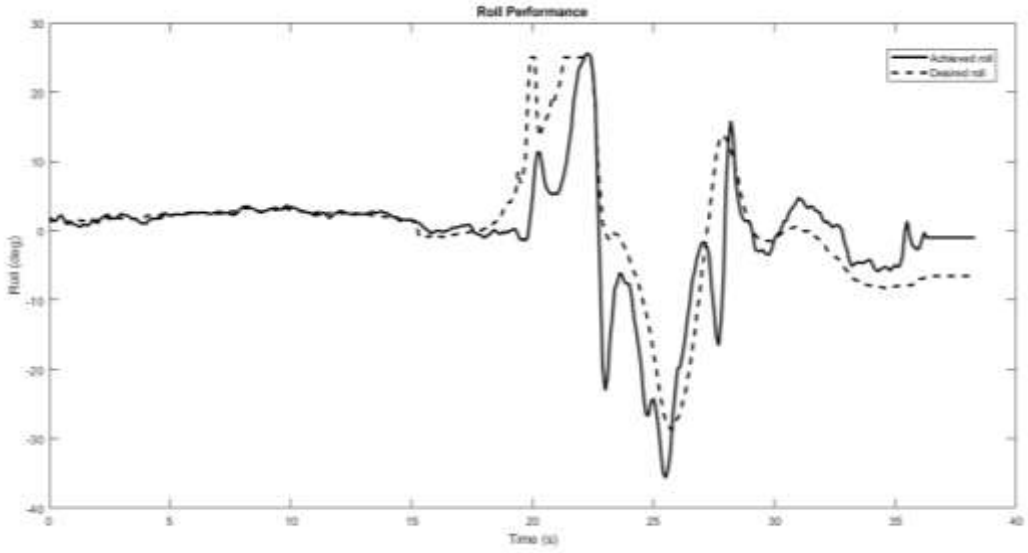

Fig 5. 19: Desired and achieved roll

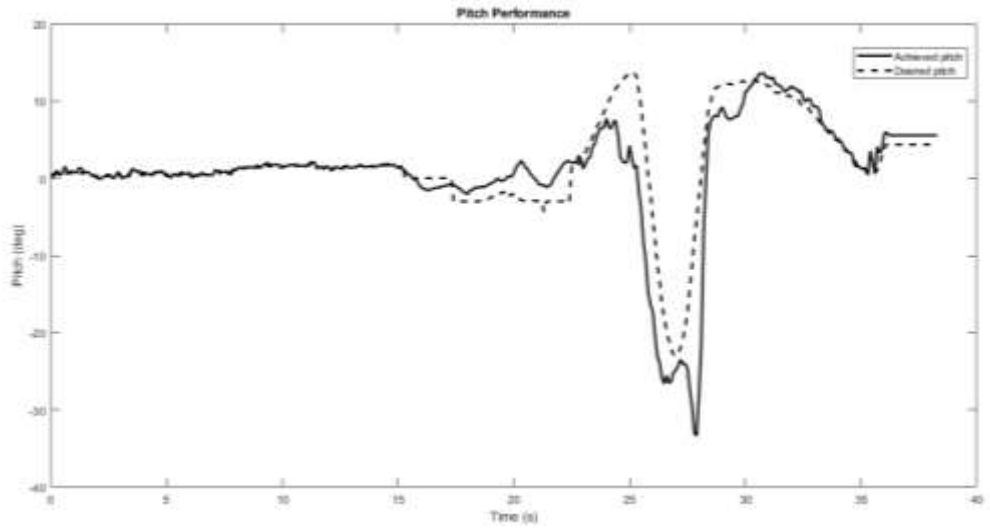

Fig 5. 20: Desired and achieved pitch

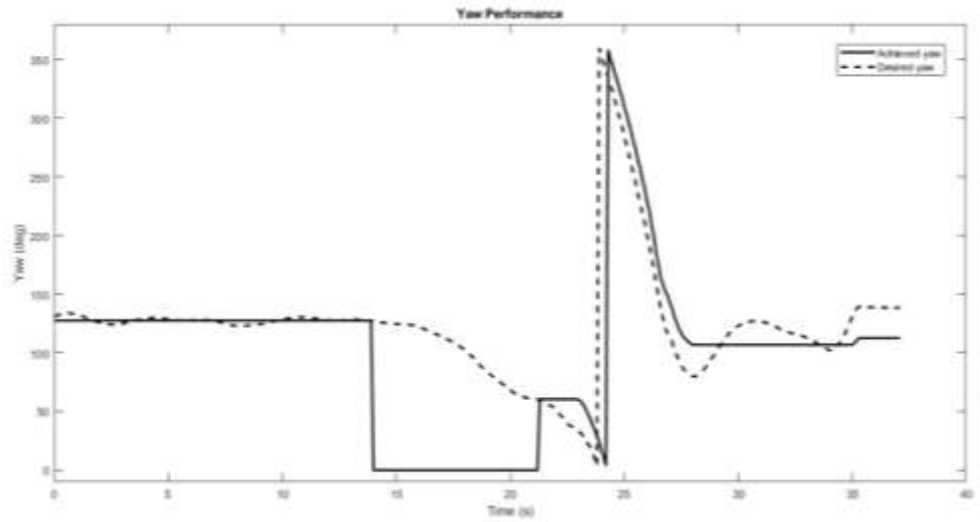

Fig 5. 21: Desired and Achieved Yaw

The desired and achieved roll, pitch and yaw shows good compliance to each other. This shows that the system was able to get the required amount of roll, yaw and pitch movement. The required roll and pitch have been zero with slight yaw throughout the cruise. These parameters have changed significantly during landing.

5.4.3.4. Ducted Fan Thrust Graph:

The graph of ducted fan thrust clearly shows how its throttle has varied throughout the mission. It shows that the fan started throttling up only when forward transition got triggered and it started throttling down only when back transition got triggered. The

throttle has ramped up from zero to maximum in about 2.5 sec. This also comply with the slew rate of 40% that we set in the parameter setup since 40% slew rate means 2.5 sec ramp up duration.

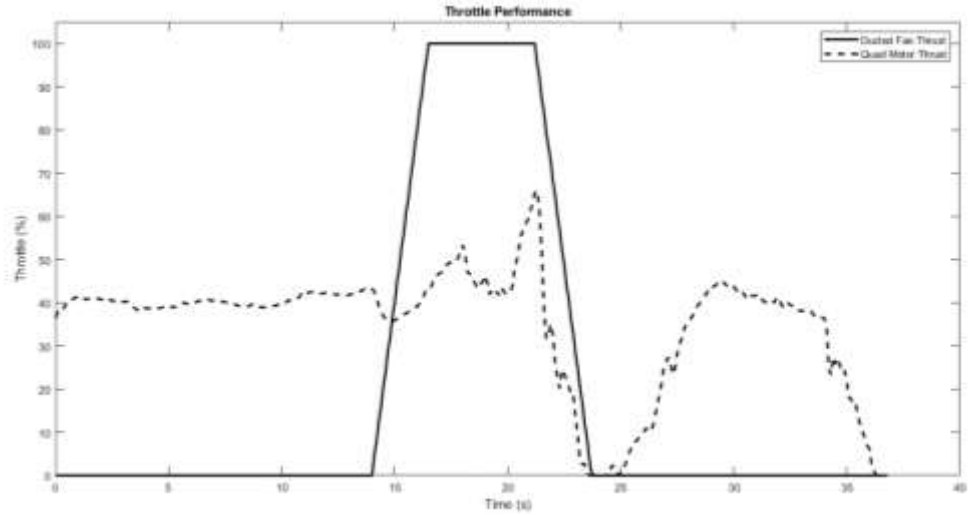

Fig 5. 22: Ducted fan thrust Vs time graph

5.4.3.5. Velocity Time Graph:

The velocity time graph for the velocity attained by ducted fan during the forward flight shows the maximum value of 16.61m/s which is significantly higher than the stall speed of the designed BWB which is 12m/s. Hence, it shows that the BWB was capable of carrying out the forward transition flight in fixed wing mode without going in stall.

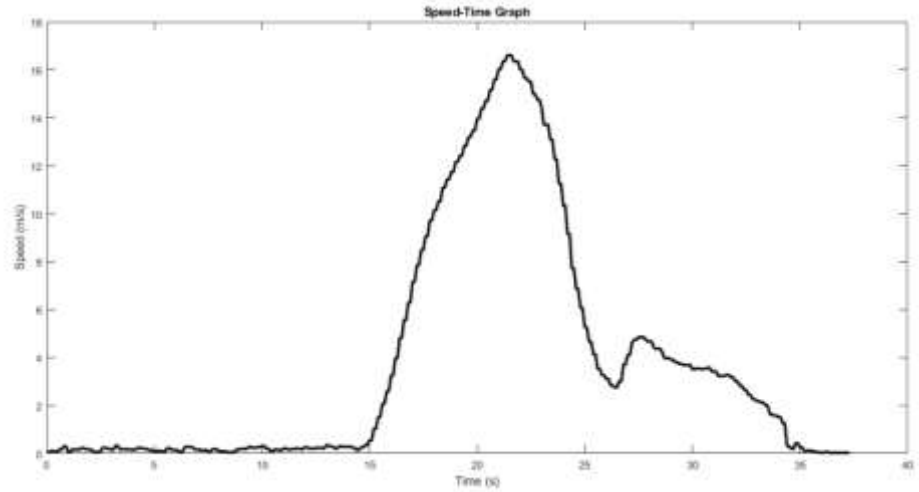

Fig 5. 23: Speed vs time

5.5. Limitations

Following are the some of the limitations of our project:

- Cutouts made on the upper body surface for electronic components and their placement caused reduction in lift and increase in drag which was not taken in consideration.
- The drag due to quad motors and vehicle frame was not considered.
- GPS error in navigating and maintaining position.

5.6. Problems Faced

The design phase wasn't much problematic considering the fact that all tasks were computer-operated. The only major problem we faced during design phase was to provide the twist and required incidence in plane maker as the software has no option for twist, so assigning twist and incidence both at once was not possible.

However, the manufacturing process was a lot more problematic. Here are some of the major problems we faced during manufacturing:

- The inability of CNC Hot Wire Cutter to cut high swept wing made us cut most of our wing sections manually.
- The assembly of wing section, spar and rib was difficult due to dihedral, variable sweep and variable twist across the wingspan.
- Limited availability of Pixhawk and Telemetry devices delayed the workflow.

CHAPTER SIX: CONCLUSION AND RECOMMENDATION

6.1. Conclusion

In this project, the detail design of a BWB UAS was presented. The design process was conducted in three major phases: conceptual, preliminary and detail design phase. The initial sizing was performed and design constraints were estimated during the conceptual design phase. Then necessary wing parameters were calculated using empirical formulas and a baseline design was made in XFLR5. The sweep, dihedral and twist angle along with few other parameters were continuously varied to achieve most efficient design. Since the BWB lacks tail, sweep and twist are two primary parameters to adjust the curves and attain required performances. Once the desired CL, Cm and L/D curves were obtained, the designed was finalized. Then, the internal structure was developed in CATIA and the design was tested in X-Plane 11. Once the flight test was completed in X-Plane 11, we started fabricating individual components. The available hot wire cutter was small for our application, so we had to cut most of the wing sections by hand. After the completion of fabrication of wing sections, each individual components were assembled together and final model was obtained. Then the electronic setup was completed and a pure fixed wing mode test was performed at first. Once it was completed, we started to perform quad mode test. One of the motor wasn't throttling up evenly with others at the initial stage. The problem was solved by replacing the 3S battery with a 4S battery. We performed few missions in quad mode to estimate the attitude variation due to heavy drag of vehicle in pitched down forward motion in pure quad mode. The effect was not significant, so we proceed toward the transition flight test. Qgroundcontrol was used initially but the ducted fan didn't respond in ground test, so after many attempts, we shifted toward missionplanner. The vehicle setup was performed as per our requirements and transition test was performed. The transition was successful but the vehicle showed left yaw which possibly was the result of slight shift in ducted fan's position after the crashes that happened during testing phase.

6.2. Recommendation

Following are the some of the recommendation for future enhancement.

- The transition parameters can be varied mission-wise to obtain more smooth transition.
- Less dense styro-foam and carbon fiber rod can be used to reduce the overall weight.
- Wing fence can be used to reduce the effect of Dutch roll.

REFERENCES

[1] E. Ordoukhanian and A. Madni, "Model-Based Approach to Engineering Resilience in Multi-UAV Systems," *Systems*, vol. 7, no. 1, p. 11, Feb. 2019, doi: 10.3390/systems7010011.

[2] N. Qin, A. Vavalle, A. Le Moigne, M. Laban, K. Hackett, and P. Weinerfelt, "Aerodynamic considerations of blended wing body aircraft," *Progress in Aerospace Sciences*, vol. 40, no. 6, pp. 321–343, Aug. 2004, doi: https://doi.org/10.1016/j.paerosci.2004.08.001.

[3] N. Qin, A. Vavalle, and A. Le Moigne, "Spanwise Lift Distribution for Blended Wing Body Aircraft.," *Journal of Aircraft*, vol. 42, no. 2, pp. 356–365, Mar. 2005, doi: https://doi.org/10.2514/1.4229.

[4] N. Qin, "Aerodynamic Studies for Blended Wing Body Aircraft," *9th AIAA/ISSMO Symposium on Multidisciplinary Analysis and Optimization*, Sep. 2002, doi: https://doi.org/10.2514/6.2002-5448.

[5] J. van Dommelen and R. Vos, "Conceptual design and analysis of blended-wing-body aircraft," *Proceedings of the Institution of Mechanical Engineers, Part G: Journal of Aerospace Engineering*, vol. 228, no. 13, pp. 2452–2474, Jan. 2014, doi: https://doi.org/10.1177/0954410013518696.

[6] S. Siouris and N. Qin, "Study of the effects of wing sweep on the aerodynamic performance of a blended wing body aircraft," *Proceedings of the Institution of Mechanical Engineers, Part G: Journal of Aerospace Engineering*, vol. 221, no. 1, pp. 47–55, Jan. 2007, doi: https://doi.org/10.1243/09544100jaero93.

[7] D. W. Casbeer, Sai-Ming Li, R. W. Beard, R. K. Mehra, and T. W. McLain, "Forest fire monitoring with multiple small UAV," *Proceedings of the 2005, American Control Conference, 2005.*, doi: https://doi.org/10.1109/acc.2005.1470520.

[8] L. Y, D. L, and McCluer, *Insights into airframe aerodynamics and rotor-on-wing interactions from a 0.25-scale tiltrotor wind tunnel model*. 2002.

[9] Kumar, R. Sharma, S. Sharma, S. Chandel, and S. Kumar, "A Review on Design Methods of Vertical take-off and landing UAV aircraft," *IOP Conference Series: Materials Science and Engineering*, vol. 1116, no. 1, p. 012142, Apr. 2021, doi: 10.1088/1757-899x/1116/1/012142

[10] E. Ordoukhanian and A. M. Madni, "Blended Wing Body Architecting and Design: Current Status and Future Prospects," *Procedia Computer Science*, vol. 28, pp. 619–625, 2014, doi: 10.1016/j.procs.2014.03.075.

[11] C. Sheng and Q. Zhao, “Numerical Investigations of Fan-in-Wing Aerodynamic Performance with Active Flow Control,” *Journal of Aircraft*, vol. 54, no. 6, pp. 2317–2329, Nov. 2017, doi: 10.2514/1.c034134.

[12] Kamal A.M and S. A.R, “Design methodology for hybrid (VTOL + Fixed Wing) unmanned aerial vehicles,” 2018.

[13] Kaparos P Bliamis C and Yakinthos K 2019 Conceptual design of a UAV with VTOL characteristics Proc. AIAA Aviation 2019 Forum Dallas TX (AIAA)

[14] D. M, L. Swathi s, and N. DC, “Airfoil Design and Optimization for tailless aircrafts Dheeraj M, Lakshmi Swathi S, Naresh D C Dayananda Sagar College of Engineering, Bangalore, 2020 DOI: 10.9790/9622-1004062130,” 2020, doi: Airfoil Design and Optimization for tailless aircrafts Dheeraj M, Lakshmi Swathi S, Naresh D C Dayananda Sagar College of Engineering, Bangalore, 2020 DOI: 10.9790/9622-1004062130.

[15] S. Paudel, “Aerodynamic and Stability Analysis of Blended Wing Body Aircraft,” *International Journal of Mechanical Engineering and Applications*, vol. 4, no. 4, p. 143, 2016, doi: https://doi.org/10.11648/j.ijmea.20160404.12.

[16] A. Hamada, A. Sultan, and M. Abdelrahman, “Design, Build and Fly a Flying Wing,” *Athens Journal of Technology & Engineering*, vol. 5, no. 3, pp. 223–250, Aug. 2018, doi: 10.30958/ajte.5-3-2.

[17] “Aerodynamic characteristics of low Reynolds number airfoils,” *Tehnicki vjesnik - Technical Gazette*, vol. 24, no. 1, Feb. 2017, doi: 10.17559/tv-20160225100019.

[18] N. Ruseno, “Modal Analysis Of Blended Wing-Body UAV,” *Jurnal Teknologi Kedirgantaraan*, vol. 6, no. 2, pp. 68–75, Aug. 2021, doi: 10.35894/jtk.v6i2.39.

[19] F. Parisa, B. Adrien, and S. Sergey, “Aerodynamic Characteristics of the Blended-Wing-Body VTOL UAV,” *Journal of Aerospace Engineering and Mechanics*, vol. 4, no. 1, Jan. 2020, doi: 10.36959/422/440.

[20] B. Yuksek, A. Vuruskan, U. Ozdemir, M. A. Yukselen, and G. Inalhan, “Transition Flight Modeling of a Fixed-Wing VTOL UAV,” *Journal of Intelligent &*

Robotic Systems, vol. 84, no. 1–4, pp. 83–105, Jan. 2016, doi: 10.1007/s10846-015-0325-9.

[21] W. Choi and S. Hampton, "Scenario-Based Strategic Planning for Future Civil Vertical Take-off and Landing (VTOL) Transport," *Journal of Aviation/Aerospace Education & Research*, 2020, doi: 10.15394/jaaer.2020.1808.

[22] R. H. Liebeck, "Design of the Blended Wing Body Subsonic Transport," *Journal of Aircraft*, vol. 41, no. 1, pp. 10–25, Jan. 2004, doi: https://doi.org/10.2514/1.9084.

[23] Diedrich A, Hileman J, Tan D, et al., "Multidisciplinary design and optimization of the silent aircraft." *Massachusetts Institute of Technology, USA*, 2006. AIAA 2006-1323.

[24] E. Ordoukhanian and A. M. Madni, "Blended Wing Body Architecting and Design: Current Status and Future Prospects," *Procedia Computer Science*, vol. 28, pp. 619–625, 2014, doi: 10.1016/j.procs.2014.03.075.

[25] I. B. Laskowitz, "VERTICAL TAKE-OFF AND LANDING (VTOL) ROTORLESS AIRCRAFT WITH INHERENT STABILITY," *Transactions of the New York Academy of Sciences*, vol. 23, no. 3 Series II, pp. 198–198, Jan. 1961, doi: 10.1111/j.2164-0947.1961.tb03113.x.

[26] W. Wisnoe, R. Nasir, W. Kuntjoro, and A. Mamat, "Wind Tunnel Experiments and CFD Analysis of Blended Wing Body (BWB) Unmanned Aerial Vehicle (UAV) at Mach 0.1 and Mach 0.3," *International Conference on Aerospace Sciences and Aviation Technology*, vol. 13, no. AEROSPACE SCIENCES, pp. 1–15, May 2009, doi: 10.21608/asat.2009.23441.

[27] H. Yeo and H. Saberi, "Tiltrotor Conversion Maneuver Analysis with RCAS," *Journal of the American Helicopter Society*, 2021, doi: 10.4050/jahs.66.042010.

[28] H. Yeo and W. Johnson, "Performance and Design Investigation of Heavy Lift Tilt-Rotor with Aerodynamic Interference Effects," *Journal of Aircraft*, vol. 46, no. 4, pp. 1231–1239, Jul. 2009, doi: 10.2514/1.40102.

BIBLIOGRAPHY

[1] D. Kurtulus, “Introduction to micro air vehicles: concepts, design and applications,” no. April 2011, pp. 219–255, 2011.

[2] K. Nonami, F. Kendoul, S. Suzuki, W. Wang, and D. Nakazawa, “Autonomous flying robots: Unmanned aerial vehicles and micro aerial vehicles,” Auton. Fly. Robot. Unmanned Aer. Veh. Micro Aer. Veh., pp. 1– 329, 2010, doi: 10.1007/978-4-431-53856-1.

[3] F. Cakici, “Control and Guidance of a Multi-Mode Unmanned Aerial Vehicle for Increased Versatility,” 2016. [3] Anderson J 1999 Aircraft performance and design (WCB/McGraw–Hill) p 383

[4] Mitridis D Bliamis C Kaparos P and Yakinthos K 2020 Design of a tilting mechanism for a VTOL flying wing UAV Proc. 10th EASN Virtual Int. Conf. (IOP Conf. Series: Mat. Sci. and Eng.)

[5] Panagiotou P Fotiadis-Karras S and Yakinthos K 2018 Conceptual design of a blended wing body MALE UAV Aerospace Science and Technology 73 32-47

[6] Spalart P R and Allmaras S A 1992 A one-equation turbulence model for aerodynamic flows Proc. 30th Aerospace Science Meeting Exhibition Reno NV (AIAA) pp 5–21

[7] Panagiotou P Kaparos P Salpingidou C and Yakinthos K 2016 Aerodynamic design of a MALE UAV Aerospace Science and Technology 50 127-38

[8] Spalart P R and Rumsey C L 2007 Effective inflow conditions for turbulence models in aerodynamic calculations AIAA J. 45 2544–53

[9] Salpingidou C Misirlis D and Yakinthos K 2015 Computational flow analysis and development of a surrogate model for the prediction of the fluid flow and 3D flow effects around a propeller Proc. 8th GRACM Int. Cong. on Computational Mechanics Volos Greece

[10] Nelson R 1997 Flight stability and automatic control (WCB/McGraw-Hill)

[11] Roskam J 2004 Airplane Design (DARcorporation)

[12] Dimopoulos T Panagiotou P and Yakinthos K 2019 Stability study and flight simulation of a blended-wing-body UAV Proc. 9th EASN Int. Conf. Athens Greece (MATEC Web of Conf.)

[13] M. U. T. Matsumoto, K. Kita, R. Suzuki, A. Oosedo, Y. Hoshino, "A Hovering Control Strategy for a Tail-Sitter VTOL UAV that Increases Stability Against Large Disturbance," 2010 IEEE International Conference on Robotics and Automation, 2010.

[14] J. Escareño, S. Salazar, and R. Lozano, "Modelling and control of a convertible VTOL aircraft," Proc. IEEE Conf. Decis. Control, pp. 69–74, 2006, doi: 10.1109/cdc.2006.376915.

[15] O. Garcia, A. Sanchez, J. Escareño, and R. Lozano, Tail-sitter UAV having one tilting rotor: Modeling, Control and Real-Time Experiments, vol. 41, no. 2. IFAC, 2008.

[16] R.H. Stone, "Control architecture for a tail-sitter unmanned air vehicle," 2004 5th Asian Control Conference (IEEE Cat. No.04EX904), Melbourne, Victoria, Australia, 2004, pp. 736-744 Vol.2.

[17] B. N. Pamadi, *Performance, Stability, Dynamics, and Control of Airplanes*. AIAA, 2004.

[18] T. R. Yechout, *Introduction to Aircraft Flight Mechanics*. AIAA, 2003.

[19] D. P. Raymer, *Aircraft Design*. 1989

APPENDICES

	y ()	chord ()	offset ()	dihedral(°)	twist(°)	foil
1	0.000	0.570	0.000	0.0	3.00	MH 78 14.47%
2	0.121	0.420	0.120	3.0	3.00	MH 78 14.47%
3	0.121	0.420	0.120	3.0	3.00	MH 78 14.47%
4	0.220	0.300	0.200	3.0	3.00	MH 78 14.47%
5	0.330	0.220	0.290	3.0	0.00	MH 80 12.72%
6	0.420	0.180	0.350	3.0	-3.00	S5010 10%
7	0.420	0.180	0.350	3.0	-3.00	S5010 10% 0_80
8	0.660	0.110	0.510	3.0	-3.00	S5010 10% 0_80
9	0.660	0.110	0.510	3.0	-3.00	S5010 10%
10	0.750	0.090	0.560		-3.00	S5010 10%

Fig A. 1: Wing parameters in XFLR5

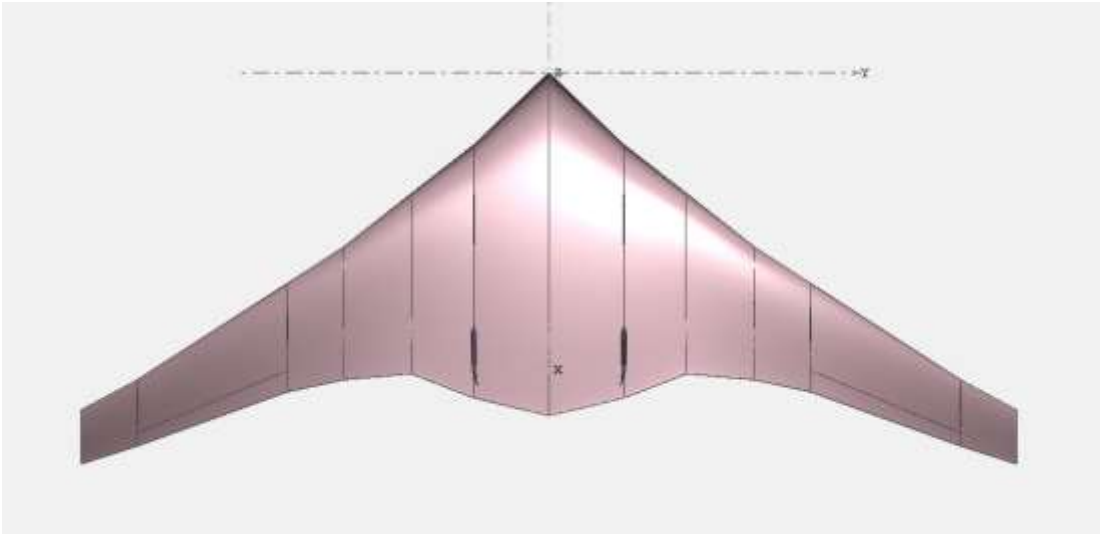

Fig A. 2: BWB design in XFLR 5

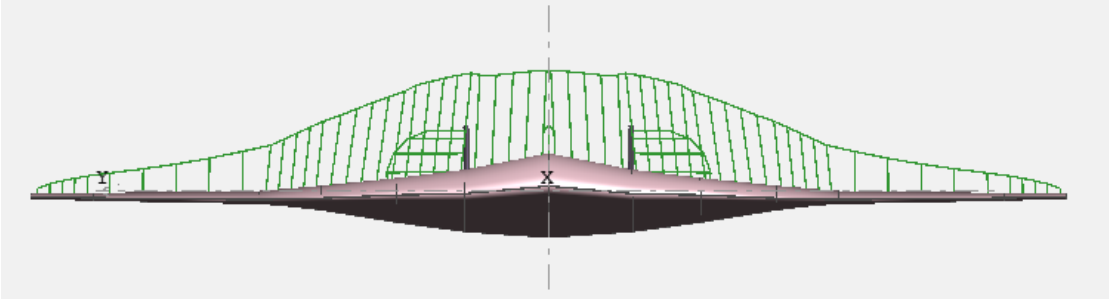

Fig A. 3: Lift distribution

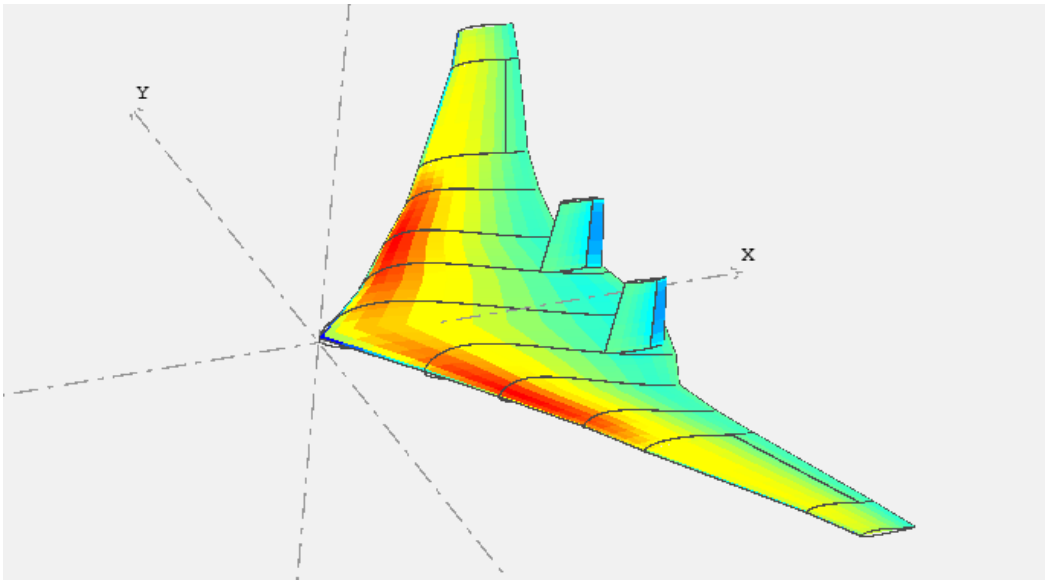

Fig A. 4: Pressure variation

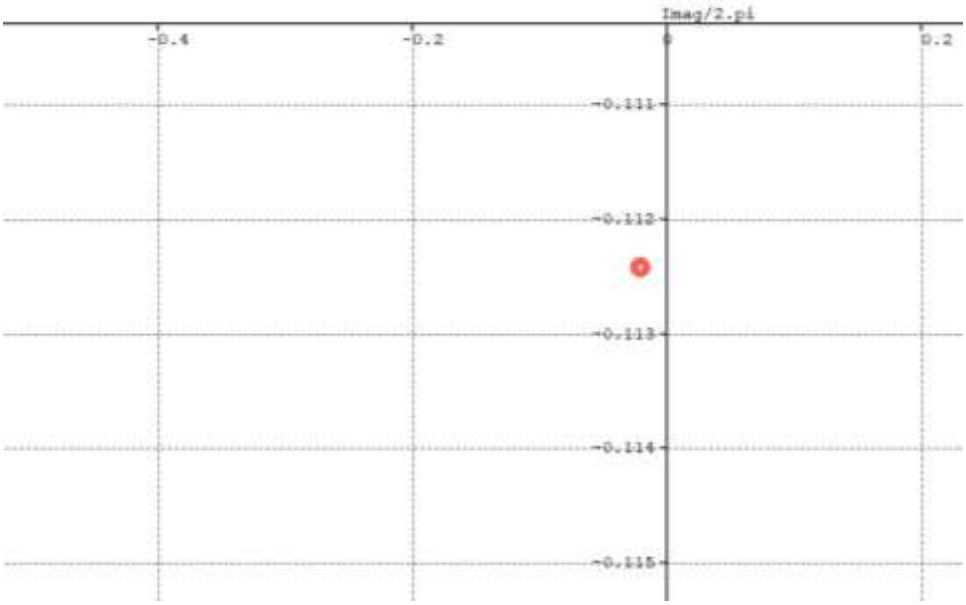

Fig A. 5: Root locus graph for longitudinal mode zoomed

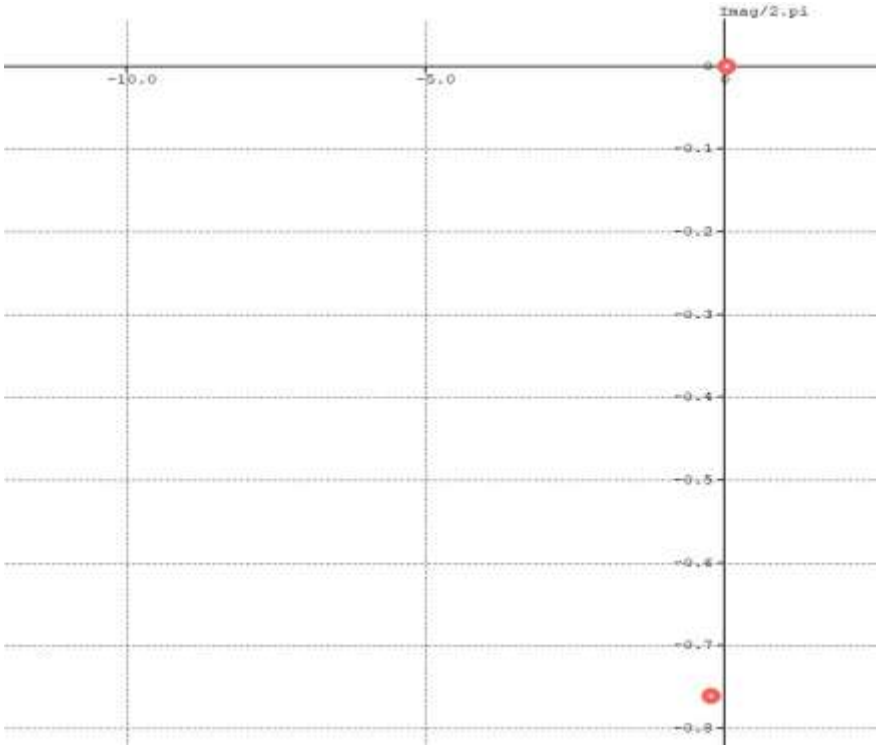

Fig A. 6: Root locus graph for lateral mode zoomed

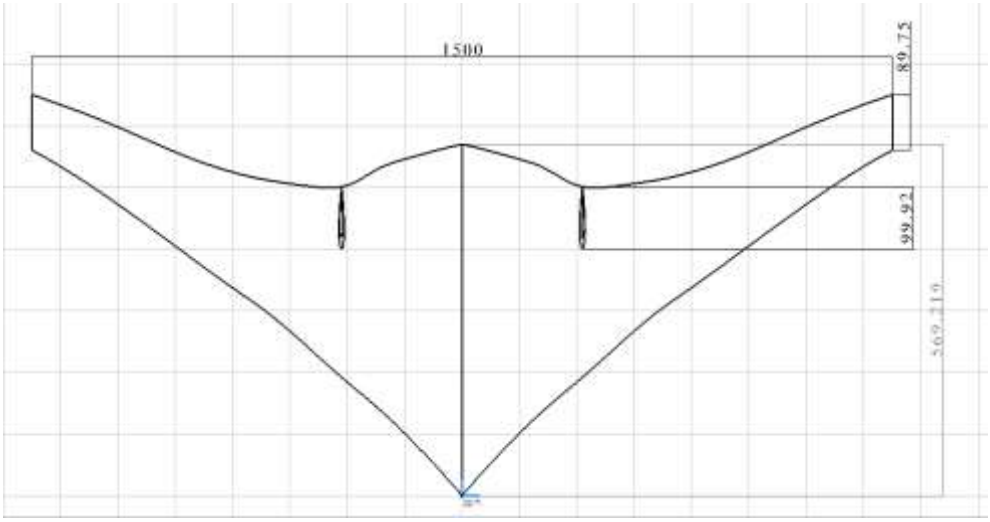

Fig A. 7: 2D- View of BWB

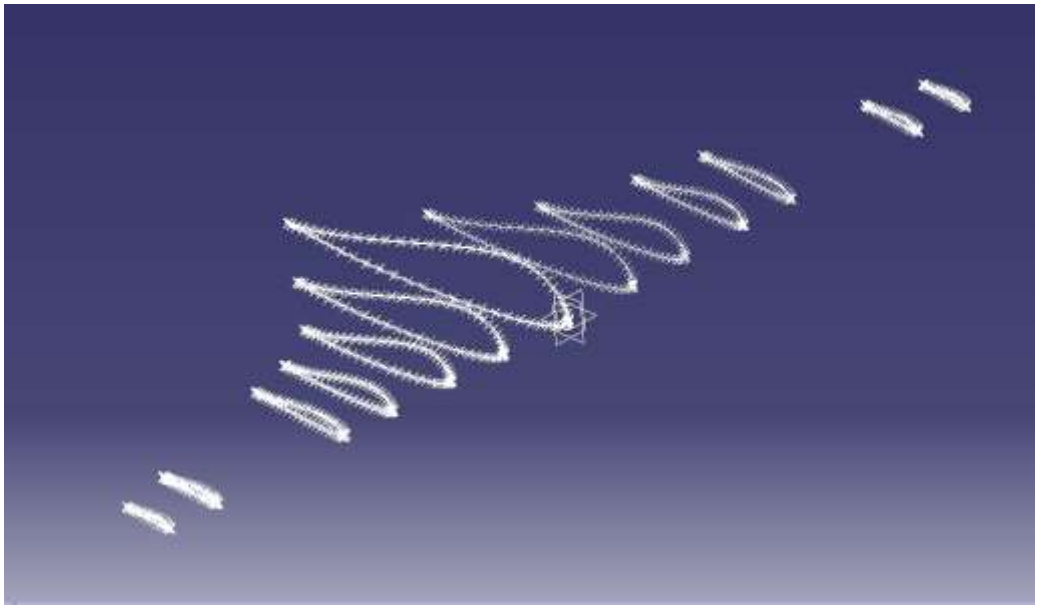

Fig A. 8: Airfoils data points importing in CATIA

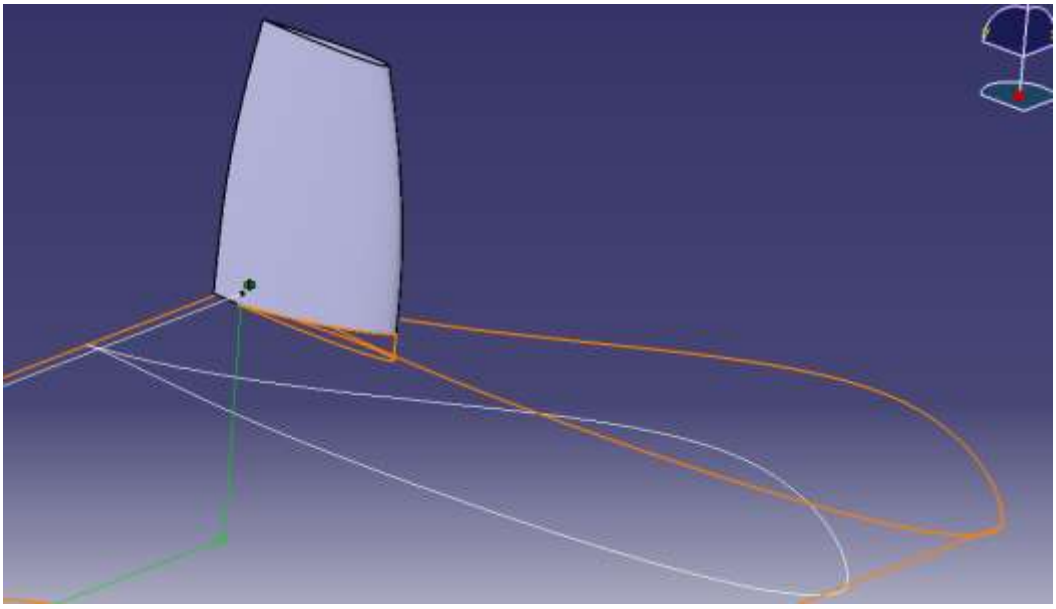

Fig A. 9: Fin placement in CATIA

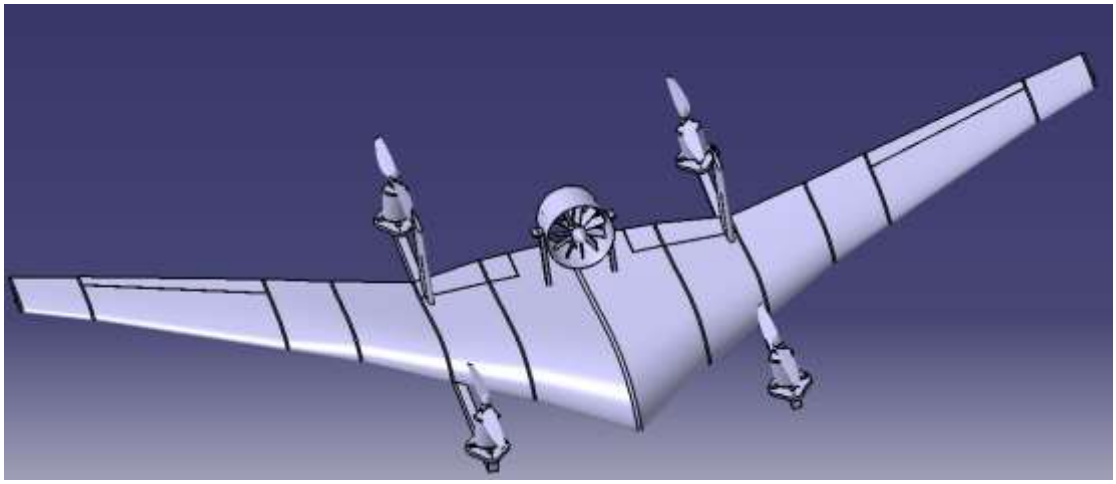

Fig A. 10: Final assembled model in CATIA

Vehicle Setup Parameters:

Q_FRAME_CLASS = 1 (for quad)

Q_FRAME_TYPE = 3 (for H frame)

SERVO9_FUNCTION = 33 (motor1)

SERVO10_FUNCTION = 34 (motor2)

SERVO11_FUNCTION = 35 (motor3)

SERVO12_FUNCTION = 36 (motor4)

SERVO1_FUNCTION = 77 (right elevon)

SERVO2_FUNCTION = 78 (left elevon)

SERVO4_FUNCTION = 21(rudder 1)

SERVO5_FUNCTION = 21(rudder 2)

SERVO3_FUNCTION = 70 (pusher motor)

Q_TKOFF_SPEED = 1 m/s

Q_LAND_SPEED = 1 m/s

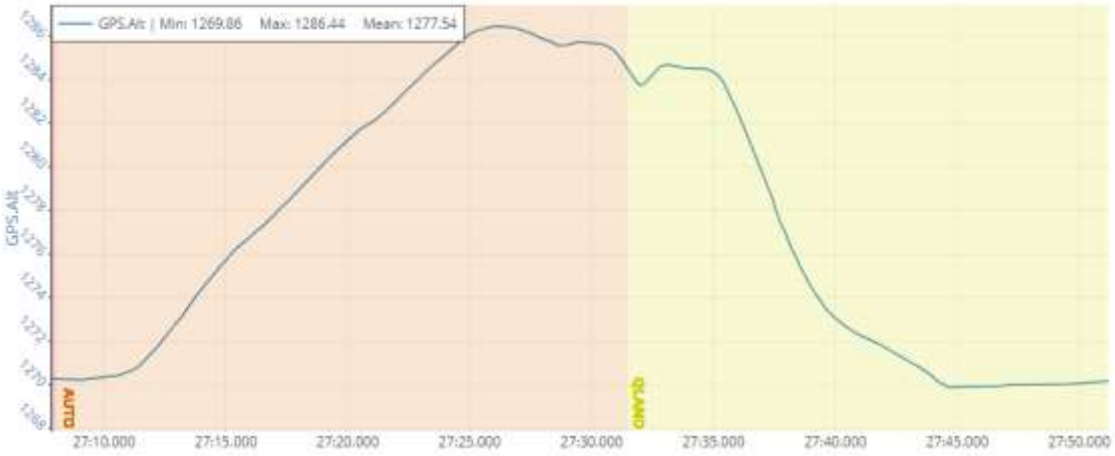

Fig A. 11: Altitude Vs time

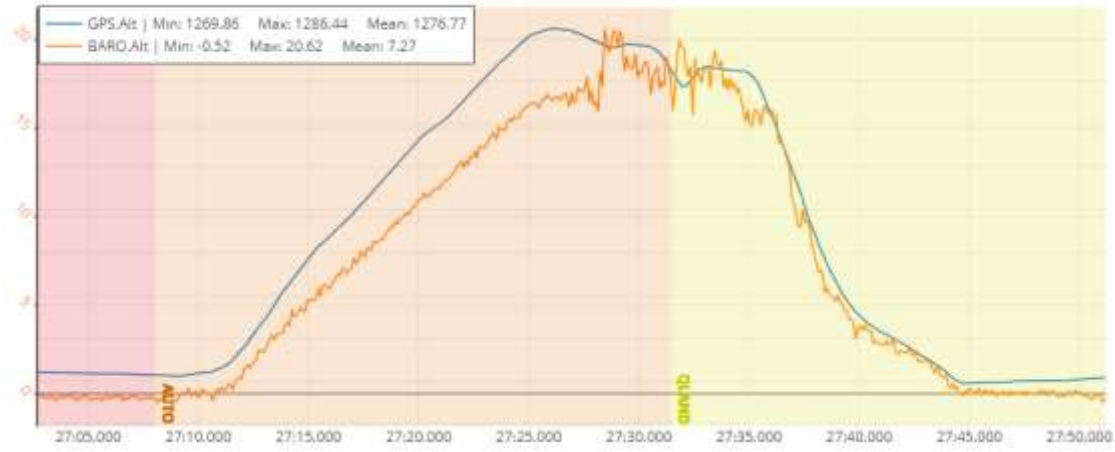

Fig A. 12: Comparison between GPS and barometric altitude

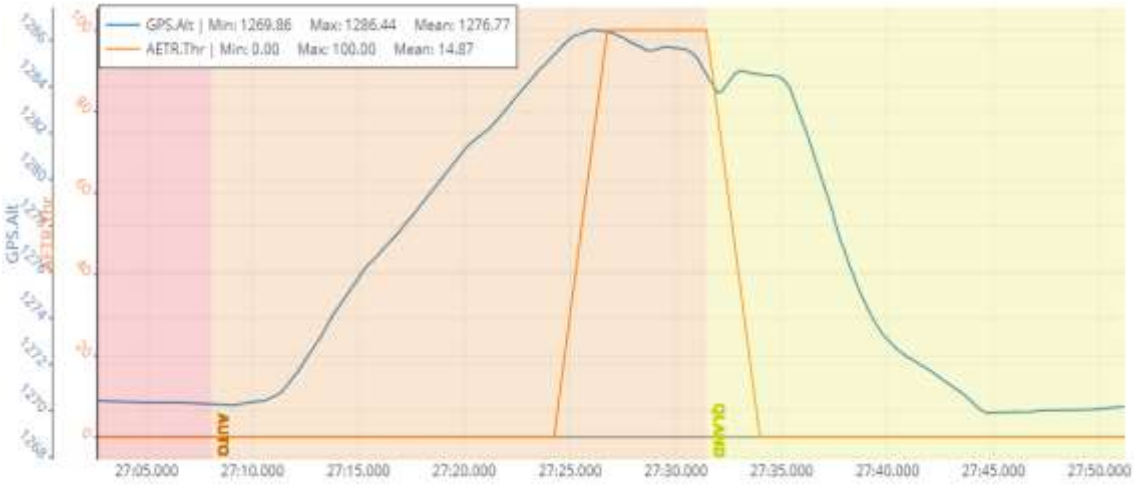

Fig A. 13: Forward Thrust variation at different Altitude

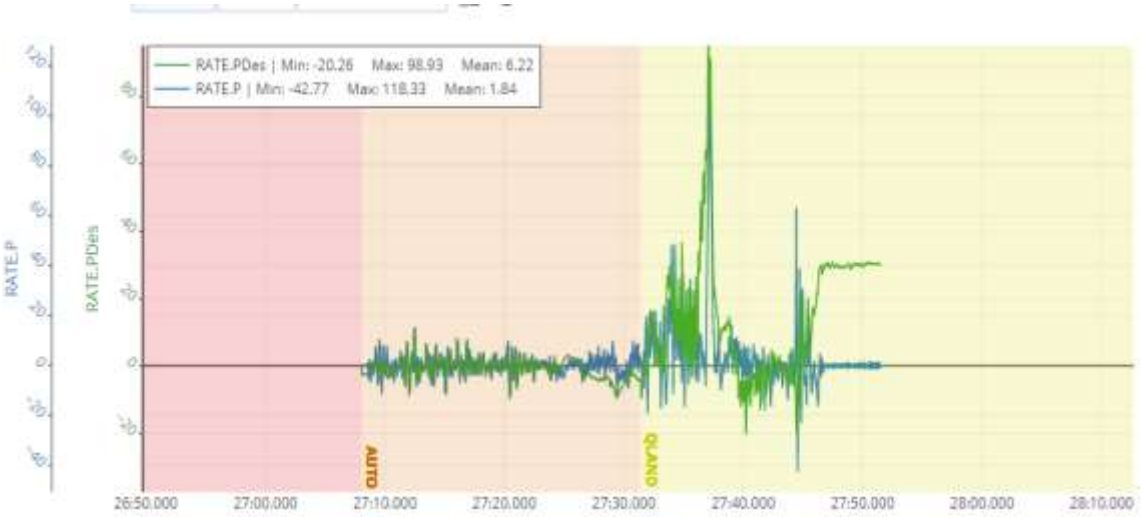

Fig A. 14: Desired and achieved pitch rate

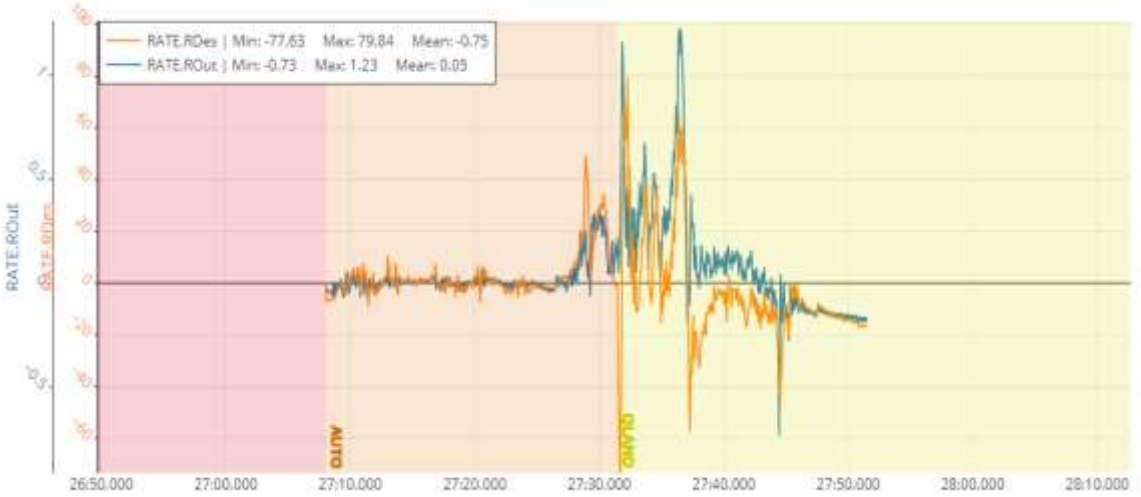

Fig A. 15: Desired and achieved roll rate

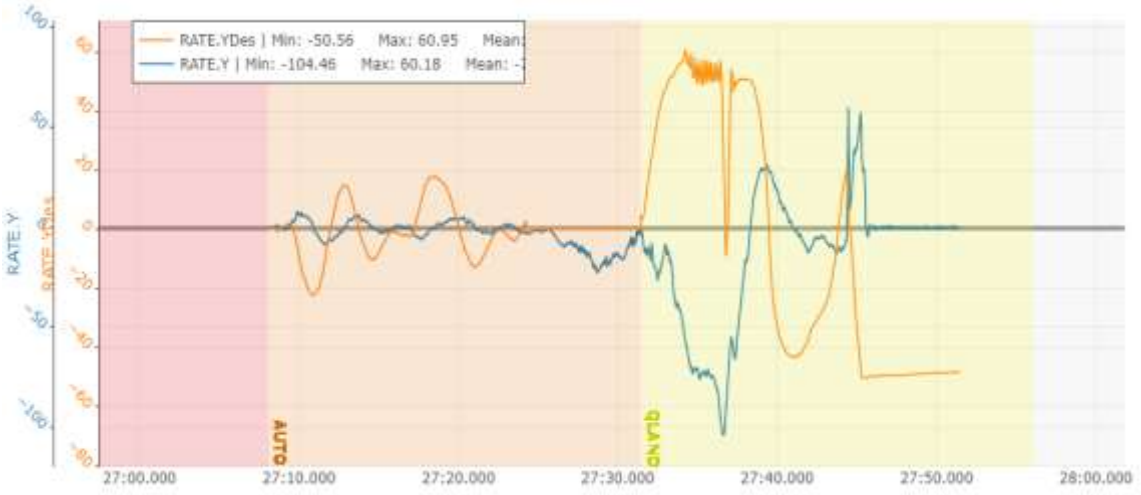

Fig A. 16: Desired and achieved yaw rate

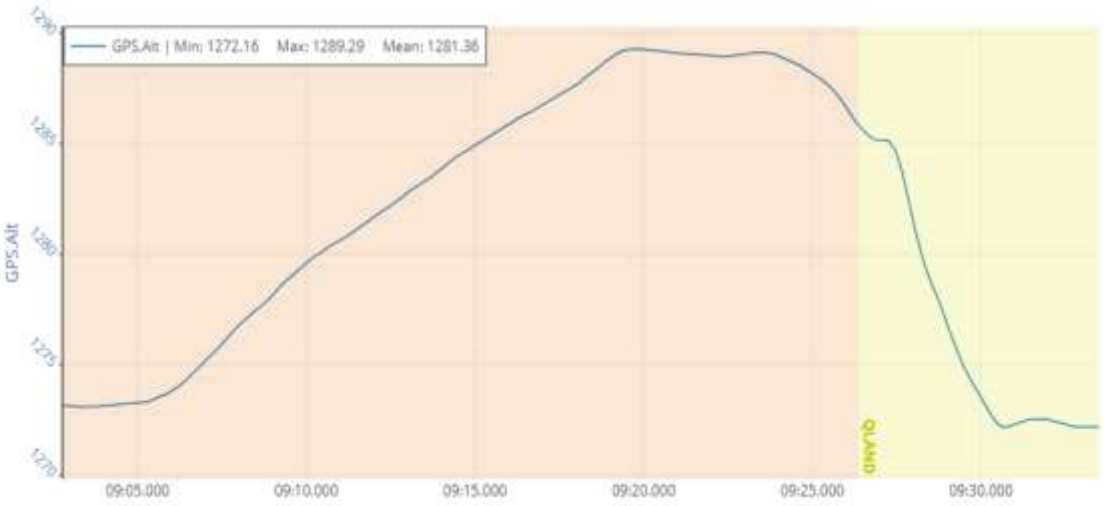

Fig A. 17: Altitude vs time

Fig A. 18: Comparison between GPS and barometric Altitude

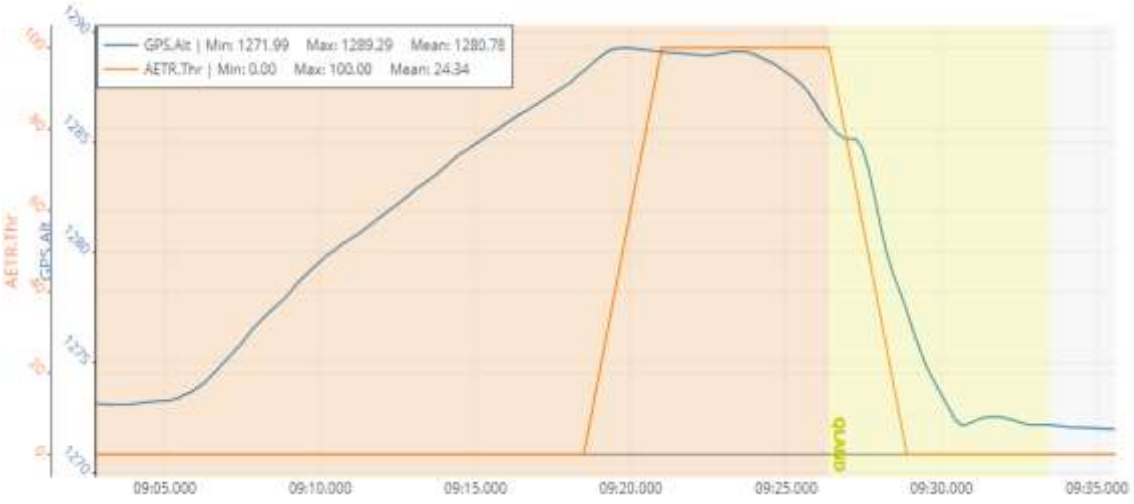

Fig A. 19: Forward thrust variation at different Altitude

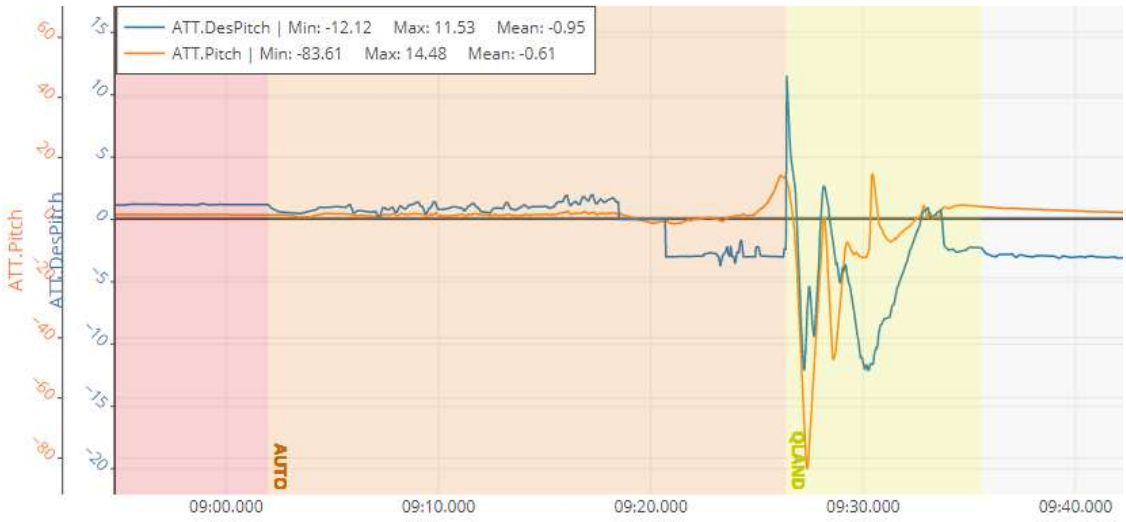

Fig A. 20: Desired and achieved pitch (deg)

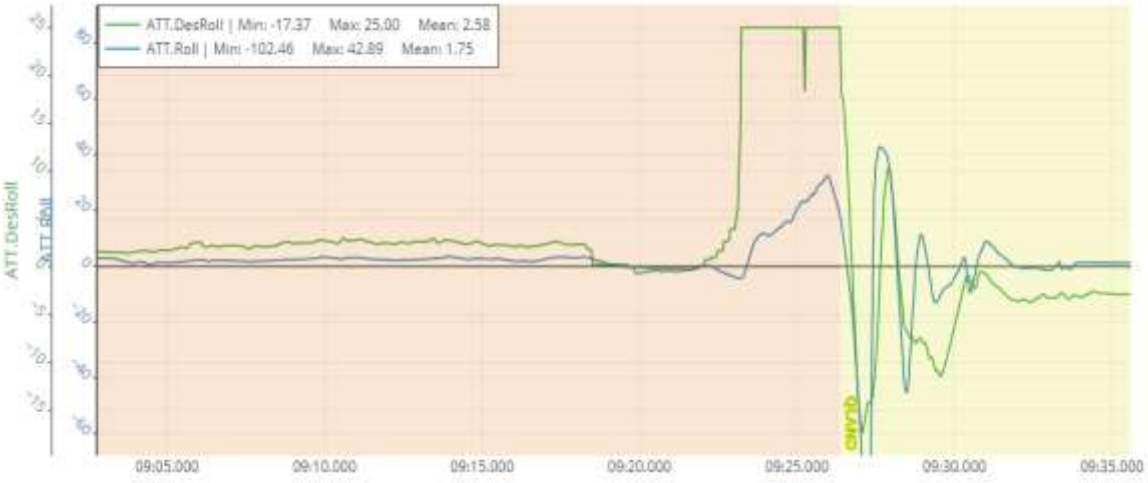

Fig A. 21: Desired and achieved roll (deg)

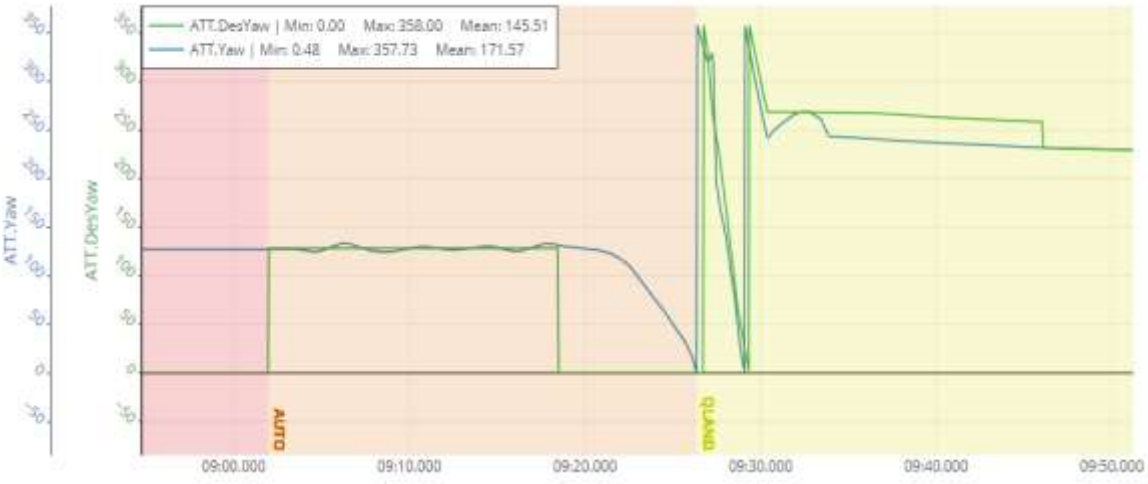

Fig A. 22: Desired and achieved yaw (deg)